

MICROREACTOR BASED SYNTHESIS OF POLYMER STABILIZED GOLD NANOCCLUSERS AND THEIR CHARACTERIZATION

A DISSERTATION

*Submitted in partial fulfillment of the
requirements for the award of the degree*

of

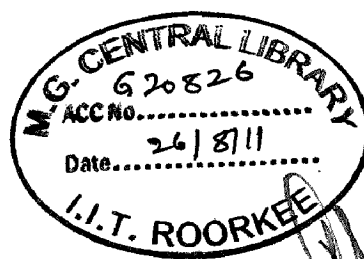
MASTER OF TECHNOLOGY

in

ADVANCED CHEMICAL ANALYSIS

By

VIJAY LAKSHMI MISHRA



DEPARTMENT OF CHEMISTRY
INDIAN INSTITUTE OF TECHNOLOGY ROORKEE
ROORKEE - 247 667 (INDIA)

JUNE, 2011

CANDIDATE'S DECLARATION

I hereby declare that the work which is being presented in this dissertation entitled "Microreactor Based Synthesis of Polymer Stabilized Gold Nanoclusters and Their Characterization" in partial fulfillment of the requirements for the award of the degree of Master of Technology in Chemistry with specialization in "Advanced Chemical Analysis (A.C.A)", and submitted in the Department of Chemistry at Indian Institute of Technology Roorkee, is an authentic record of work carried out by me during the period August 2010 to June 2011, under the guidance of Dr. P. Jeevanandam, Assistant Professor, Department of Chemistry, Indian Institute of Technology Roorkee, Roorkee and Prof. H. Sakurai, Research Center for Molecular Scale Nanoscience, Institute for Molecular Science, Myodaiji, Okazaki, Japan.

The matter presented in this dissertation work has not been submitted by me for the award of any other degree of this or any other Institute/ University. In keeping with the general practice of reporting scientific observation, due acknowledgement has been made wherever the work described is based on the findings of other investigators.

Date June 2011

Place Roorkee


(Vijay Lakshmi Mishra)

CERTIFICATE

This is to certify that above statement made by the candidate is correct to the best of our knowledge.



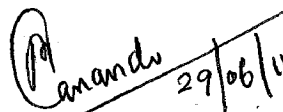
Dr. Hidehiro Sakurai

Professor

Research Centre for Molecular Scale Nanoscience

Institute for Molecular Science

Myodaiji, Okazaki 444-8787, Japan



Dr. P. Jeevanandam

Assistant Professor


Department of Chemistry

Indian Institute of Technology Roorkee

Roorkee-247667, Uttarakhand, India

To my parents, Jainath Mishra and Shanti Mishra, my first teacher, who showed me the bright path of education and gave me the greatest treasure of spirituality.

PREFACE



The work embodied in this thesis entitled “**Microreactor Based Synthesis of Polymer Stabilized Gold Nanoclusters and Their Characterization**” consists of five chapters; Introduction, Experimental, Results and Discussion, Au:PVP as a catalyst and Conclusions. Gold nanoclusters stabilized by poly(*N*-vinyl-2-pyrrolidone) (Au:PVP) and gold nanoclusters stabilized by star poly(2-methoxy ethoxy vinyl ether) (Au:star poly(MOVE)) were synthesized using microreactors and the catalytic properties were investigated after thorough characterization by transmission electron microscopy (TEM) and UV-visible spectroscopy. The yield of the products of the catalytic aerobic oxidation reaction were estimated by gas chromatography (GC). The gold nanoclusters were also explored as a catalyst for the growth of carbon nanotubes.

ACKNOWLEDGEMENT



I express my deepest gratitude to **Dr. P. Jeevanandam**, Assistant Professor, Department of Chemistry, IIT Roorkee, Roorkee for sparing his valuable time, suggestion and providing useful guidance for completion of this dissertation. He has the unique ability of identifying strengths and weaknesses to bring out the best in every student, and he worked with me patiently bringing me up to speed in my understanding of research. He is the best supervisor I ever met.

I am highly obliged to **Prof. V. K. Gupta**, Head, Department of Chemistry, **Prof. Kamaluddin**, **Dr. R. K. Dutta**, Course Coordinator of M.Tech and **Prof. M. R. Maurya**, for allowing me to do a part of my dissertation at IMS (Institute for Molecular Science), Okazaki, Japan. I would like to thank Prof. Hidehiro Sakurai for his invaluable help and guidance. I greatly appreciate all of his time and hard work he invested in me. I would also like to thank Dr. Hiroaki Kitahara for his unstinted cooperation and encouragement for the successful completion of this work. I truly appreciate his immense patience and tolerance. Special thanks to Noriko Kai. Thanks to all the members in Prof. Sakurai group for all their helpful suggestion, discussion, and generous assistance. I avail the opportunity to express thanks to my labmates at IIT Roorkee, Manu Sharma, Nisha Bayal, Geetu Sharma and Naga Ratna Kishore for their kind help, care, encouragement and moral support. In addition, I would also like to thank the JENESYS program and the Ministry of Human Resource, Government of India for their financial supports.

Finally, I would like to thank my family members for their moral support and blessing, which helped me to complete the dissertation.

Vijay Lakshmi Mishra


← ABBREVIATIONS →

Abbreviation	Full Form
PVP	Poly (<i>N</i> -vinyl-2-pyrrolidone)
KDa	Kilo Dalton
TEM	Transmission electron microscopy
GC	Gas chromatography
M	Molar
K	Kelvin
mg	Milligram
mmol	Millimol
mm	Millimeter
Rpm	Rotations per minute
BnOH	Benzyl alcohol
p-OMe BnOH	para methoxy benzyl alcohol
p-NO ₂ BnOH	para nitro benzyl alcohol
min	Minute
nm	Nanometer
mL	Milliliter
hr	Hour
NCs	Nanoclusters
° C	Degrees Centigrade
Star poly(MOVE)	Star poly(2-methoxy ethoxy vinyl ether)

ABSTRACT

Synthesis of ultra fine particles of metals, which are referred as clusters or nanoclusters, has been the subject of considerable interest. Small size is needed for effective catalysis. Gold clusters protected by a hydrophilic polymer acts as a superior quasi-homogeneous catalyst for aerobic oxidation in water. Synthesis of gold nanoclusters protected by poly(*N*-vinyl-2-pyrrolidone) (PVP) with three different molecular weights namely K-15 (average molecular weight, $M_w = 10$ kDa), K-30 (average molecular weight, $M_w = 40$ kDa), K-90 (average molecular weight, $M_w = 360$ kDa) and star polymer have already been prepared using batch process and successful results have been obtained using PVP(K-15) and PVP(K-30), giving mono-dispersed gold clusters with 1.3 nm mean size. However, there are some problems regarding the size and reproducibility in the case of useage of PVP(K-90) and star polymer due to their high molecular weight and high viscosity. In the present study, flow reaction conditions were applied to conquer the viscosity problem. Two different types of micro reactors, Techno-applications COMET X-01 and Sigma-Aldrich type S02, were used. Under the optimized conditions of Sigma-Aldrich type S02 microreactor, mono-dispersed clusters of Au:PVP(K-90) with 1.15 nm mean size were successfully produced and the size of Au:star poly(MOVE) nanoclusters varies from 1.9 to 4 nm using Techno-applications COMET X-01 microreactor. The Au:PVP (K-90) and Au:Star poly(MOVE) nanoclusters were characterized by UV-Vis spectroscopy and transmission electron microscopy. Catalytic activity of gold nanoclusters towards the aerobic oxidation of alcohols and growth of carbon nanotubes using Au:PVP(K-90) nanoclusters as a catalyst is also discussed.

TABLE OF CONTENTS



Candidate's declaration	i
Preface	iii
Acknowledgement	iv
Abbreviation	v
Abstract	vi
Contents	vii
List of tables	viii
List of figure	ix
CHAPTER 1: GENERAL INTRODUCTION	1
1.1. Nanoparticles as catalysts	
1.2. Gold nanoclusters	
1.3. Gold nanoclusters as catalysts	
1.3.1: Polymer-stabilized gold nanoclusters	
1.3.2: Dendrimer-stabilized gold nanoclusters	
1.3.3: Ligand-stabilized gold nanoclusters	
1.3.4: Surfactant-stabilized gold nanoclusters	
1.3.5: Ionic liquids as media for gold nanoclusters	
1.4: Au:PVP as an oxidation catalyst	
1.4.1: Aerobic oxidation of alcohols	
1.4.2: Homocoupling reaction of organoboron compounds	
1.4.3: Hydroxylation of organoboron compounds	
1.5: Au:PVP as a Lewis acid catalyst	

1.6: Objective of the present study

CHAPTER 2: EXPERIMENTAL

21

2.1: Materials used

2.2: Experimental procedure

2.2.1: Batch synthesis

2.2.2: Microreactor based synthesis

2.3: Preparation of Au: PVP (K -90)

2.3.1: Batch process

2.3.2: Microreactor process

2.4: Preparation of Au:star poly(MOVE) by microreactor

2.5: Methods and characterization of the samples

2.5.1: UV-Visible spectroscopy

2.5.2: Transmission electron spectroscopy (TEM)

2.5.3: Scanning electron microscopy (SEM)

2.5.4: Gas chromatography

2.5.5: Freeze dryer

2.5.6: Electric furnace

2.5.7: Centrifuge

2.5.8: Parallel chemical reactor

CHAPTER 3: RESULTS AND DISCUSSION

38

3.1: TEM and UV-visible spectroscopy

3.1.1: TEM and UV-visible results of Au:PVP(K-15)

3.1.2: TEM and UV-visible results of Au:PVP(K-30)

3.1.3: TEM and UV-visible results of Au:PVP(K-90)

3.2: Optimization conditions for Au:PVP(K-90) using Sigma-aldrich S02 microreactor

3.3: Au:Star poly(MOVE) synthesis

CHAPTER 4: Au:PVP NANOCCLUSERS AS A CATALYST

52

4.1: Aerobic oxidation reactions

4.1.1: Oxidation of benzyl alcohol

4.1.2: Oxidation of p-methoxy benzyl alcohol

4.1.3: Oxidation of p-nitro benzyl alcohol

4.2: Some preliminary studies on the catalytic growth of carbon nanotubes

4.2.1: Carbon nanotubes

4.2.2: Fabrication methods

4.2.2a: Chemical vapor deposition

4.2.3: Experimental procedure

4.2.3a: Preparation of Au supported catalyst

4.2.3b: Growth of carbon nanotubes

CHAPTER 5: CONCLUSIONS

69

CHAPTER 6: REFERENCES

70

LIST OF TABLES



Table (2.1.1) Chemicals used in the present study

Table (3.1.1) Different conditions used during the optimization of Sigma Aldrich microreactor for Au:PVP (K-90)

Table (3.3.1) Different optimization conditions for the preparation of Au:star poly(MOVE)

Table (4.1.1) Yield and rate constants for different aerobic oxidation reactions

Table (4.2.1) Process conditions for the carbon nanotubes growth in CVD

LIST OF FIGURES

- Figure 1.2.1:** Illustration of electronic states in a nanocluster
- Figure 1.2.2:** Size dependence on the character of gold
- Figure 1.2.3:** Size dependence of Au nanocluster for CO oxidation
- Figure 1.2.4:** Activation of Au cluster by adsorption of molecular oxygen
- Figure 1.3.1:** Poly(*N*-vinylpyrrolidone) stabilizer for metal nanoparticles
- Figure 1.3.2:** The structure of PAMAM and PPI dendrimers
- Figure 1.3.3:** Structures of ionic liquids
- Figure 1.4.1:** Aerobic oxidation of alcohols catalyzed by Au:PVP
- Fig 1.4.1:** Catalytic activity of Au:PVP for aerobic oxidation of alcohol
- Figure 1.4.2:** Proposed mechanism
- Figure 1.4.3:** Preparation and characterization of Au@star-poly(EOEOVE)₂₀₀
- Figure 1.4.4:** Reusability of Au nanocluster@star-poly(EOEOVE) for aerobic oxidation of benzyl alcohol
- Figure 1.4.5:** Homocoupling reaction of phenylboronic acid catalyzed by Au:PVP
- Figure 1.4.6:** Homocoupling reaction of potassium phenyl trifluoroborate catalyzed by Au:PVP
- Figure 1.4.7:** Hydroxylation of phenylboronic acid catalyzed by Au:PVP
- Figure 1.5.1:** The role of molecular oxygen in the oxidation of alcohol
- Figure 2.2.1:** Preparation of Au:PVP by Batch Method
- Figure 2.2.2:** Reaction progress using catalyst synthesized in batch process
- Figure 2.2.3:** Reaction progress using catalyst synthesized in Microreactor
- Figure 2.2.4:** Heat distributions in a batch synthesis vessel and the temperature ranges from 293.15 K (blue) to 303.15 K (red)
- Figure 2.2.5:** Heat distribution in a micro reactor. Temperatures are given according to the scale (above right) in Kelvin
- Figure 2.2.6:** Precise temperature control in a microreactor enhances the product quality by suppression of side reactions
- Figure 2.2.7:** Mixing efficiency in a microreactor. Compound B is injected into a flow of compound A (blue)

- Figure 2.2.8:** Mixing efficiency in a stirred batch reactor. Concentration equivalents (ranging from 0.8 (blue) to 1.2 (red) according to the colour scale top left)
- Figure 2.2.9:** Chemical progress diagram
- Figure 2.2.10:** a) Techno-applications COMET X-01 microreactor, b) Sigma-Aldrich type S02 microreactor
- Figure 2.2.11:** Mixing of HAuCl_4 and NaBH_4 in microreactor
- Figure 2.2.12:** Preparation of Au:PVP by the batch method
- Figure 2.2.13:** Preparation of Au:PVP nanoclusters using a microreactor
- Figure 2.2.14:** Structure of star poly(MOVE)
- Figure 2.5.5:** Centrifuge KUBOTA 7780II
- Figure 2.5.6:** Freeze dryer
- Figure 2.5.6:** Electric furnace
- Figure 2.5.4:** Parallel chemical reactor
- Figure 3.1.1:** UV-visible spectra of Au:PVP(K-15) synthesized by different methods
- Figure 3.1.2:** TEM images and particle size distributions of Au:PVP(K-15) prepared using a) batch process, b) COMET X-02 microreactor and c) Aldrich microreactor
- Figure 3.1.3:** UV-visible spectra of Au:PVP(K-30) synthesized by different methods
- Figure 3.1.4:** TEM images and particle size distributions of Au:PVP (K-30) prepared using a) batch process, b) COMET X-02 microreactor and c) Aldrich microreactor
- Figure 3.1.5:** UV-visible spectra of Au:PVP (K-90) synthesized by different methods
- Figure 3.1.6:** TEM images and particle size distributions of Au:PVP(K-90) prepared using a) batch process, b) COMET X-02 microreactor and c) Aldrich microreactor
- Figure 3.2.1:** TEM image, UV-vis spectrum and size distribution of gold nanoclusters stabilized by PVP(K-90) at conditions I using Sigma-Aldrich microreactor
- Figure 3.2.2:** TEM image, UV-vis spectrum and size distribution of gold nanoclusters stabilized by PVP(K-90) at conditions II using Sigma-Aldrich microreactor
- Figure 3.2.3:** TEM image, UV-vis spectrum and size distribution of gold nanoclusters stabilized by PVP(K-90) at conditions III using Sigma-Aldrich microreactor
- Figure 3.2.4:** TEM image of gold nanoclusters stabilized by PVP(K-90) at conditions IV using Sigma-Aldrich microreactor
- Fig 3.2.5:** TEM image, UV-vis spectrum and size distribution of gold nanoclusters stabilized by PVP(K-90) at conditions V using Sigma-Aldrich microreactor

- Figure 3.2.6:** TEM image, UV-vis spectrum and size distribution of gold nanoclusters stabilized by PVP(K-90) at conditions VI using Sigma-Aldrich micro reactor
- Figure 3.2.7:** TEM image, UV-vis spectrum and size distribution of gold nanoclusters stabilized by PVP(K-90) at conditions VII using Sigma-Aldrich micro reactor
- Figure 3.2.8:** TEM image, UV-vis spectrum and size distribution of gold nanoclusters stabilized by PVP(K-90) at conditions VIII using Sigma-Aldrich microreactor
- Figure 3.2.9:** TEM image, UV-vis spectrum and size distribution of gold nanoclusters stabilized by PVP(K-90) at conditions IX using Sigma-Aldrich microreactor
- Figure 3.3.1:** TEM images, UV-vis spectrum and size distribution of gold nanoclusters stabilized by star MOVE at condition I using Techno-application COMET X-01 microreactor
- Figure 3.3.2:** TEM images, UV-vis spectrum and size distribution of gold nanoclusters stabilized by star MOVE at condition II using Techno-application COMET X-01 microreactor
- Figure 4.1.1:** Oxidation of benzyl alcohol
- Figure 4.1.2:** Progress of oxidation of benzyl alcohol with Au:PVP(K-30) and Au:PVP(K-90)
- Figure 4.1.3:** Kinetics of oxidation reaction of benzy lalcohol with Au:PVP(K-30) and Au:PVP(K-90)
- Figure 4.1.4:** Oxidation of benzyl alcohol
- Figure 4.1.5:** Progress of oxidation reaction of p-methoxy benzyl alcohol with Au:PVP(K-30) and Au:PVP(K-90)
- Figure 4.1.6:** Kinetics of oxidation reaction of p-methoxy benzyl alcohol with Au:PVP(K-30) and Au:PVP(K-90)
- Figure 4.1.8:** Oxidation of p-nitro benzyl alcohol
- Figure 4.2.1** Schematic diagram of a chemical vapor deposition system.
- Figure 4.2.2:** Schematic diagram of base growth model of carbon nanotubes
- Figure 4.2.3:** Temperature program of electric furnace for the growth of carbon nanotubes
- Figure 4.2.4:** SEM image of product obtained under the condition listed in Entry 1
- Figure 4.2.5:** SEM image of product obtained under the condition listed in Entry 2
- Figure 4.2.6:** SEM image of product obtained under the condition listed in Entry 3
- Figure 4.2.7:** SEM image of product obtained under the condition listed in Entry 4

Figure 4.2.8: SEM image of product obtained under the condition listed in Entry 5

Figure 4.2.9: SEM image of product obtained under the condition listed in Entry 6

1. General introduction

1.1 Nanoparticles as catalysts

A catalyst is a species that is added to a chemical reaction but does not get consumed. It works by providing an alternative reaction pathway for the reaction in which the activation barriers are lowered and the reaction rate is increased [1]. Catalysts are used widely in chemical industry. Metal nanoparticles are promising catalysts for a variety of reactions, for example, oxidation, hydrogenation, and C-C coupling reactions [2], given that they have large surface to volume ratio. Metal nanoparticles (colloids or clusters) have been used as catalysts since the 19th century [3] and industries have involved the nanoparticles since the beginning of 20th century [4, 5]. A major achievement in the area of nanoparticles catalysts came with Haruta's report that oxide supported gold nanoparticles can be an effective catalyst for low temperature oxidations of H₂ and CO in 1987 [6]. Since then, nanocatalysts have attracted more and more attention and an exponential growth has been seen in the number of publications in the literature.

"Naked" metal nanoparticles are unstable and tend to agglomerate, aggregate and even precipitate out of solution and lose their catalytic activity. Therefore, metal nanoparticles traditionally need to be supported on a solid surface (e.g. oxide, carbon) [3] to form heterogeneous catalysts. The advantages of heterogeneous catalysts are that they are easy to separate from reactants and products for recovery and reuse. Also, they can be used at high temperature and pressure. However, they often have poor catalytic activity and reactivity compared to homogeneous catalysts [7]. An alternative method to stabilize metal nanoparticles is using polymer, block polymer, dendrimers, surfactants or organic ligands as stabilizers [3]. Polymer or ligand stabilized metal nanoparticles can be uniformly dispersed in organic solvents or water and mixed with reactant and products in a way resembling a homogeneous catalytic system [8]. Such a catalytic system is often called *quasi*-homogeneous nanoparticle catalyst.

Quasi-homogeneous catalysts can have high catalytic activity and selectivity. However, insufficient stability and high costs, due to difficulties in recovery and reuse, are major drawbacks. Based on the properties of gold nanoclusters, there are ongoing and potential applications in the fields of catalysis [9-12], electronic and electro optical devices [13-15], biomedicine [16-20], etc, that extend far beyond imagination.

1.2 Gold Nanoclusters

Gold particles generally of size 1-20 nm are considered as nanoclusters. Nanoclusters have a band gap which bulks do not have (Figure 1.2.1). Specific properties are obtained from this band gap.

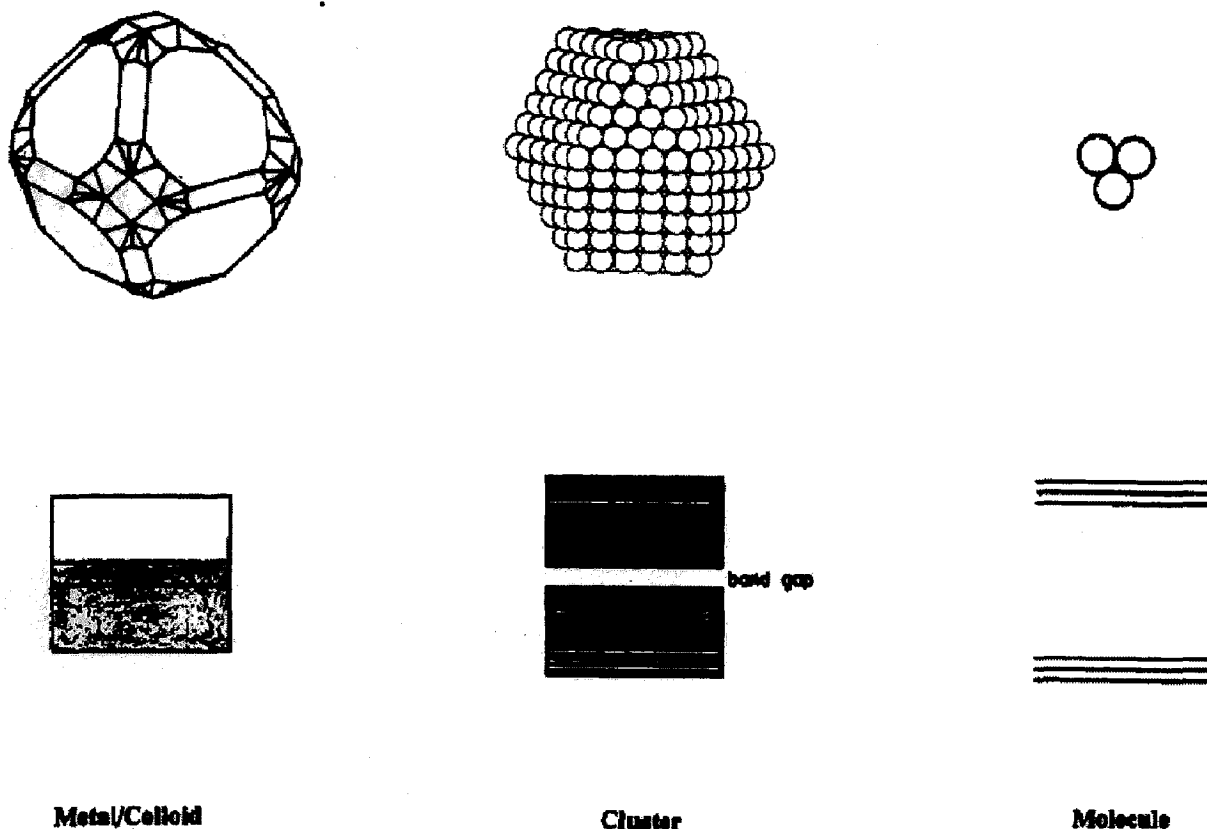


Figure 1.2.1: Illustration of electronic states in a nanocluster (from Schmid, G. *Chem. Rev.* 1992, 92, 1709-1727)

Plasmon resonance occurs for the gold nanoclusters in the range of 500-600 nm that depend on the size, shape and support of particles [21]. Gold complexes having Au (I) or Au (III) states possess catalytic activity (e.g. Lewis acid catalyst) and there are many reports involving oxidation, reduction, formation of carbon-carbon, carbon-heteroatom bonds and so on [22]. In contrast, metallic gold has been believed to be catalytically inactive due to its highest ionization energy. There are remarkable differences of chemical character between metallic gold and gold complexes (Figure 1.2.2).

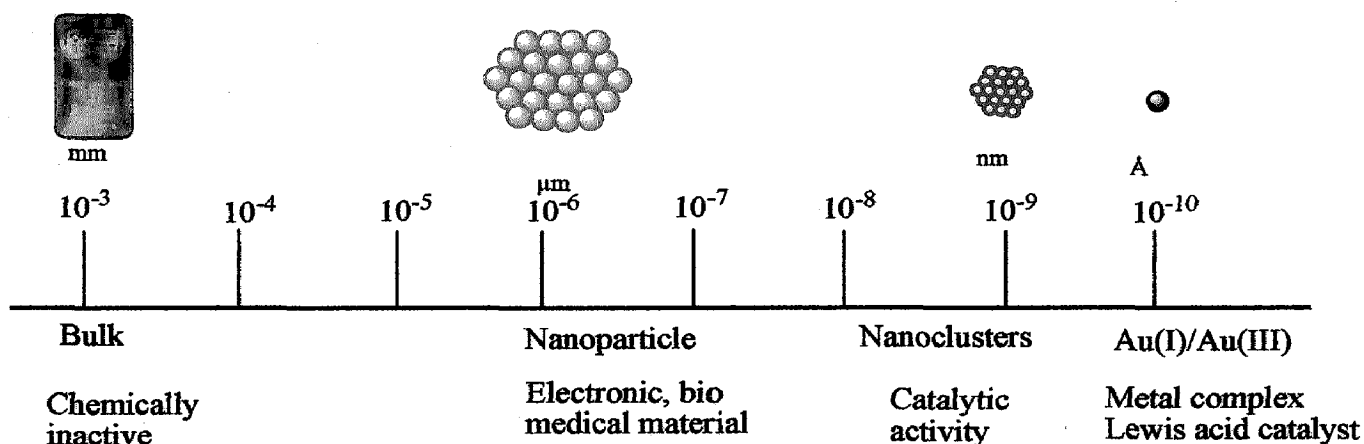


Figure 1.2.2: Size dependence on the character of gold

In 1987, Haruta reported that the zero valent nano-sized gold clusters supported on a metal oxide catalyze the CO oxidation [23a].

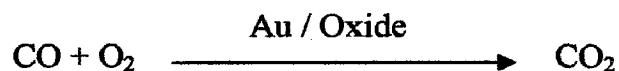


Figure 1.2.3 shows the turnover frequency (TOF) of CO oxidation as a function of the mean diameter of gold particles [23b]. The size dependence of cluster was observed. The TOF drastically increased with a decrease in the diameter from 3-4 nm size of gold cluster at 273 K. In contrast, Pt cluster showed a decrease of TOF with decrease in gold diameter. The binding energy between molecular oxygen and Pt is higher than that in Au due to vacant *5d* orbital of Pt. Therefore, higher activation energy should be the barrier for the reaction even at 437 K.

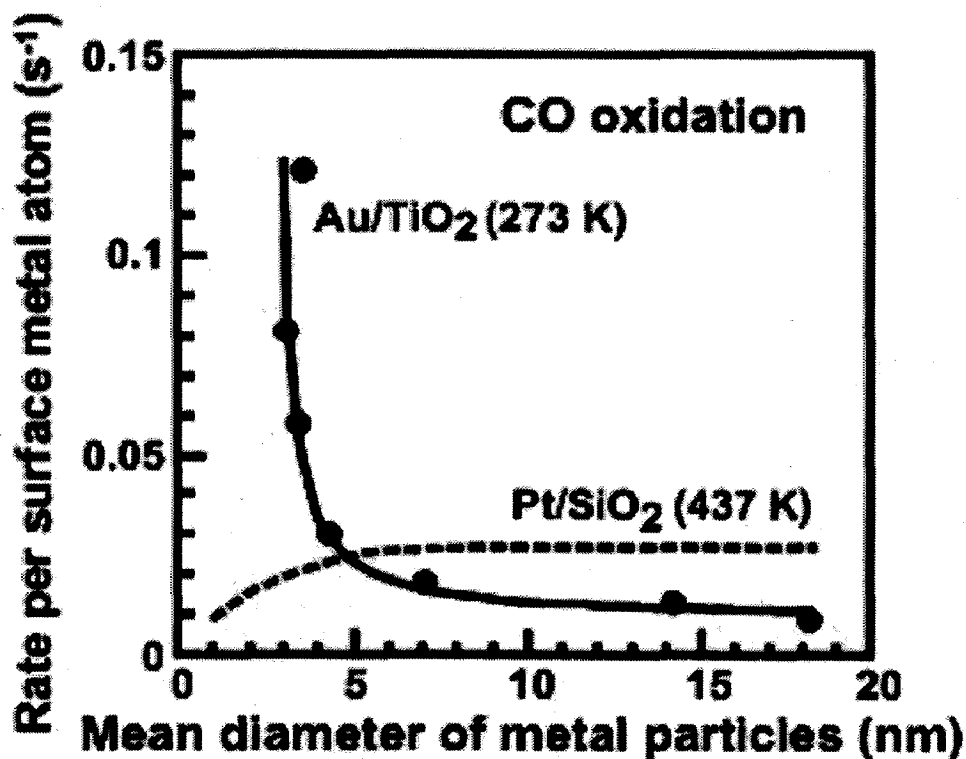
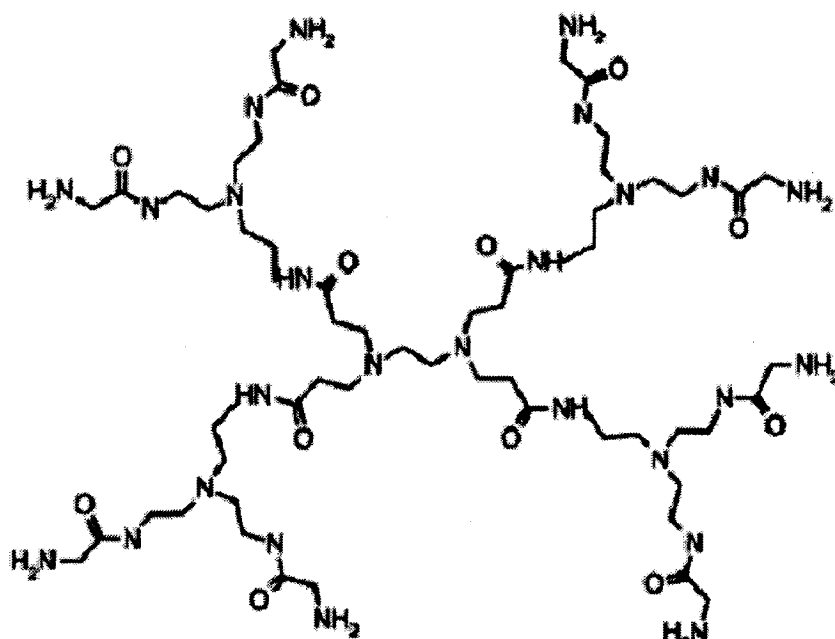


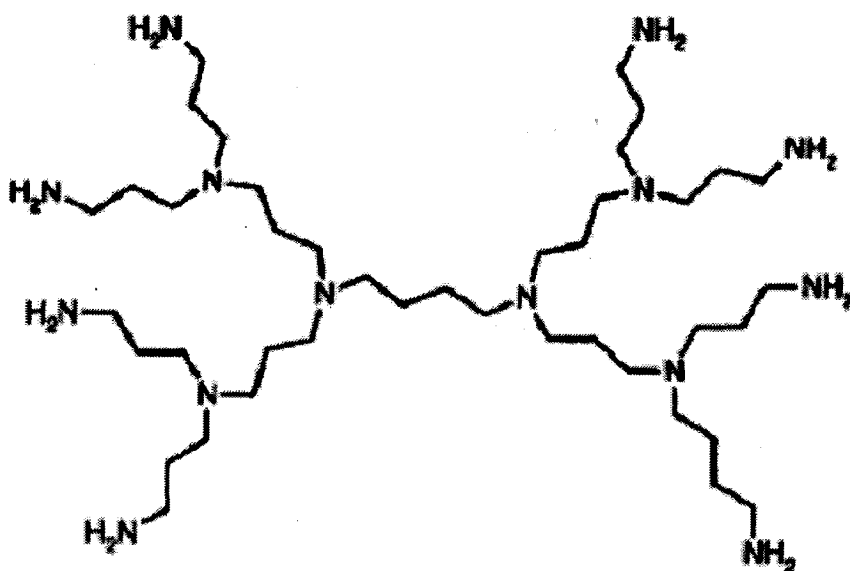
Figure 1.2.3: Size dependence of Au nanocluster for CO oxidation (From M. Haruta, *Chem. Record* 2003, 3, 75)

With respect to the mechanism of CO oxidation, the adsorption of molecular oxygen on to the gold nanoclusters has been proposed as shown in Fig 1.2.4 [24a]. The activation of Au cluster by electron transfer from metal oxide is followed by electron transfer of molecular oxygen. Since water is known to increase the activity, adsorption of water is also expected to assist the electron donation [24b]. In both the cases, electron rich gold nanocluster is important to adsorb molecular oxygen on to the cluster surface. Oxygen molecule can be adsorbed by the electron transfer from the *5d* orbital of gold nanocluster to the anti-bonding orbital of molecular oxygen.

This means higher generation dendrimers have higher steric crowding on the periphery [42] compared to lower generation. For a particular generation, the PPI dendrimers are substantially smaller than PAMAM dendrimers (2.8 nm versus 4.5 nm for G4, respectively) [42].



G1 PAMAM Dendrimer



G1 PPI Dendrimer

Figure 1.3.2: The structure of PAMAM and PPI dendrimers

1.3.3 Ligand-stabilized Gold Nanoclusters

Organic ligands, such as amine, phosphine, and thiol molecules, also can be used as stabilizers. Au nanoparticles stabilized by amines, phosphines, and thiols have been prepared [11, 43-45]. Polymers, dendrimers, and ligands sometimes have been combined by other groups in order to stabilize metal nanoclusters with novel activity, selectivity, and recycling potentials [46].

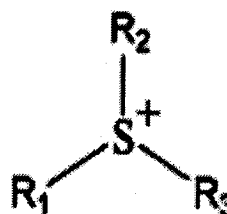
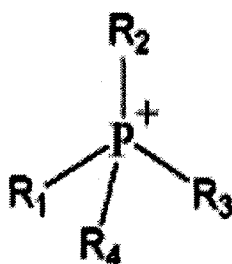
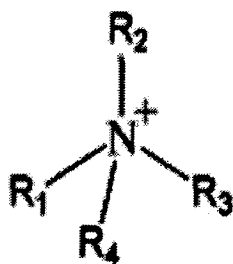
1.3.4 Surfactant-stabilized Gold Nanoclusters

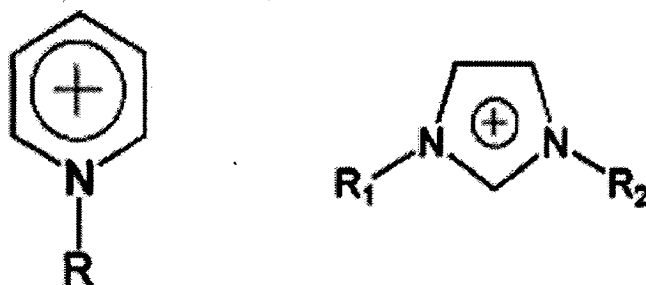
Several surfactants, for example, tetraoctylammonium bromide (TOAB) [47] and sodium bis(2-ethylhexyl) sulfosuccinate (AOT) [8], have been reported to stabilize metal nanoparticle catalysts. However, TOAB-stabilized gold nanoclusters have unsatisfactory long-term stability, though Isaacs *et al.* found that the use of thiosulfate anions instead of bromide anions can greatly improve both the chemical and thermal stability of tetraoctylammonium-stabilized Au nanoparticles [47]. Surfactants are generally not preferred stabilizers for nanoparticle catalysts as the catalytic activity of metal nanoparticles is typically inhibited by them [48].

1.3.5 Ionic Liquids as Media for Gold Nanoparticles

Ionic liquids are solvents that are composed entirely of ions. Room temperature ionic liquids are generally salts of organic cations such as tetraalkylammonium tetraalkylphosphonium, N-alkylpyridinium, 1,3-dialkylimidazolium and trialkylsulfonium cations, paired with highly diffuse anions (Figure 1.3.3) [49]. Some of the example of cations and anions in ionic liquids are given below.

Cations:





Anions:

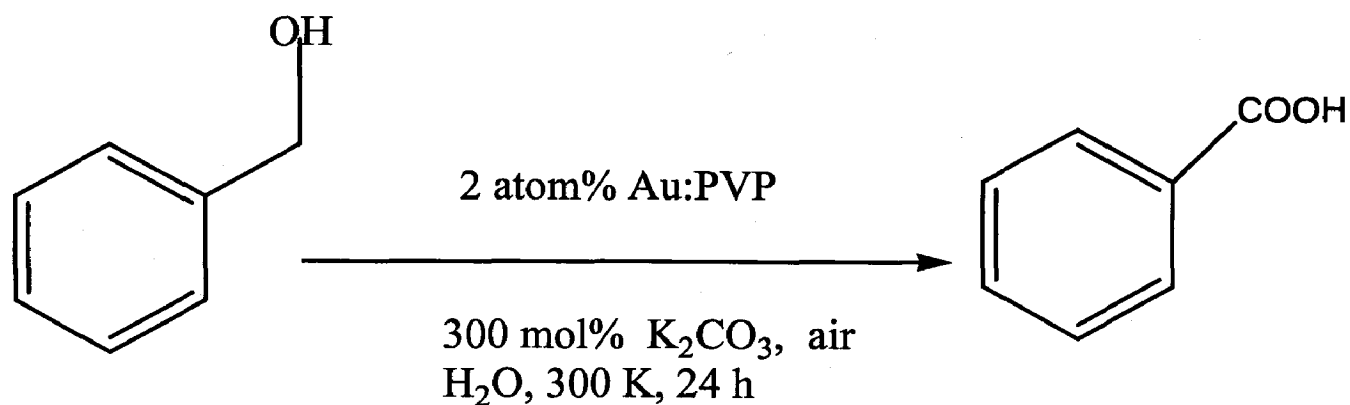


Figure 1.3.3: Structures of ionic liquids [50].

1.4 Au:PVP as an Oxidation Catalyst

1.4.1 Aerobic Oxidation of Alcohols [51a, 51b, 51e]

Au:PVP behaves as an oxidation catalyst, which promotes the aerobic oxidation of primary and secondary alcohols (benzylic, aliphatic) in basic aqueous conditions, giving corresponding carboxylic acids and ketones, respectively (Figure 1.4.1).



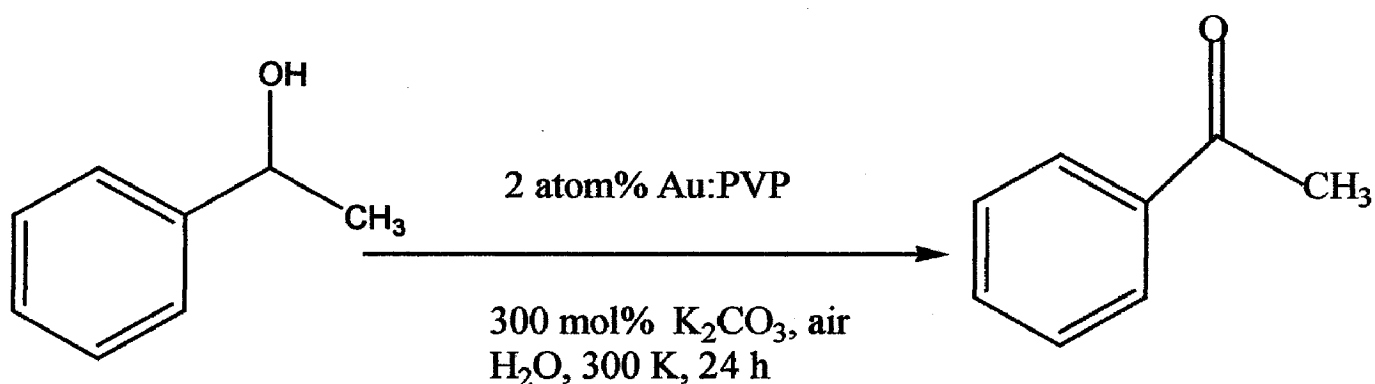


Figure 1.4.1: Aerobic oxidation of alcohols catalyzed by Au:PVP.

As a mechanistic consideration, cluster size dependence for catalytic activity was investigated (Fig 1.4.1). *p*-Hydroxybenzyl alcohol was used as the substrate, because it affords only *p*-hydroxybenzaldehyde and further oxidation into the corresponding carboxylic acid is suppressed due to the mesomeric effect of [O-C₆H₄-CH=O]⁻.

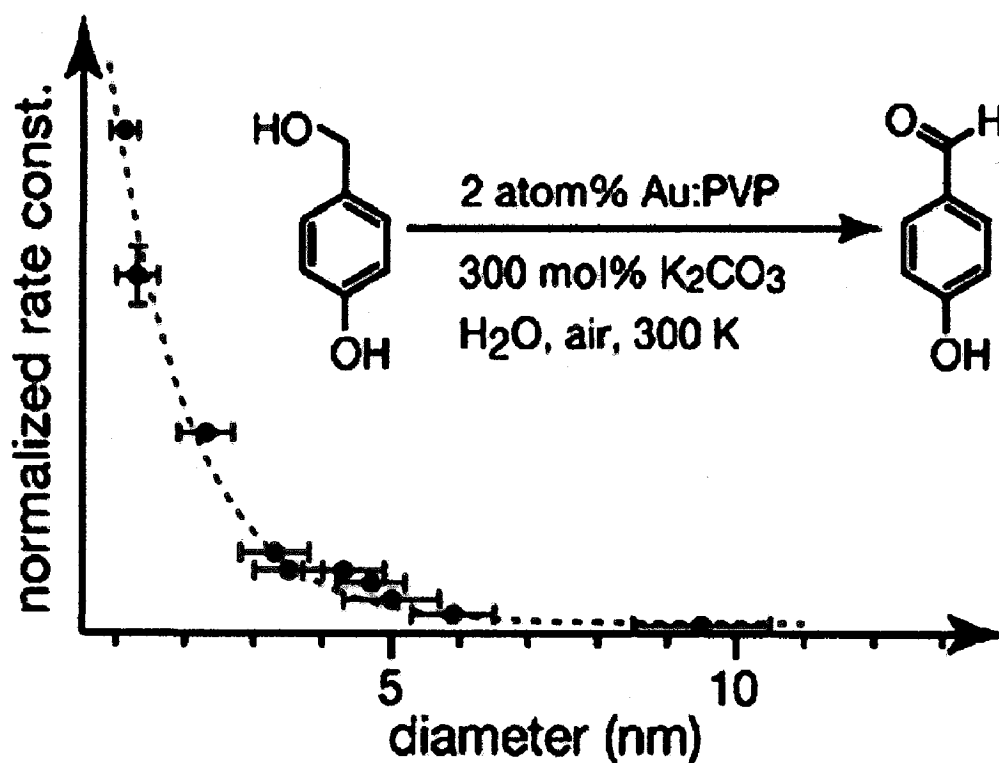


Figure 1.4.1: Catalytic activity of Au:PVP for aerobic oxidation of alcohol (from H. Tsunoyama, *et al*, *Chem. Phys. Lett.* 2006, 429-528)

The catalytic activity was drastically increased with decrease in the Au cluster size. It means that the catalytic active species is not a leached atomic or ionic species from the cluster. The oxidation of alcohols catalyzed by Pd clusters go on till the oxidative addition of alcohol followed by β -hydrogen elimination as a rate determining step giving the corresponding aldehyde. Finally, the molecular oxygen removes the hydride species to activate the Pd catalyst [52]. On the other hand, Au cluster is activated by molecular oxygen adsorption, giving species which has negative charge on oxygen with cationic site on the gold cluster surface. The adsorption of alkoxide in basic condition followed by β -hydrogen extraction by superoxo-like oxygen as a rate-determining step afford corresponding aldehyde with regeneration of the Au cluster. As an alternative mechanism for oxidation of alcohols, β -hydrogen shift was proposed to form Au-H intermediate as a key step. The proposed mechanism is shown in Figure 1.4.2.

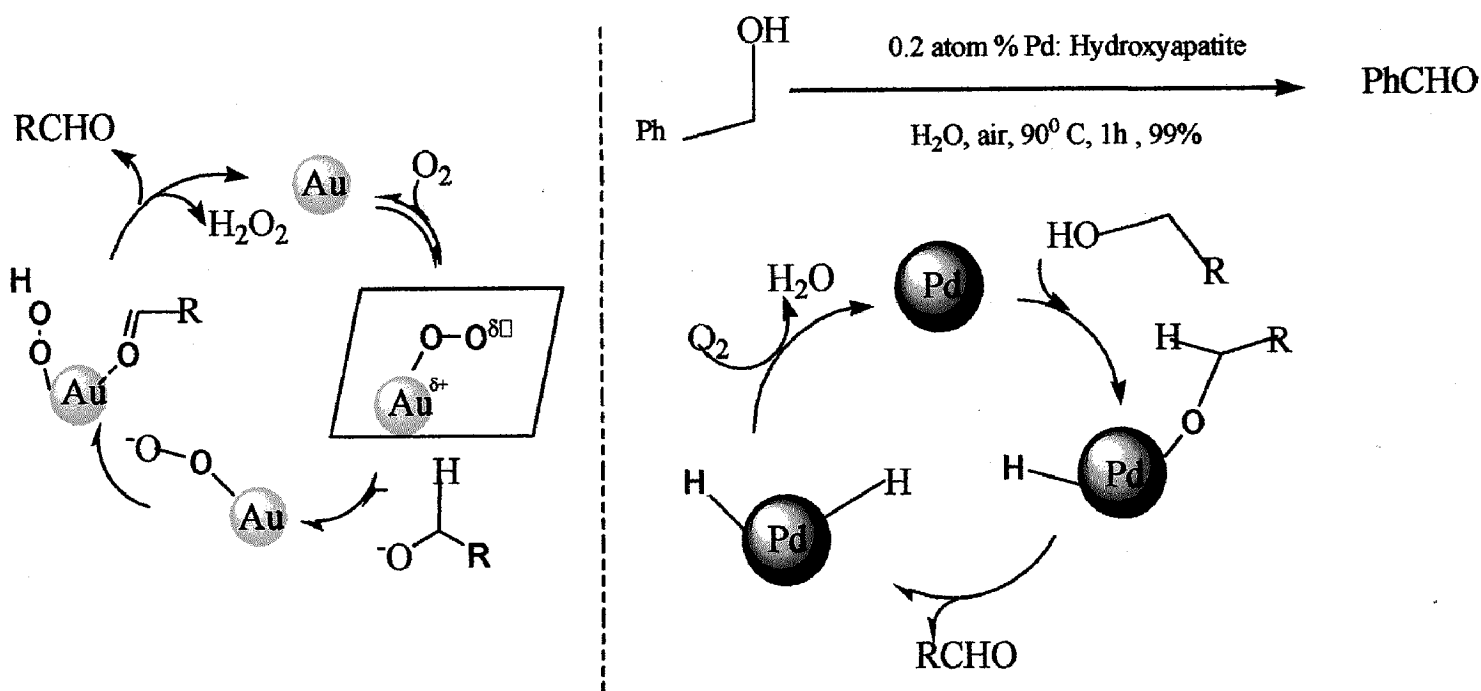
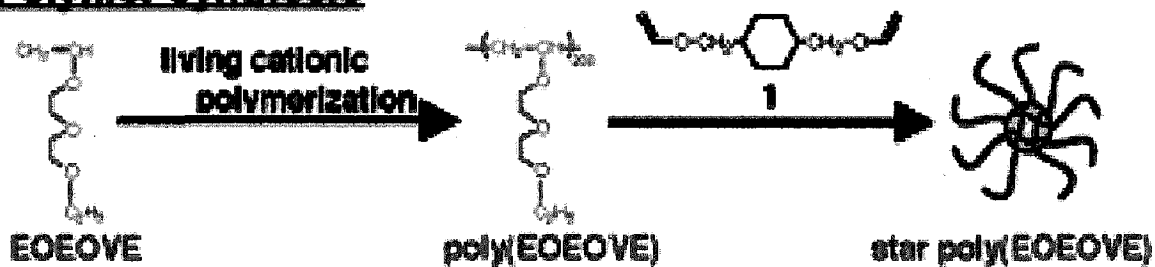


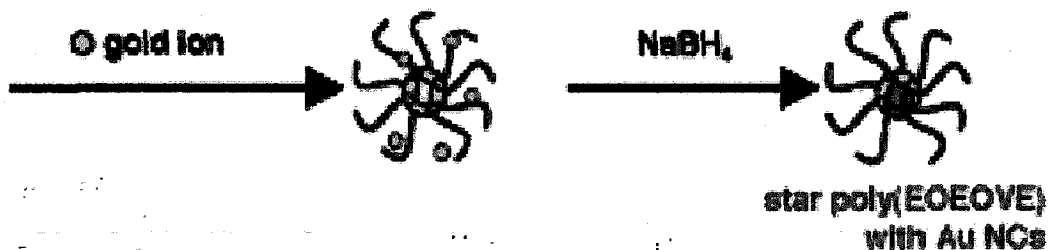
Figure 1.4.2: Proposed mechanism (from H. Tsunoyama, H. Sakrai, T. Tsukuda, *Chem. Phys. Lett.* 2006, 429, 528).

As described above, Au:PVP behaves as a *quasi*-homogeneous catalyst in aqueous condition by the coordination of hydrophilic polymer, PVP. Its stabilization ability is not high. Reuse of Au:PVP is not easy, and aggregation of the gold clusters is often observed.

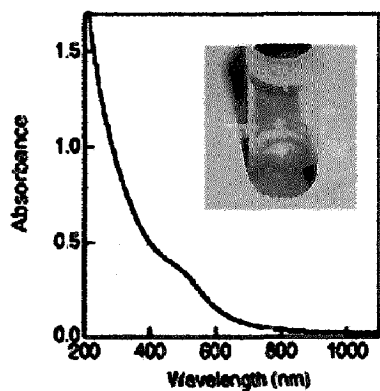
Polymer synthesis



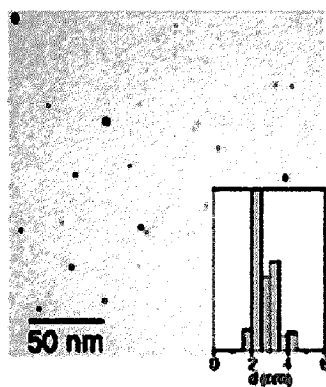
Preparation of Au NCs



UV-Vis



TEM



LCST behavior

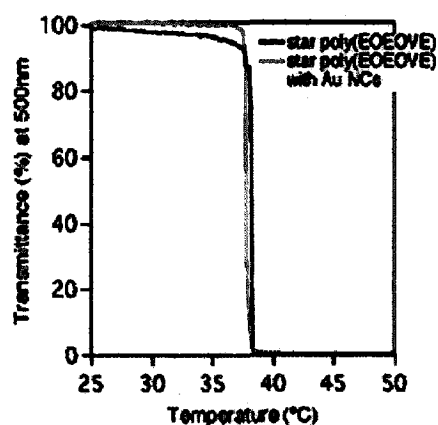
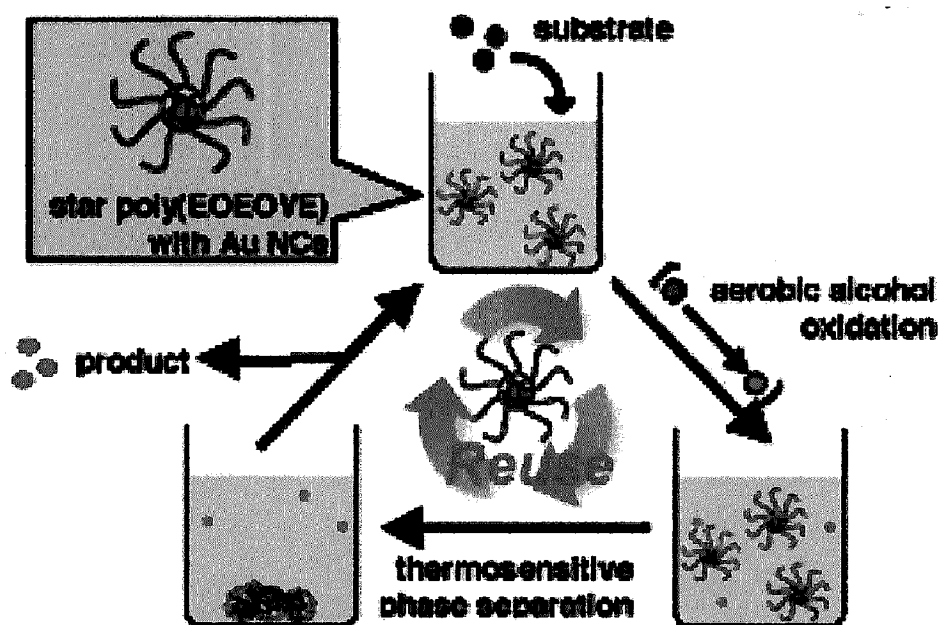


Figure 1.4.3: Preparation and characterization of Au@star-poly(EOEOVE)₂₀₀ (from S. Kanaoka, *et al*, *J. Am. Chem. Soc.* 2007, 129, 12060)

As a reusable system of Au nanocluster catalyst, thermoresponsible vinyl ether star polymer was used as a stabilization polymer (Figure 1.4.3) [53]. This star polymer was prepared by living cationic polymerization of 2-(2-ethoxy) ethoxyethyl vinyl ether (EOEOVE) as hydrophilic part and divinyl ether as hydrophobic part. Reduction of HAuCl_4 in the presence of star-polymer (EOEOVE) in water affords Au nanocluster@star-polymer (EOEOEVE).

Au nanocluster@star-polymer(EOEOVE) was found to have small size with narrow size distribution as shown in the UV-vis spectrum and the TEM image. The nanoclusters exhibit thermally induced lower critical solution temperature (LCST) type phase separation reversibility in aqueous solution at around 40°C due to the hydrophilic parts of EOEOEVE. The Au nanocluster@star-polymer(EOEOVE) showed excellent catalytic activity towards the aerobic oxidation of primary and secondary alcohols giving corresponding carboxylic acids and ketones in good yield at 27°C , respectively (Figure 1.4.4). The Au nanocluster@star-poly(EOEOVE) was recovered by heating the reaction mixture up to 60°C (higher than the clouding point of star-poly(EOEOVE)) followed by decantation of the aqueous phase. The catalytic activity was maintained at least until the sixth use. No aggregation of the clusters were observed throughout the reaction, indicating that this polymer possesses superior stabilizing ability compared to PVP. In the Au nanocluster@star-poly(EOEOVE), the design of functionality of polymer and combination are important for a good catalyst.



The Au:PVP did not promote cross coupling reaction including oxidative addition of organohalide.

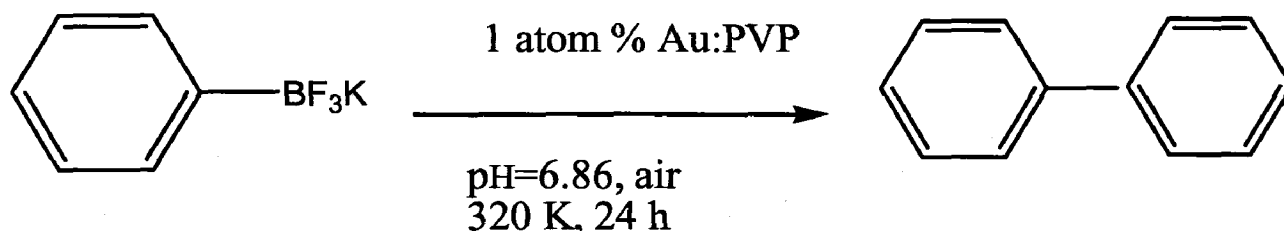


Figure 1.4.6: Homocoupling reaction of potassium phenyl trifluoroborate catalyzed by Au:PVP

1.4.3 Hydroxylation of organoboron compounds [54b]

As shown in Figure 1.4.7, phenol was formed via oxidation of the C-B bond of phenylboronic acid by hydrogen peroxide, arising from boron peroxide and water [57e]. When HCO_2NH_4 was used to generate the peroxide phenol was obtained in high yield.

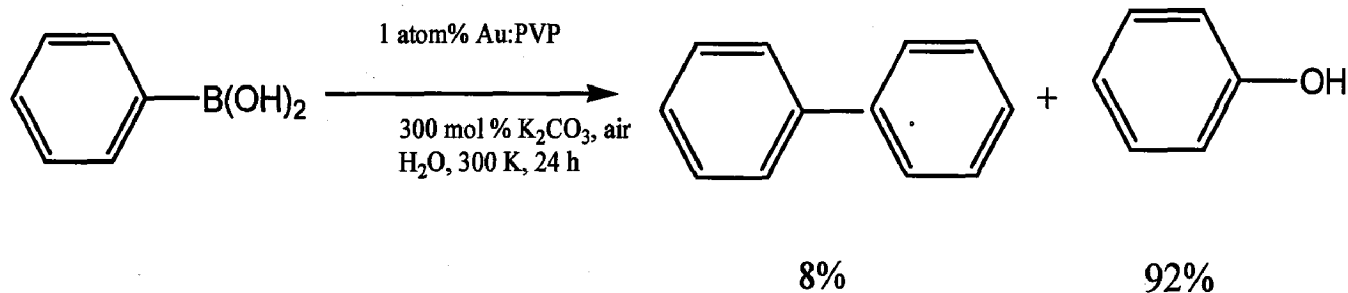
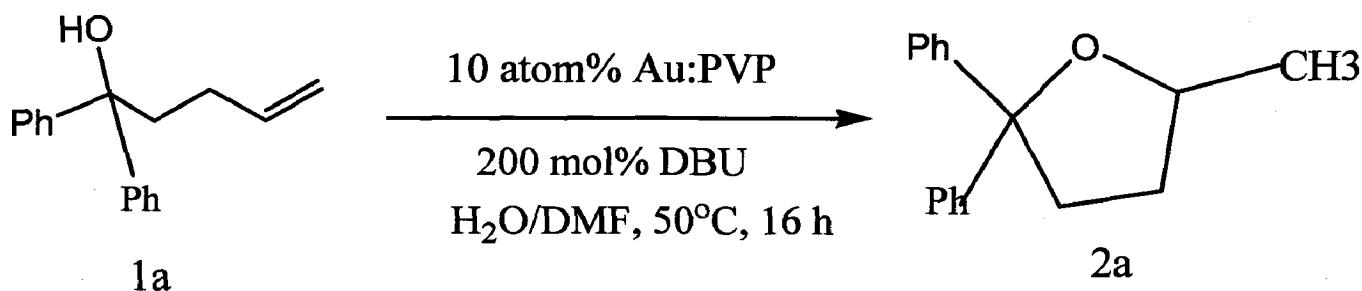


Figure 1.4.7: Hydroxylation of phenylboronic acid catalyzed by Au:PVP

1.5 Au:PVP as a Formal Lewis Acid Catalyst [55]

Superoxo-like species act as a key active species for the oxidation reaction [56]. It should have cationic site on the gold nanocluster, which behaves as a formal Lewis acid catalyst.

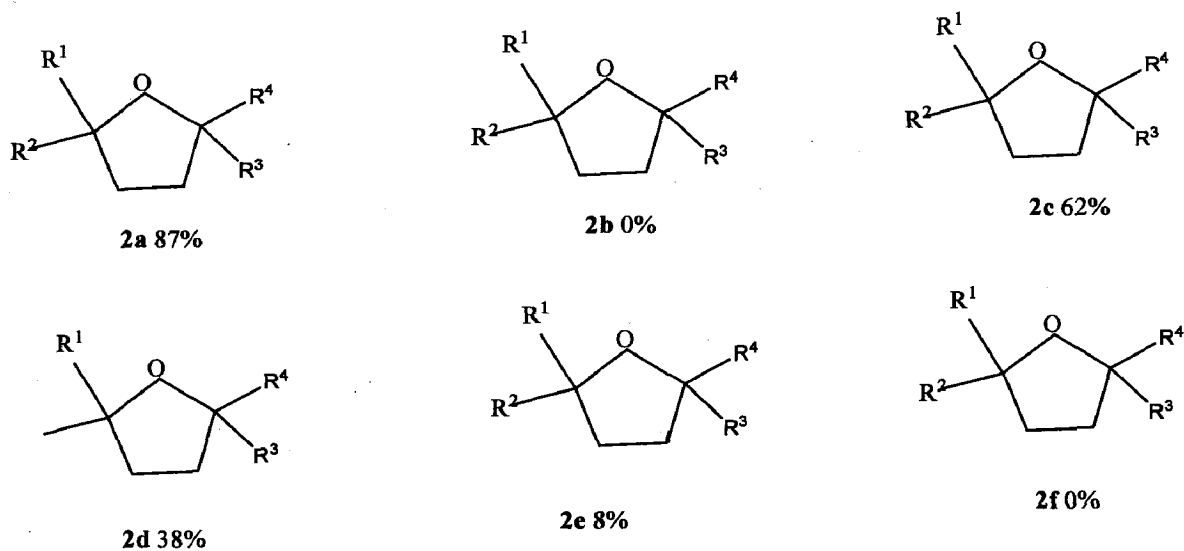
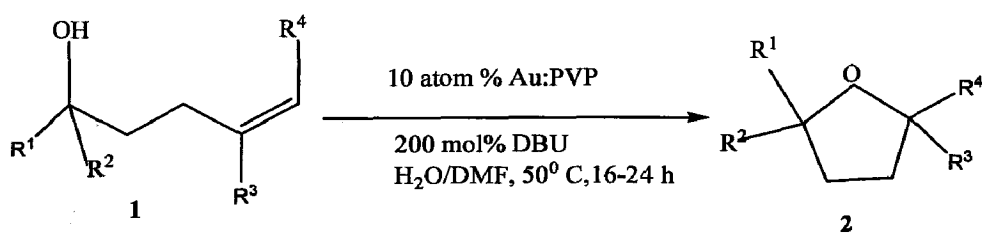
To demonstrate Au:PVP as a formal Lewis acid catalyst, the following reaction has been carried out. When alkenylalcohol **1a** was treated with 10 atom% Au:PVP in the presence of 1,8-Diazabicyclo[5.4.0] undec-7-ene (DBU) as a base in H₂O/DMF mixed solvent at 50°C under aerobic conditions, tetrahydrofuran derivative **2a** was obtained in 87% yield (Figure 1.5.1). The hydroalkoxylation did not occur under Au:PVP (1.3 nm)/Ar conditions and under Au:PVP (9.5 nm)/ aerobic conditions indicating that molecular oxygen is essential and ionic species of gold is not the active species for this reaction.



d_{av} of Au:PVP = $1.3 \pm 0.3 \text{ nm}$	under air	87%
$1.3 \pm 0.3 \text{ nm}$	under Ar	0%
$9.5 \pm 1.0 \text{ nm}$	under air	0%

Figure 1.5.1: The role of molecular oxygen in the oxidation of alcohol

The substrate dependence at α -position of the alcohol was observed in this reaction (Scheme 1.5.1). The reaction proceeds smoothly, giving diphenyl-substrate **2a**, but phenyl-methyl-substrate **2b** was not obtained. Methyl- α -naphthyl substrate **2c** affords the product in 62% yield. Introduction of methyl group substituent at internal/terminal of olefin decreased yield of the products **2d-2f** due to steric hindrance of the methyl groups.



Scheme 1.5.1: Intramolecular hydroalkoxylation catalyzed by Au:PVP along with the yield
 (from H. Sakurai *et al*, *Pure Appl. Chem.*, 2010, 82, 2005-2016)

1.6 Objective of the Present Study

Research involving gold nanoparticle catalysts stabilized by hydrophilic polymers has attracted a great deal of attention and gained numerous achievements in the past ten years. However, the catalytic activity, selectivity and reusability of the catalyst still need to be improved for many systems for commercial applications. The present study focuses on Au:PVP that acts as quasi-homogeneous catalyst, which is stable under aerobic conditions. It is anticipated that Au:PVP can be an alternative catalyst for many catalytic reactions which are sensitive under aerobic conditions. The objectives of this thesis are: (i) to exploit a new preparation method to get small (< 2nm) Au nanoclusters which are stabilized by PVP(K-90), a polymer with $M_w = 360$ kDa and (ii) to study the effect of viscosity on the aerobic oxidation reaction by comparing the results obtained with those of Au:PVP(K-30).

2.1 Materials Used

All the chemicals were commercially available and used without purification for the synthesis of Au nanoclusters. The chemicals that were used are listed in Table 2.1.1. All the glassware were rinsed with aqua regia, sodium bicarbonate followed by sonication and lastly with demonized water before use. Deionized water with a resistivity of $> 18 \text{ M}\Omega \cdot \text{cm}$ was used in this study.

Table 2.1.1 Chemicals used in the present study

S.No.	Chemical	Company
1	PVP	Tokyo Kasei Kogyo
2	Star poly(2-methoxyethoxyvinyl ether)	Aldrich
3	NaBH_4	Wako
4	HAuCl_4	Tanaka Kikinzoku
5	Benzyl alcohol	Wako
6	p-methoxy bezyl alcohol	Wako
7	p-nitro benzyl alcohol	Wako
8	Hexadecane(C_{16})	Aldrich
9	K_2CO_3	Wako

2.2 Experimental Procedure

Au:PVP can be synthesized using chemical reduction of metal salts [1]. It is one of the most frequently used method to prepare Au:PVP. NaBH_4 is commonly used as the reducing agent [2]. The gold metal salt and the reducing agents are dissolved in the same solvent (water). Two typical processes are used for the preparation of Au:PVP. One is the batch method and other one is microreactor based method. They are described below.

2.2.1 Batch Method

In this process, the gold solution containing PVP and the reducing agent were mixed rapidly in a flask, as shown in Figure 2.1.1, at 0°C . The mixture was stirred for 1 hour. The obtained Au:PVP nanoclusters were subsequently dialyzed overnight to remove inorganic impurities such as Na^+ and Cl^- which is crucial to enhance the stability of Au:PVP nanoclusters against coalescence. The progress of the reaction is shown in Figure 2.2.2. These NCs can be used as catalyst for many aerobic oxidation reactions.

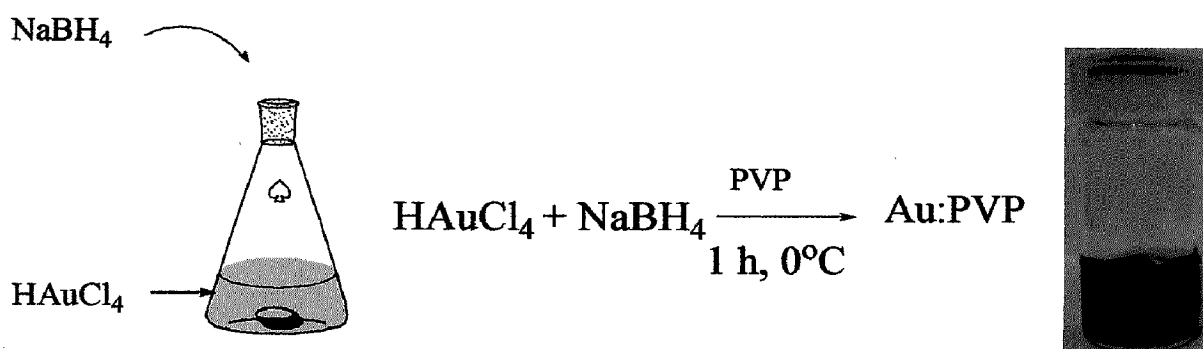


Figure 2.2.1: Preparation of Au:PVP by Batch Method

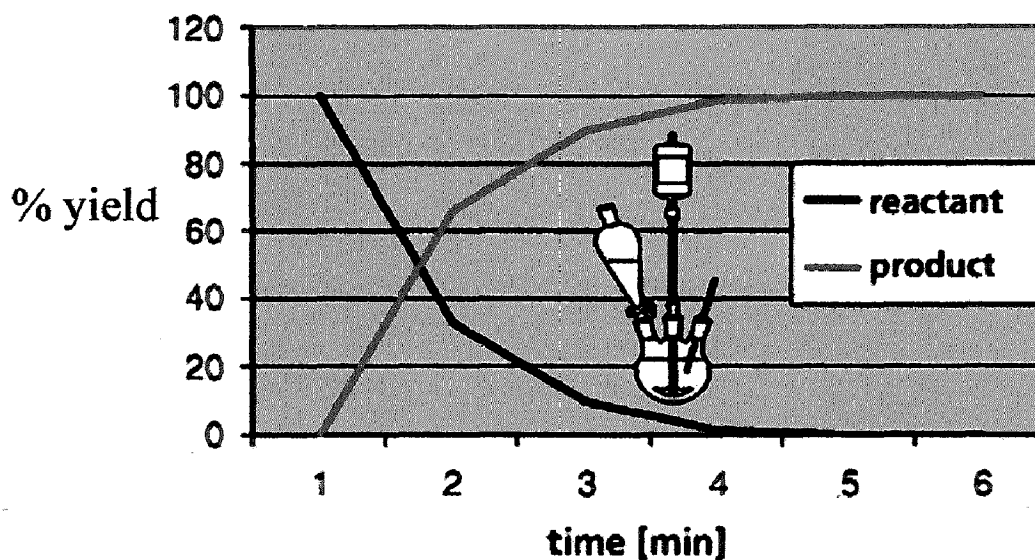


Figure 2.2.2: Reaction progress using catalyst synthesized in batch process (from ChemFiles vol. no. 9, page no. 4)

2.2.2 Microreactor Method

This method is less common and it is based on continuous flow using specialized equipment. In sharp contrast to the batch mode, the synthesis becomes a time resolved process in the flow method. Reagent streams are continuously pumped into a flow reactor where they are mixed and allowed to react. The product instantaneously leaves the reactor as a continuous stream. Therefore, only the flow rate and operation time determine the synthesis scale. A reactor with an inner diameter of less than a millimetre will produce kilogram quantities of the product when operated for a whole day at a fast flow rate, or small milligram batches if operated for a few minutes. The progress of an oxidation reaction catalyzed by thus obtained catalyst is shown in Figure 2.2.3.

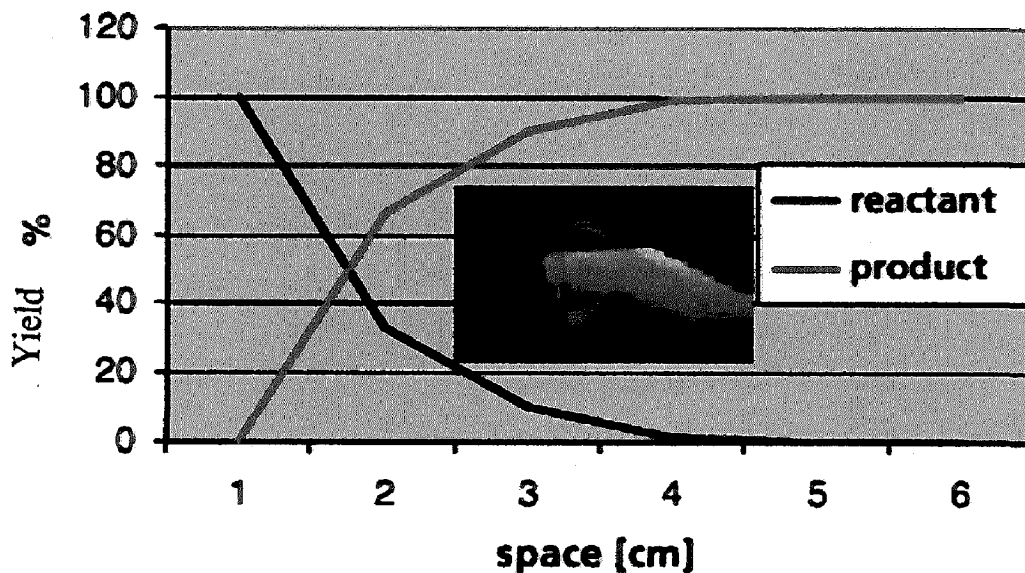


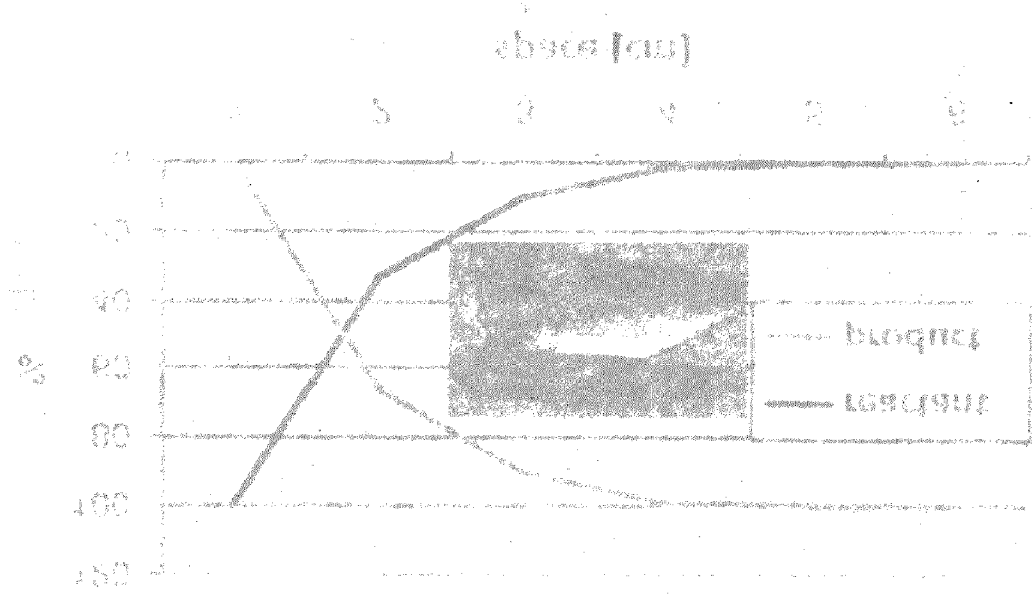
Figure 2.2.3: Reaction progress using catalyst synthesized in Microreactor (from ChemFiles vol. no. 9, page no. 4)

Figure 2.2.2 and Fig 2.2.3 looks similar but a closer look at the x-axis demonstrates the difference between a batch, time resolved chemical process, and a micro structured surface where the process is space resolved.

Rather than the size of the microreactor, other parameters define the performance of a microreactor. First of all, the reactor material needs to be selected. Microreactors are readily available as metal, glass or silicon made. Each material offers specific advantages and disadvantages regarding price, compatibility with reagents and heat conductivity. The preferred material is glass since it offers the highest compatibility with aggressive media and reagents.

Independently from the reactor materials, microreactors offer two major features that clearly make a difference vis-à-vis classical batch process. The neutralization of hydrochloric acid with sodium hydroxide (Scheme 2.2.1) can be taken as a model reaction to visualize the superior performance of microreactor compared to the batch process.

The text in this section is extremely faint and largely illegible. It appears to be a series of paragraphs or a list of items, but the specific content cannot be discerned.



1. Efficient heat transfer

Microreactors with their small surface to volume ratio are able to absorb the heat generated from a reaction much more efficiently than the batch process. Figure 2.2.4 shows the initial heat distribution for the model reaction (Scheme 2.2.1) in a simulated 5 m³ batch reactor stirred at 500 rpm [3].



Scheme 2.2.1: Exothermic model reaction

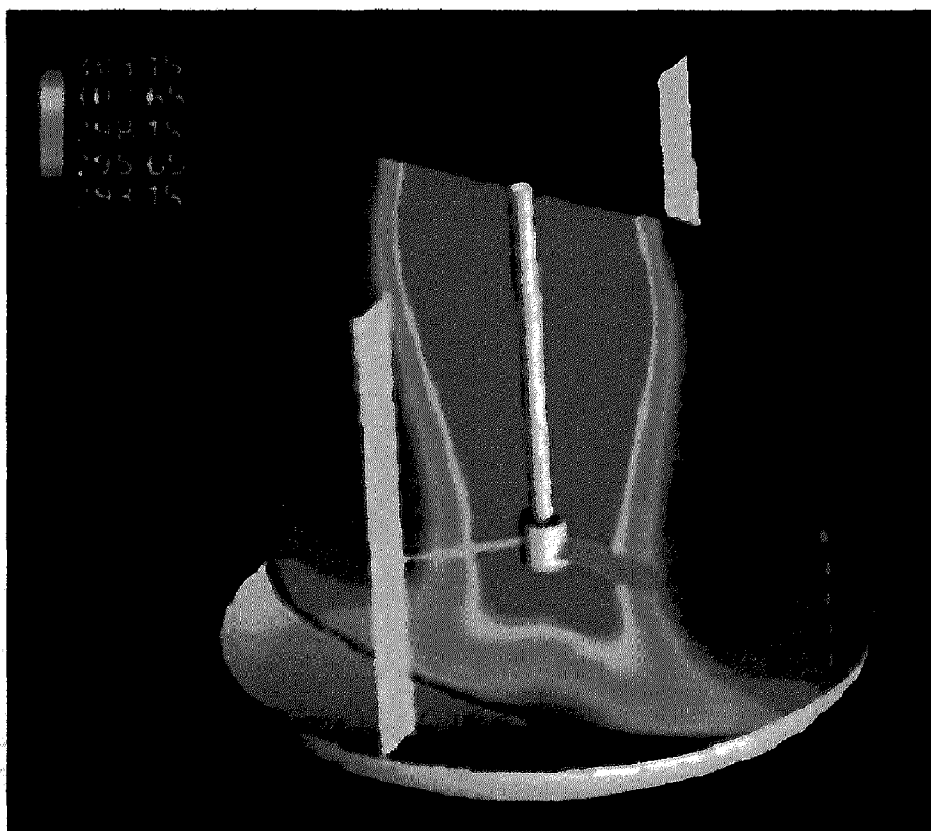
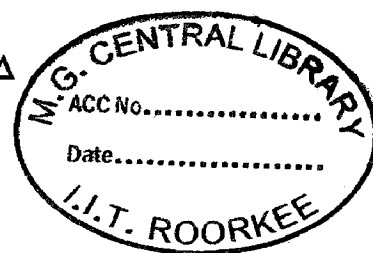


Figure 2.2.4: Heat distributions in a batch synthesis vessel and the temperature ranges from 293.15 K (blue) to 303.15 K (red) (from ChemFiles vol. no. 9, page no. 4)

The batch reactor is heated up by the exothermic reactions. Cooling only takes place at the surface of the vessel. As a result, there is a strong temperature gradient from the surface of vessel to the centre. In a microreactor, the heat created by mixing of two reagents is also detectable but the temperature gradient is a lot smaller (Figure 2.2.5). Additionally, it takes only a millimetre of path length for the reagent stream to cool down to the temperature of the outside cooling medium. The formation of hot spots or the accumulation of heat inside a reaction container may favor undesirable side reactions or fragmentation. Microreactors with their superior heat exchange efficiency present a perfect solution.

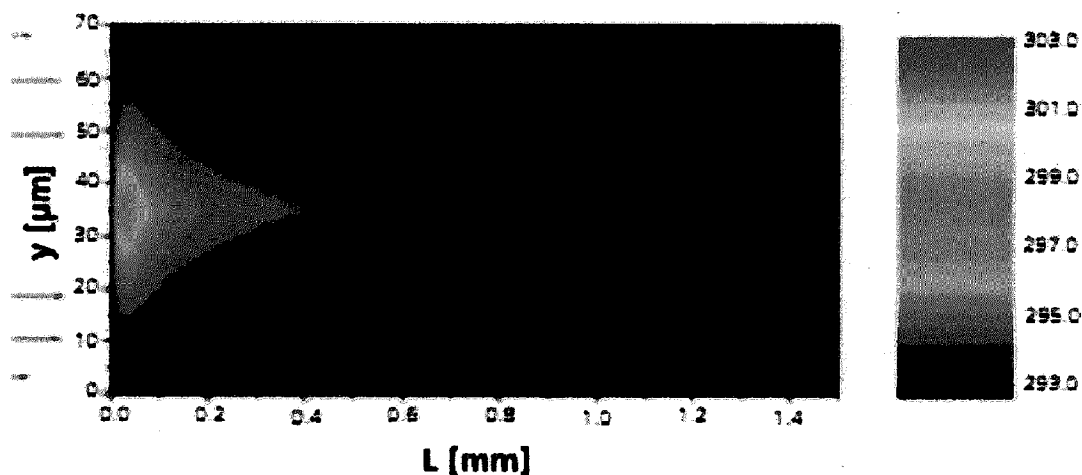


Figure 2.2.5: Heat distribution in a micro reactor. Temperatures are given according to the scale (above right) in Kelvin (y is the cell thickness and L the channel length) (from ChemFiles vol. no. 9, page no. 4)

Precise temperature control offers suppression of undesired by products (Figure 2.2.6). This becomes even more evident when looking at the scaling up of a production. The surface to volume ratio is a function of reactor size and bigger reactors have small surface to volume ratio.

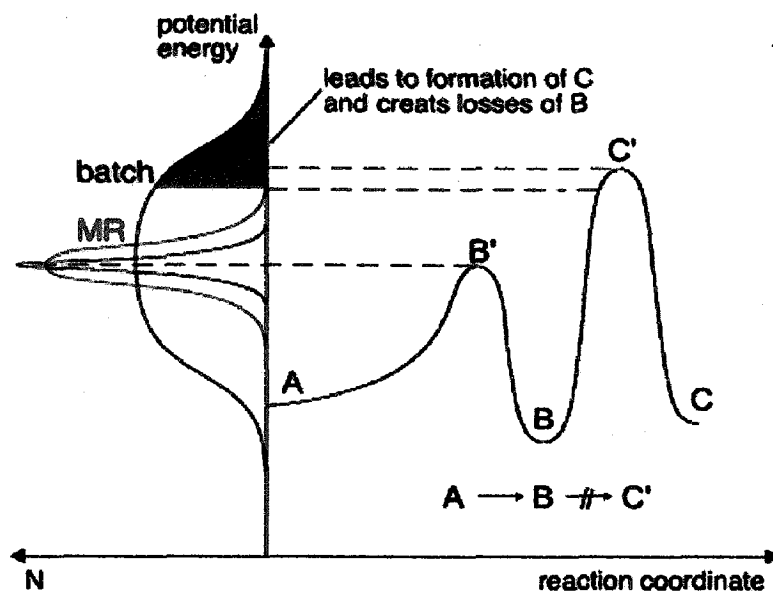


Figure 2.2.6: Precise temperature control in a microreactor enhances the product quality by suppression of side reactions (from ChemFiles vol. no. 9, page no. 4)

2. Efficient Mixing

In addition to the above mentioned heat transfer, mass transport is also considerably improved in microreactors. Mixing in microreactors can occur through diffusion between laminar flow layers. This can be visualized in Figure 2.2.7 for the same reaction. It can be compared with mixing in a batch reactor (Figure 2.2.8).

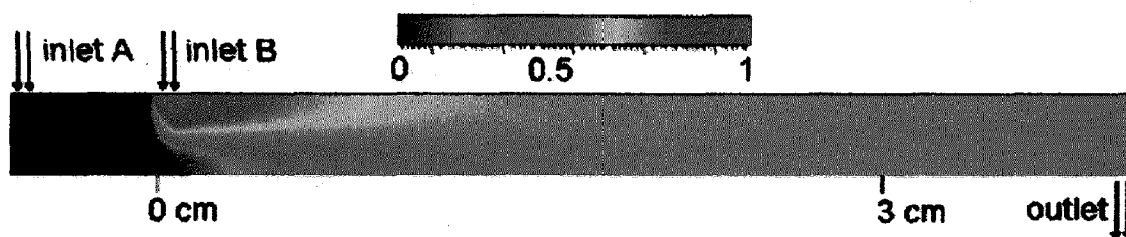


Figure 2.2.7: Mixing efficiency in a microreactor. Compound B is injected into a flow of compound A (blue). The green colour indicates the 1:1 mixing (from ChemFiles vol. no. 9, page no. 4)

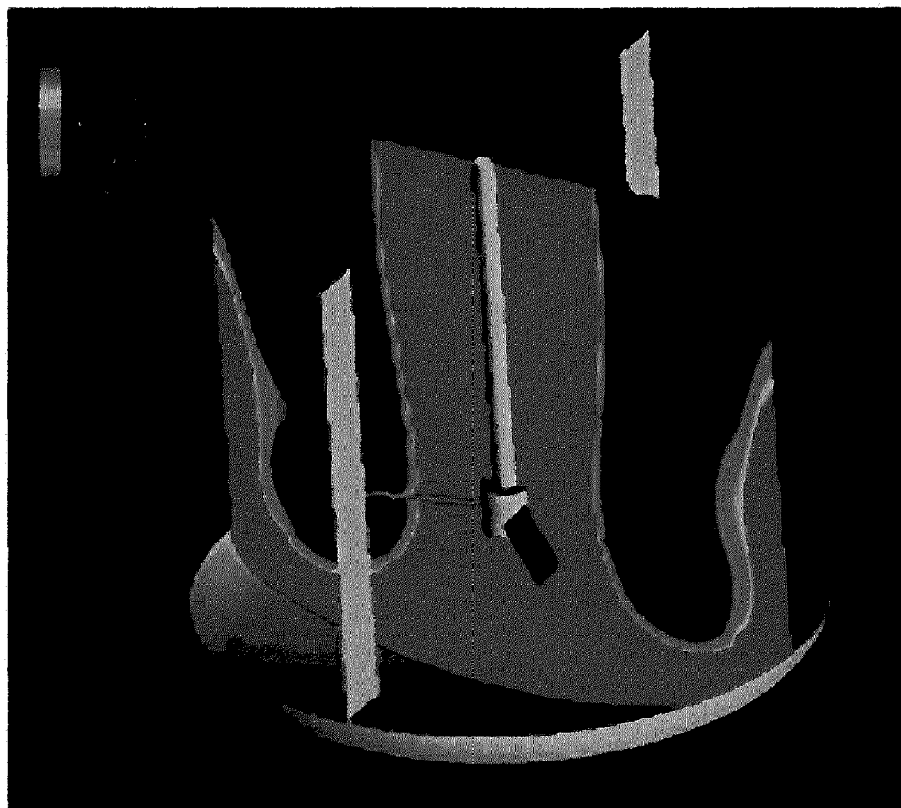


Figure 2.2.8: Mixing efficiency in a stirred batch reactor. Concentration equivalents (ranging from 0.8 (blue) to 1.2 (red) according to the colour scale top left) (from ChemFiles vol. no. 9, page no. 4)

3. Small Volume Reaction

Process parameters such as pressure, temperature, residence time, and flow rate in a microreactor are more easily controlled in a reaction that takes place in small volumes. The hazard potential of strongly exothermic reactions can also be drastically reduced [4, 5]. All of these advantages can be used most favorably in kinetic controlled reactions. Figure 2.2.9 shows the classical text book graph. This meets the most common thinking of organic chemists to discuss products distribution. In this figure, product C is favored if the activation energy provided to the reaction is limited.

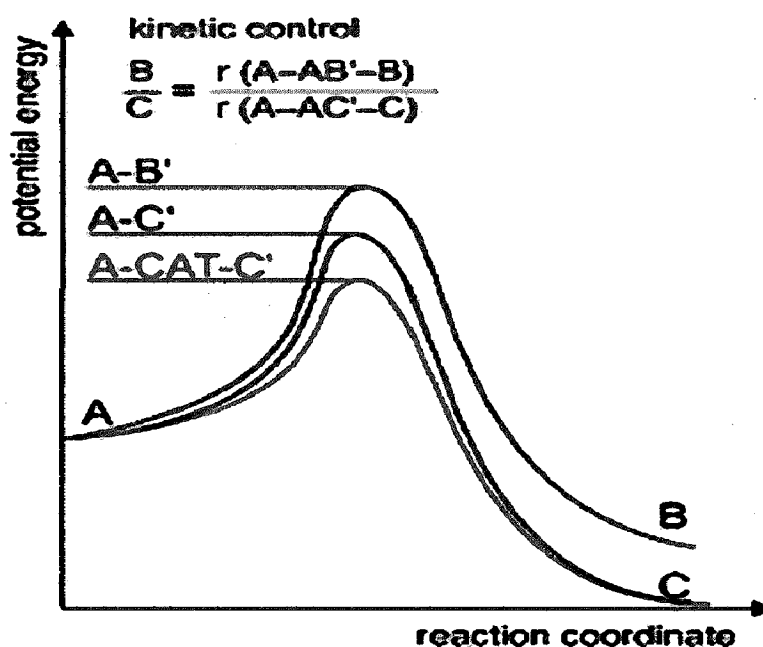


Figure 2.2.9: Chemical progress diagram (from ChemFiles vol. no. 9, page no. 4)

A narrow size distribution is essential for investigating small (< 2nm) metal clusters. Conventionally, polymer stabilized metal clusters are prepared by reducing corresponding metal ions in the presence of a polymer in macroscopic vessels [57]. Under such conditions, any variation in local conditions across the vessel influences the kinetics of cluster growth and result in polydispersity of nanoclusters. Especially, when a strong reducing reagent such as NaBH₄ is used to prepare small clusters, inhomogeneous mixing of the reactant is the main cause of polydispersity. Thus, a straight forward approach to suppress size distribution of the clusters generated under such diffusion controlled condition is to mix the metal ions and reductants homogeneously on the molecular mixing using miniaturized reaction chambers [58]. In this regard, microfluidic synthesis of organic stabilized metal nanoparticles has been attracting growing interest.

Gold nanoclusters protected by three different poly(*N*-vinyl-2-pyrrolidone) (PVP) named K-15 (average molecular weight, $M_w = 10$ kDa), K-30 (average molecular weight, $M_w = 40$ kDa), and K-90 (average molecular weight, $M_w = 360$ kDa) have already been prepared using batch process and successful results have been obtained using PVP(K-15) and PVP(K-30) giving mono-dispersed clusters with 1.3 nm mean size [59].

However, there are some problems regarding size and monodispersity in the case of the usage of PVP(K-90) due to its high molecular weight and high viscosity. In the present study, flow reaction conditions were applied to conquer this viscosity problem [60, 61]. Two different types of microreactors (Figure 2.2.10), Techno-applications COMET X-01 and Sigma-Aldrich type S02 were chosen.

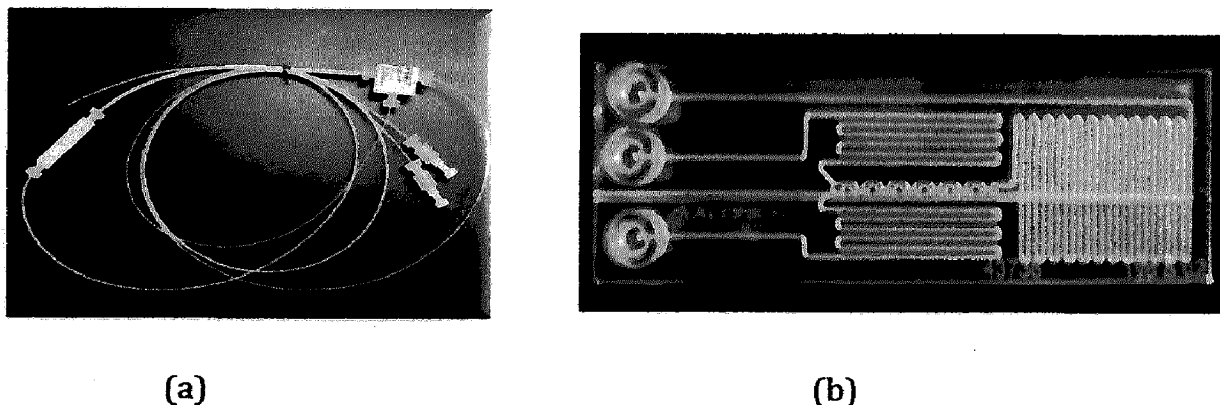


Figure 2.2.10: a) Techno-applications COMET X-01 microreactor, b) Sigma-Aldrich type S02 microreactor

The synthesis of Au:PVP in a micro reactor is shown in Figure 2.2.11

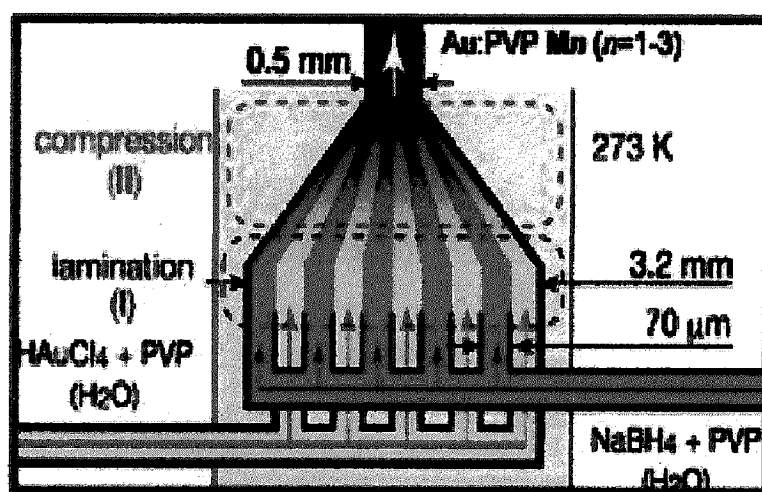


Figure 2.2.11: Mixing of HAuCl_4 and NaBH_4 in microreactor (from H. Tsunoyama, *et al.* *Langmuir*, 2008, 24, 11327-11330)

2.3. Preparation of Au: PVP (K-90) by batch and microreactor methods

2.3.1 Batch method: In the present study, typical method for the preparation of Au:PVP nanoclusters by the batch process is as follows. To an aqueous solution of HAuCl_4 (1mmol, 50 ml) 555 mg (5mmol) of PVP was added so that the molar ratio of AuCl_4^- and PVP was kept as 1:100. The mixture was further stirred for 30 mins in a bath kept at 0°C . Then, an aqueous solution of NaBH_4 (100 mmol, 5ml) was rapidly added into the mixture under vigorous stirring. The colour of mixture turned from pale yellow to dark brown indicating the formation of Au:PVP nanoclusters (Figure 2.2.12).

The Au:PVP nanoclusters were subsequently filtered with vivaspin tube (30,000 M.wt. cut off) at 0°C , centrifuged (4800 rpm) and washed with milliQ water three times to remove inorganic impurities such as Na^+ and Cl^- , which is crucial to enhance the stability of Au:PVP NPs against aggregation. The obtained hydrosol of Au:PVP NPs was diluted to 100 ml and stored at 4°C or stored after freeze drying. The Au:PVP nanoclusters thus prepared were characterized by UV-vis absorption spectroscopy and transmission electron spectroscopy (TEM).

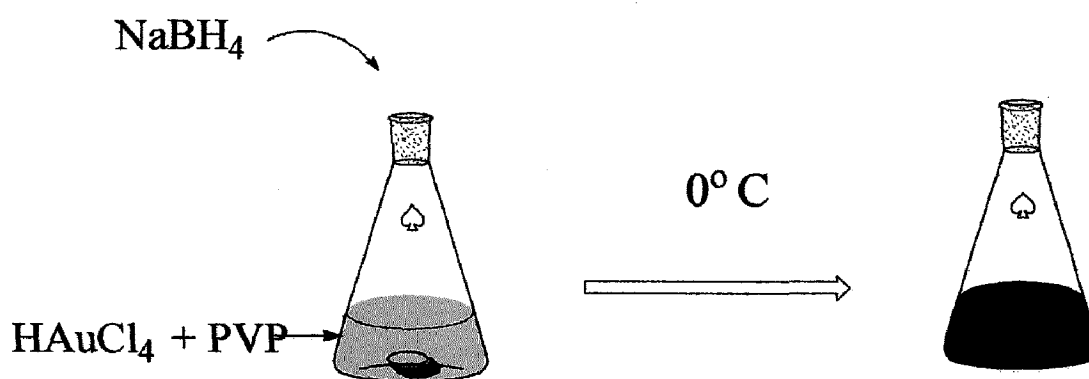


Figure 2.2.12: Preparation of Au:PVP by the batch method

2.3.2 Microreactor method

Au:PVP nanoclusters were prepared, in the present study, by using two microreactors, Techno-applications COMET X-01 and Sigma-Aldrich type S02. Aqueous solutions of HAuCl_4 (0.05 mmol) and PVP (5 mmol) were mixed at room temperature for 15 min and then cooled at 0°C for 30 mins (solution A). During cooling, the micro reactor was set up on an ice bath and NaBH_4 (0.5 M) was cooled to 0°C (Solution B). These solutions were sucked by syringe (size = 50 mL, 28.90 mm. id for solution A and size = 25 mL, 22.5 mm.id for solution B) with the addition of air (3 ml) and pushed through the microreactor using two syringe pumps. In the mixing process, firstly, solution B was pushed through the microreactor using flow rate 55.8 ml/h for 0.9 ml and then solution A was pushed using a flow rate 300 mL/h (Figure 2.2.13). The mixed solution eluted from the outlet was collected in an Erlenmeyer flask placed on an ice bath and stirred for 30 mins before washing followed by centrifuge (4800 rpm) at 0°C .

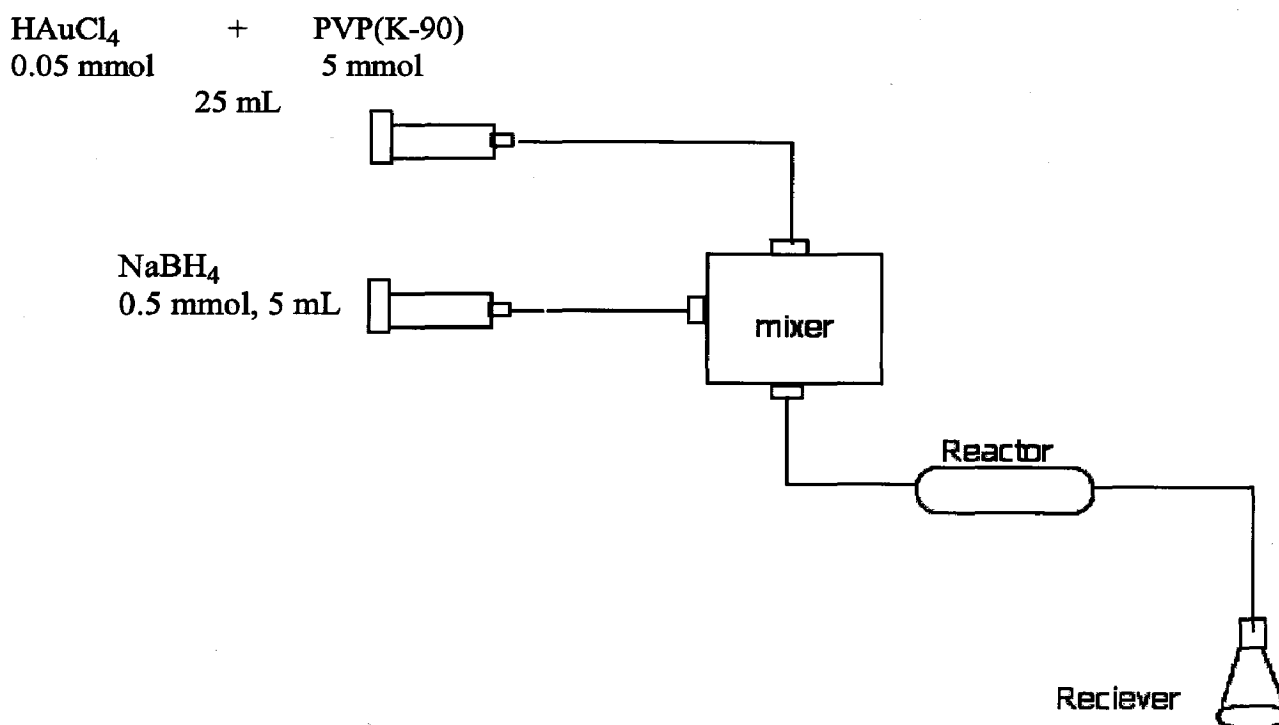


Figure 2.2.13: Preparation of Au:PVP nanoclusters using a microreactor

2.4 Preparation of Au:star poly (MOVE) Nanoclusters using a Microreactor

A star polymer [11,12] consisting of many hydrophilic arms and a hydrophobic core, prepared via polymer-linking reaction can be regarded as a unimolecular micelle. Recently, Aoshima et al. achieved a significant advance in star polymer synthesis, demonstrating quantitative formation of vinyl ether star polymers with low polydispersity (M_w/M_n) 1.1-1.2 [13].

In addition, it has been found that poly(vinyl ethers) with oxyethylene side chains exhibit lower critical solution temperature (LCST)-type phase-separation behavior in water. [13-15]. In the present study, star poly(MOVE) (Figure 2.2.14) was used.

Au:star poly(MOVE) nanoclusters were prepared using the microreactor Techno-applications COMET X-01. Aqueous solutions of HAuCl_4 (0.05 mmol) and star poly(MOVE) (5 mmol) were mixed at room temperature for 15 min and then cooled at 0°C for 30 mins (solution A). During cooling, the microreactor was set up on an ice bath and NaBH_4 (0.5 M) was cooled to 0°C (Solution B). These solutions were sucked by syringes (size= 50 mL, 28.90 mm. id for solution A and size = 25 mL, 22.5 mm.id for solution B) with the addition of air (3 ml) and pushed through the microreactor using two syringe pumps. In the mixing process, firstly, solution B was pushed through the microreactor using flow rate 55.8 ml/h for 0.9 ml and then solution A was pushed using a flow rate 300 ml/ h. The mixed solution eluted from the outlet was collected in an Erlenmeyer flask place on an ice bath and stirred for 30 mins before washing followed by centrifuge (4800 rpm at 0°C).

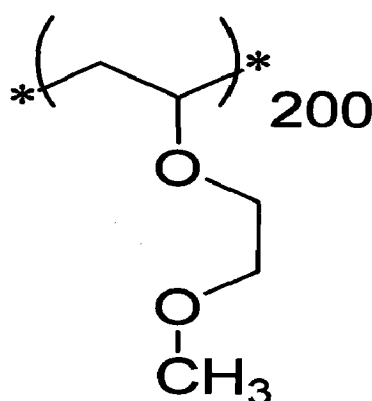
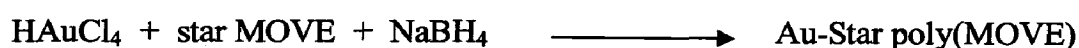


Figure 2.2.14: Structure of star poly(MOVE)

2.5 Characterization of the nanoclusters

Characterization of the nanostructures requires extreme sensitivity, accuracy and atomic level resolution. The Au nanoclusters protected by different polymers were characterized by an array of techniques. In the following section, these techniques are discussed briefly.

2.5.1 UV-Visible Spectroscopy

UV-Visible spectroscopy measurements were performed to study the surface plasmon resonance of Au nanoclusters. The instrument used was JASCO UV-Vis spectrophotometer model V-670. Au nanoclusters shows a surface plasmon resonance band at about 520 nm. Au nanoparticles with size below 2 nm show no surface plasmon resonance.

2.5.2 Transmission Electron Microscopy (TEM)

Transmission electron microscopy (TEM) is a technique whereby a beam of electrons is transmitted through an ultra thin specimen, interacting with the specimen as it passes through. An image is formed from the interaction of the electrons transmitted through the specimen; the image is magnified and focused onto an imaging device such as a fluorescent screen, a layer of photographic film, or to be detected by a sensor such as a CCD camera. TEM analysis was performed to get the average particle size. The instrument used was JEOL JEM-2010F and the operating voltage was 200 kV.

2.5.3 Scanning Electron Microscopy

A scanning electron microscope (SEM) is a type of electron microscope that images a sample by scanning it with a high energy beam of electrons in a raster scan pattern. The electrons interact with the atoms that make up the sample producing signals that contain information about the sample's surface topography, composition, and other properties such as electrical conductivity. The instrument used was JEOL FE-SEM:JSM-6700F.

2.5.4 Gas Chromatography

Gas chromatography (GC) is a common type of chromatography used in analytical chemistry for separating and analysing compounds that can be vaporized without decomposition. Typical uses of GC include testing the purity of a particular substance, or separating the different components of a mixture (the relative amounts of such components can also be determined after calibration). In some situations, GC may help in identifying a compound. The instrument used in the present study, was Shimadzu GC-2010 with the column RESTEK Rtx-5MS (Crossbond 5% diphenyl and 95% dimethyl polysiloxane, length: 30m and i.d: 0.25mm).

2.5.5 Centrifuge

A centrifuge separates a heterogeneous mixture of a solid and a liquid by spinning it. After a successful centrifugation, the solid precipitate settles to the bottom of the test tube and the solution, called the centrifugate, is clear. The centrifuge used was KUBOTA 7780II (Figure 2.5.5) and the rpm range was 0 to 4800. This centrifuge can be also operated at low temperatures (40 to -20°C)

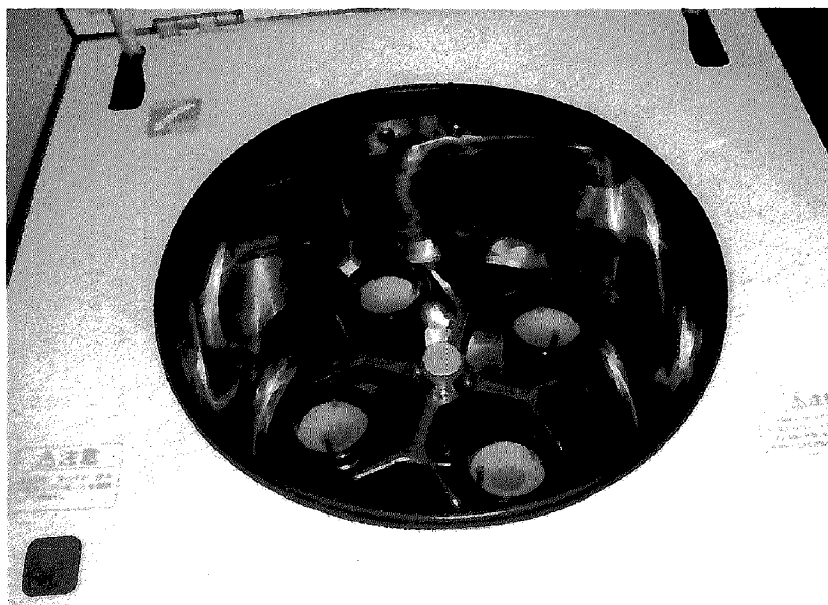


Figure 2.5.5: Centrifuge KUBOTA 7780II

2.5.6 Freeze Dryer

Freeze drying is a dehydration process typically used to preserve a perishable material or make the material more convenient for transport. Freeze drying works by freezing the material and then reducing the surrounding pressure to allow the frozen water in the material to sublime directly from the solid phase to the gas phase. The instrument used was EYELA FDU-2200 (Figure 2.5.6).



Figure 2.5.6: Freeze dryer

2.5.6 Electric Furnace

It was used to grow carbon nanotubes by chemical vapour deposition in which Au nanoclusters were used as the catalyst. In a typical CVD process, the wafer (Au supported catalyst) is exposed to one or more volatile precursors, which react and/or decompose on the substrate surface to produce the desired deposit. Frequently, volatile by-products are also produced which are removed by gas flow (Ar) through the reaction chamber. The instrument used was Koyo Thermo Systems Co. Ltd(model KTF035N1).

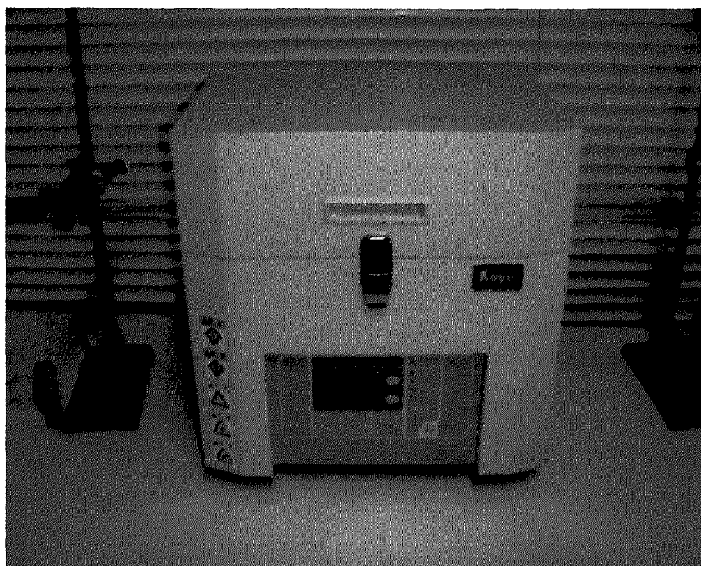


Figure 2.5.6: Electric furnace

2.5.8 Parallel Chemical Reactor

This instrument was used for aerobic oxidation reactions. More than one chemical reactions were performed parallelly. Temperature and stirring condition of the solution were maintained by this instrument. The instrument used was EYELA Chemistation series (Fig 2.5.3).



Figure 2.5.4: Parallel chemical reactor

3.1 UV-visible and TEM analysis

3.1.1 UV-visible spectra and TEM of Au:PVP(K-15)

A comparison was made among the nanoclusters prepared by the batch process, Techno-applications COMET X-01 microreactor and Sigma-Aldrich type S02 microreactor.

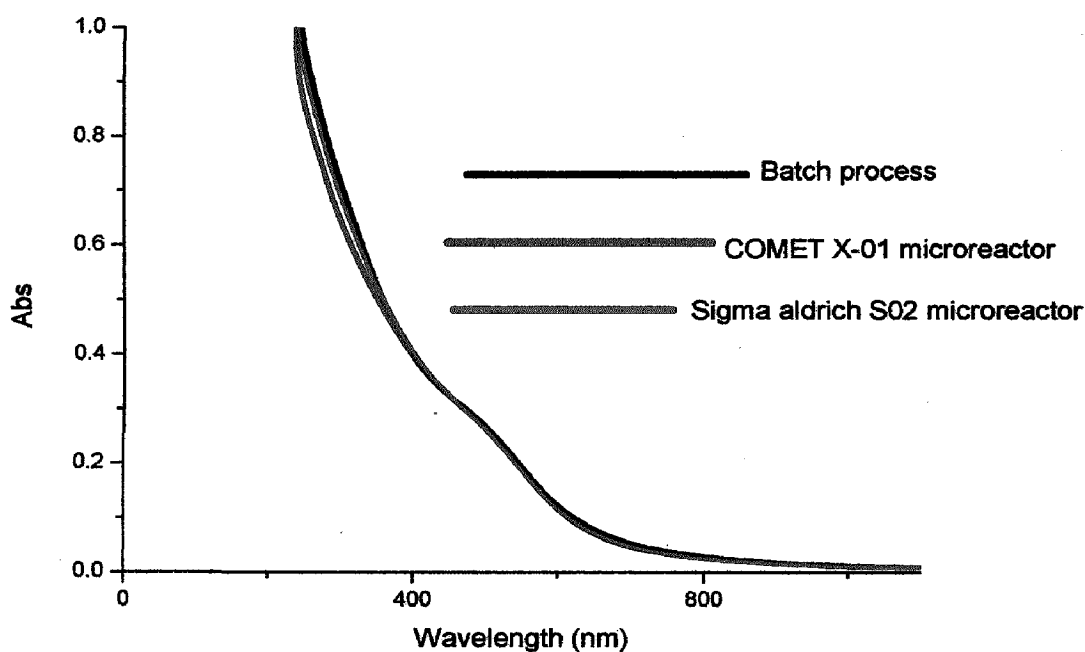
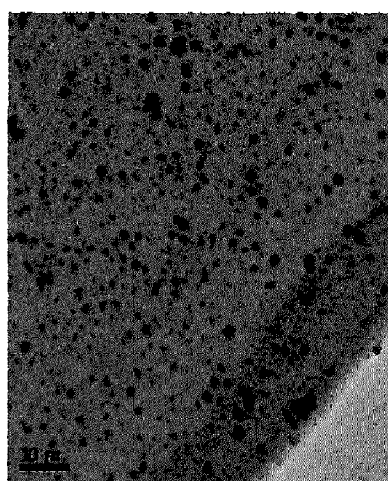
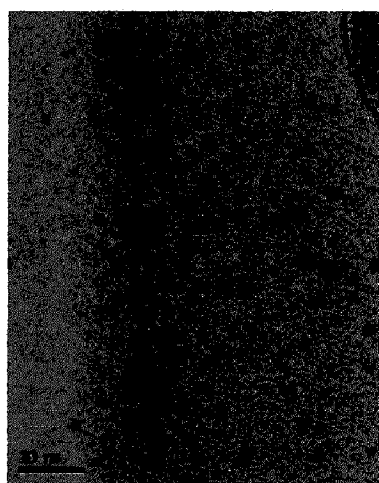
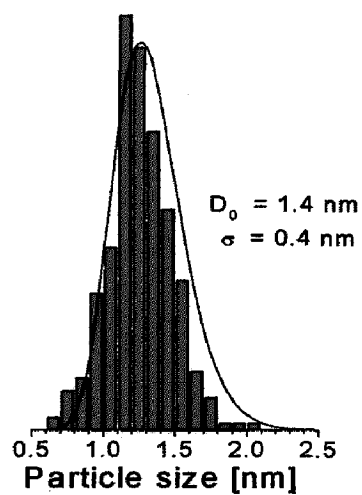


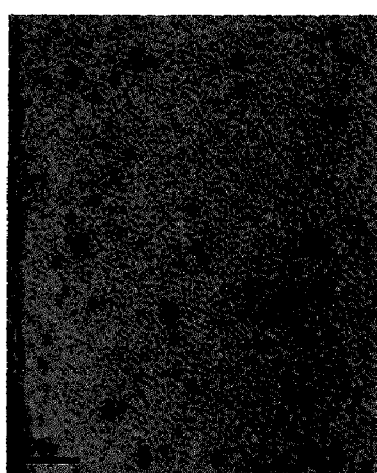
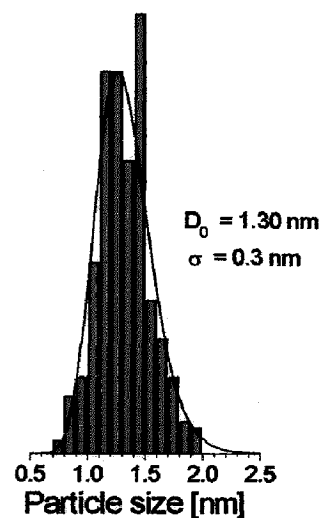
Figure 3.1.1: UV-visible spectra of Au:PVP(K-15) synthesized by different methods



(a)



(b)



(c)

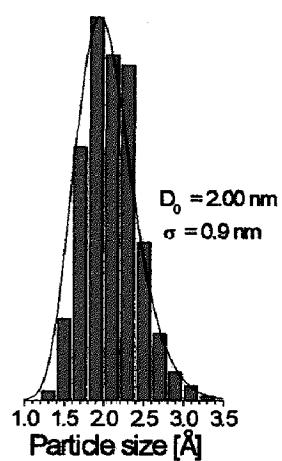


Figure 3.1.2: TEM images and particle size distributions of Au:PVP(K-15) prepared using a) batch process, b) COMET X-02 microreactor and c) Aldrich microreactor

3.1.2 UV-visible spectra and TEM of Au:PVP(K-30)

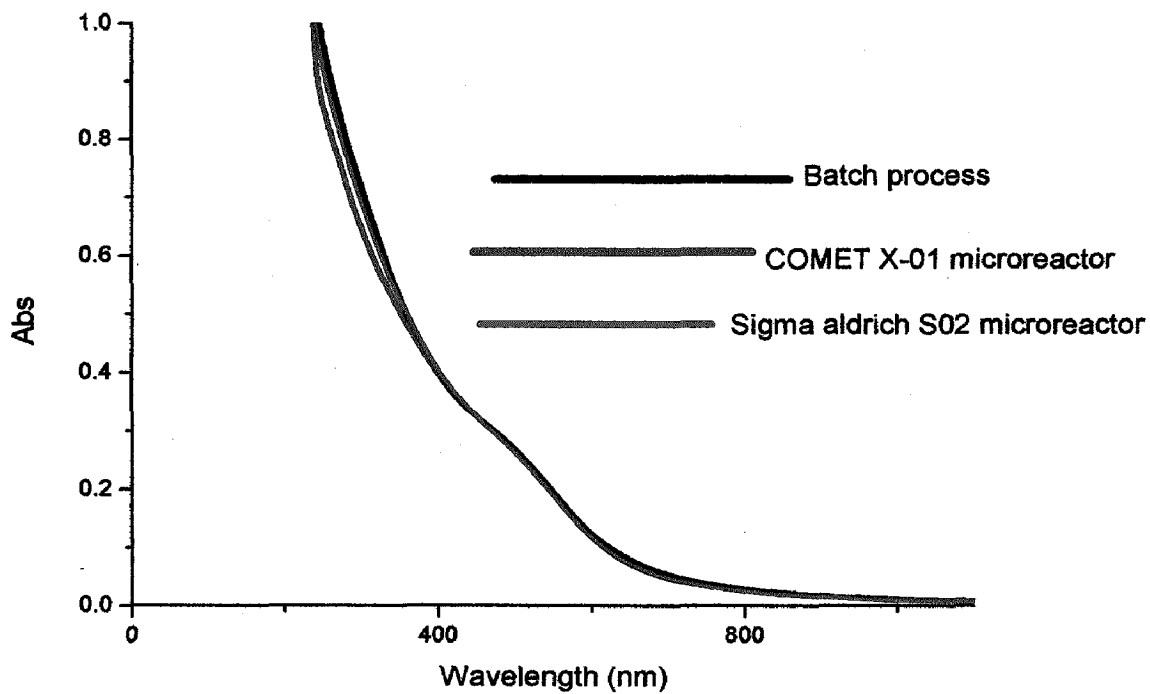
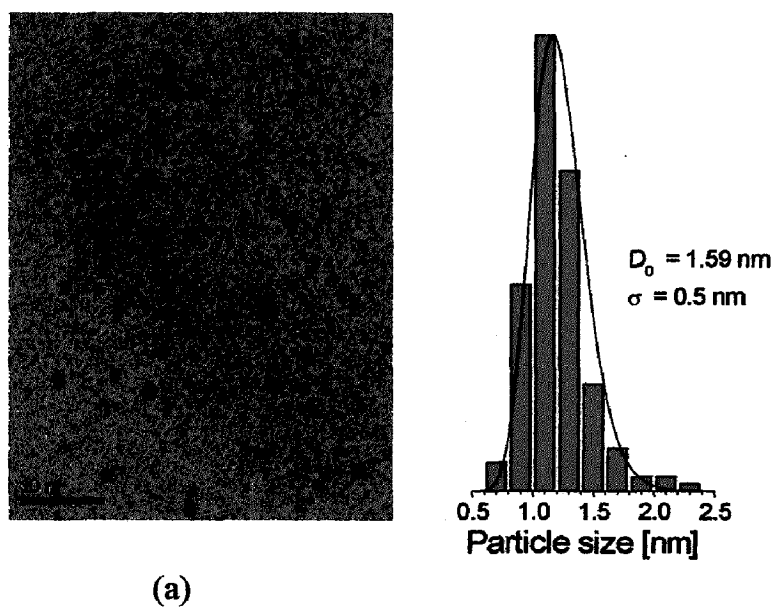
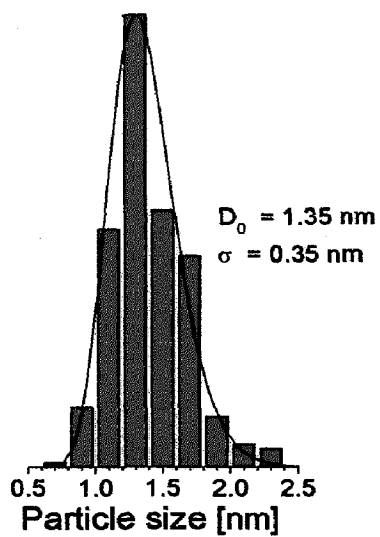
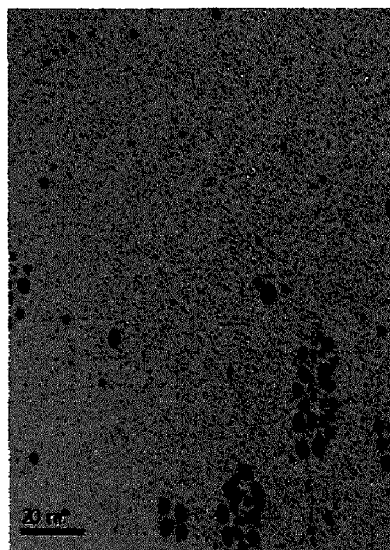
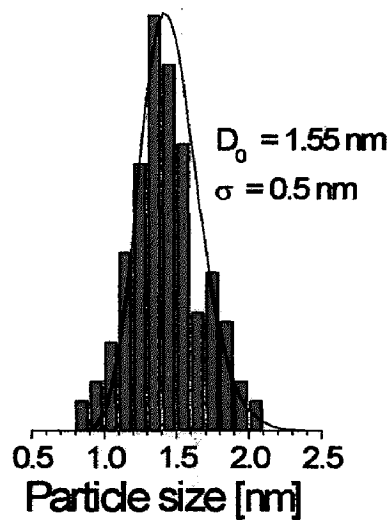
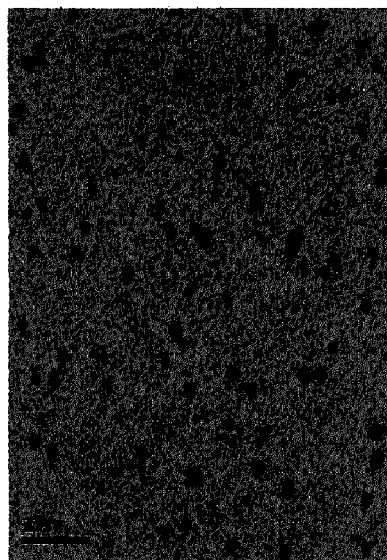


Figure 3.1.3: UV-visible spectra of Au:PVP(K-30) synthesized by different methods





(b)



(c)

Figure 3.1.4: TEM images and particle size distributions of Au:PVP (K-30) prepared using a) batch process, b) COMET X-02 microreactor and c) Aldrich microreactor

3.1.3 UV-visible spectra and TEM of Au:PVP(K-90)

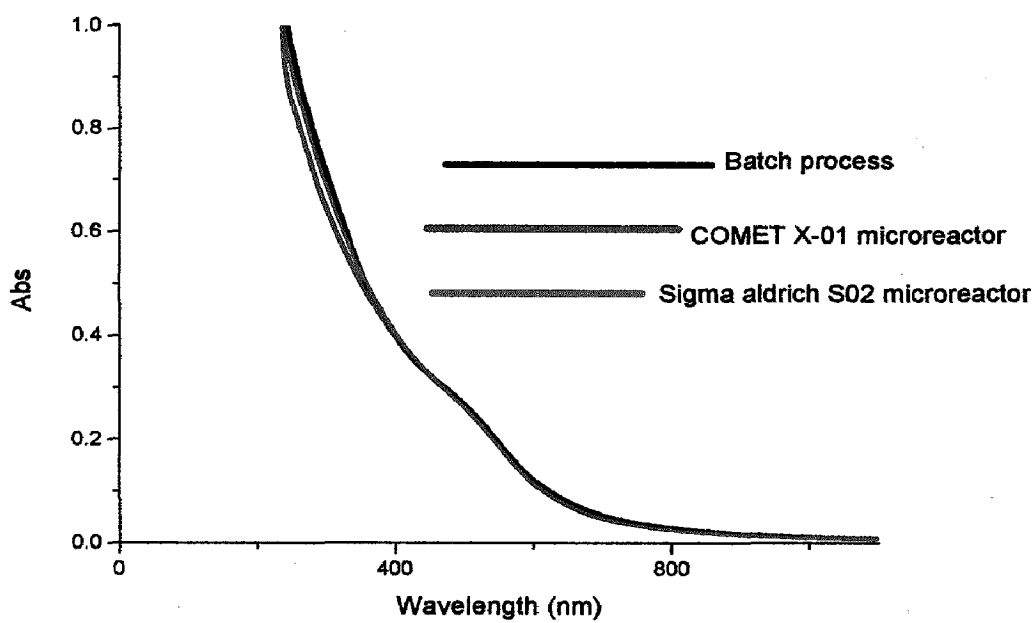
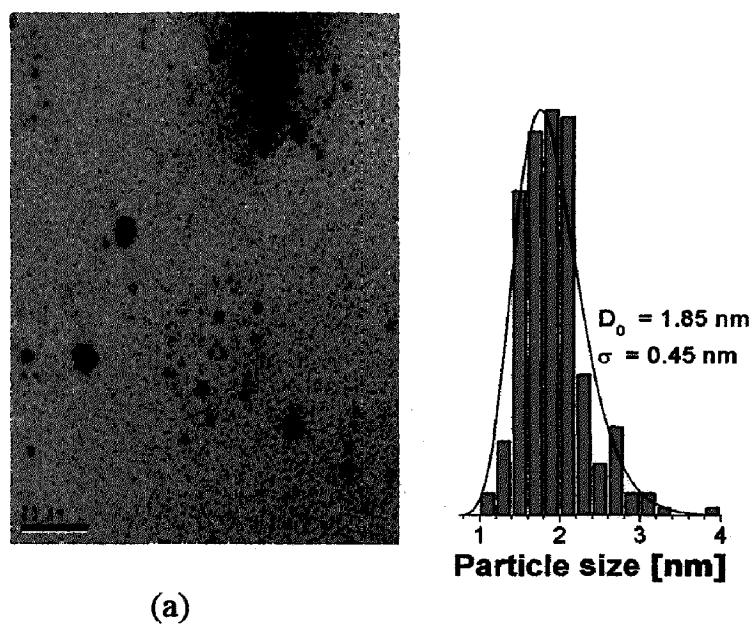
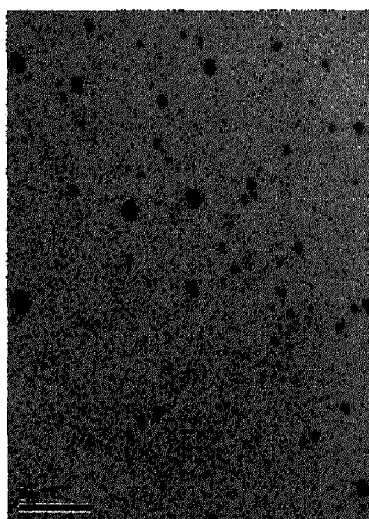


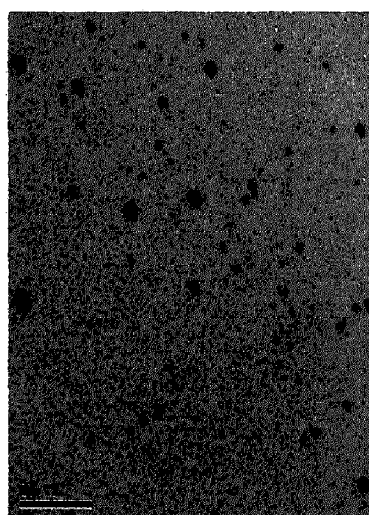
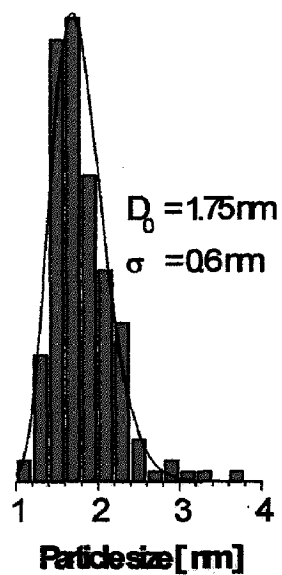
Figure 3.1.5: UV-visible spectra of Au:PVP (K-90) synthesized by different methods



(a)



(b)



(c)

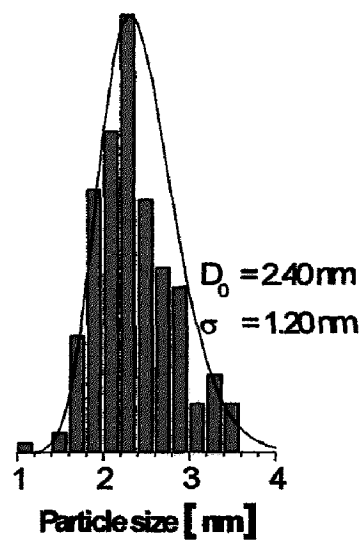


Figure 3.1.6: TEM images and particle size distributions of Au:PVP(K-90) prepared using a) batch process, b) COMET X-02 microreactor and c) Aldrich microreactor

The above figures show typical TEM images and particle size distribution of the Au nanoparticles stabilized by three different PVPs. The diameters of more than 500 particles were measured and plotted as the histograms in the figures. The average diameter of Au:PVP(K-15) nanoclusters synthesized using the batch process, COMET X-02 microreactor and Sigma Aldrich S02 microreactor were determined to be 1.4 ± 0.4 nm, 1.3 ± 0.3 nm, and 2.0 ± 0.9 nm, respectively. The average diameters of Au:PVP(K-30) synthesized by the batch process, COMET X-02 microreactor and Sigma Aldrich S02 microreactor were determined to be 1.6 ± 0.5 nm, 1.3 ± 0.35 nm, and 1.5 ± 0.5 nm, respectively. The average diameters of Au:PVP(K-90) synthesized by the batch process, COMET X-02 microreactor and Sigma Aldrich S02 microreactor were determined to be 1.8 ± 0.4 nm, 1.7 ± 0.6 nm, and 2.4 ± 1.2 nm, respectively. In the case of microreactors, the optimized conditions of COMET X-02 were used for the sigma Aldrich micro reactor just to make the comparison between these two microreactors.

The Au:PVP nanoclusters, prepared in the present study by microreactors based synthesis, are significantly smaller and monodispersed as compared with the literature [61]. Since the size of the nanoclusters is generally determined by relative rates between nucleation and particle growth, the formation of the small Au NPs can be ascribed to suppression of the growth of the Au nuclei under the present preparative conditions. The strong reducing agent NaBH_4 instantaneously produces a large number of Au nuclei [61], whose growth into larger particles is retarded by the low temperature of the medium. It is noticeable that among all the gold nanoclusters prepared, the average particle size of Au:PVP (K-15) and Au:PVP (K-30) are significantly smaller than that of Au:PVP (K-90), although the relative concentration of AuCl_4^- versus PVP monomer units was kept constant for all the samples. This result indicates that the Au NPs are stabilized more efficiently by PVP (K-15) and PVP(K-30) compared to PVP(K-90). The reason for the larger size of Au:PVP(K-90) nanoclusters may due to insufficient mixing. Sigma Aldrich microreactor was expected to have better mixing lines compared to COMET X-02. So further optimization of Sigma Aldrich microreactor for Au:PVP (K-90) synthesis was performed by changing the parameters such as concentration of PVP, NaBH_4 , HAuCl_4 and the flow rate of solutions (NaBH_4 and HAuCl_4).

3.2 Optimization conditions for Au:PVP(K-90) synthesis using Sigma-Aldrich type S02 microreactor

Au:PVP nanoclusters were prepared using Sigma-Aldrich Type S02 microreactor. The effect of change in concentrations of NaBH₄, HAuCl₄ and PVP and flow rate were investigated. All the conditions that were applied for the optimization are listed below in Table 3.1.1. A brown solution was obtained after mixing and no surface plasmon band was observed at $\lambda = 520$ nm by UV-vis spectroscopy indicating very small size of the Au nanoclusters were generated. From the result, it can be concluded that Au:PVP can be prepared in very small size compared to the batch method and Techno-applications COMET X-01 microreactor.

Table 3.1.1: Different conditions used during the optimization of Sigma Aldrich microreactor for the synthesis of Au:PVP (K-90)

Entry	HAuCl ₄ (mmol)	NaBH ₄ (mmol)	PVP (mmol)	Flow rate of HAuCl ₄ (ml/h)	Flow rate of NaBH ₄ (ml/h)	Particle diameter(nm)
I	0.01	0.5	1	300	55.8	1.5±0.8
II	0.01	0.5	1	300	230	1.6±1.0
III	0.005	1.5	0.51	55.8	300	1.8±1.1
IV	0.005	1.5	0.05	55.8	300	Precipitation
V	0.0025	1.5	0.734	55.8	300	1.2±0.5
VI	0.05	5	0.5	400	55.8	2.3±1.2
VII	0.05	5	0.5	200	55.8	1.1±0.4
VIII	0.05	5	0.5	500	55.8	1.2±0.6
IX	0.05	5	0.5	300	80	1.5±1.0

The UV-vis spectra, TEM images and the size histograms for all the conditions are given below.

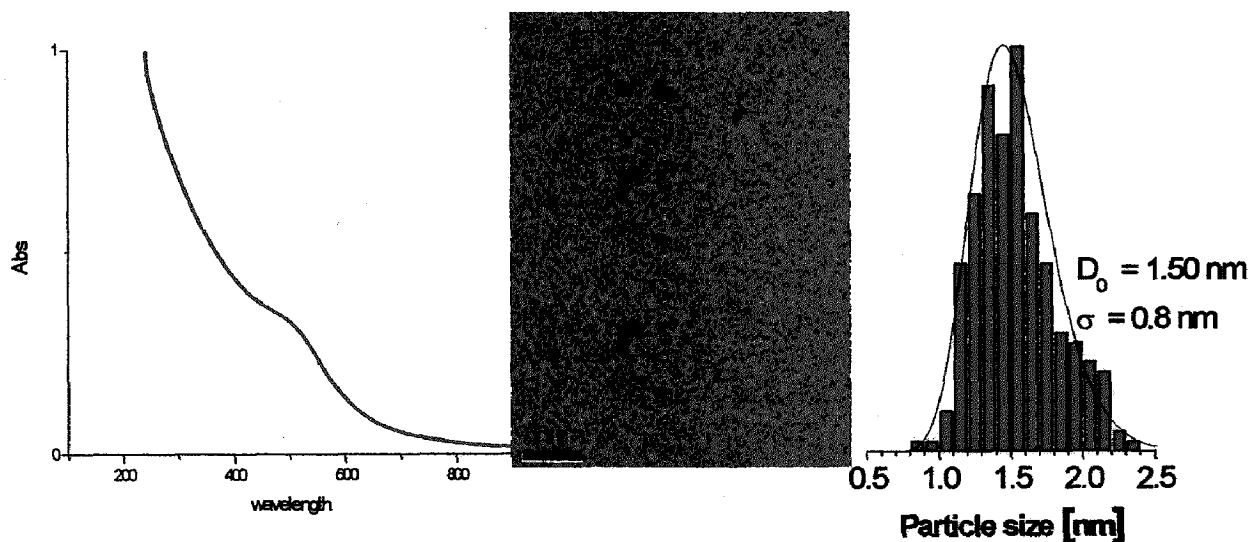


Figure 3.2.1: TEM image, UV-vis spectrum and size distribution of gold nanoclusters stabilized by PVP(K-90) at conditions I using Sigma-Aldrich microreactor

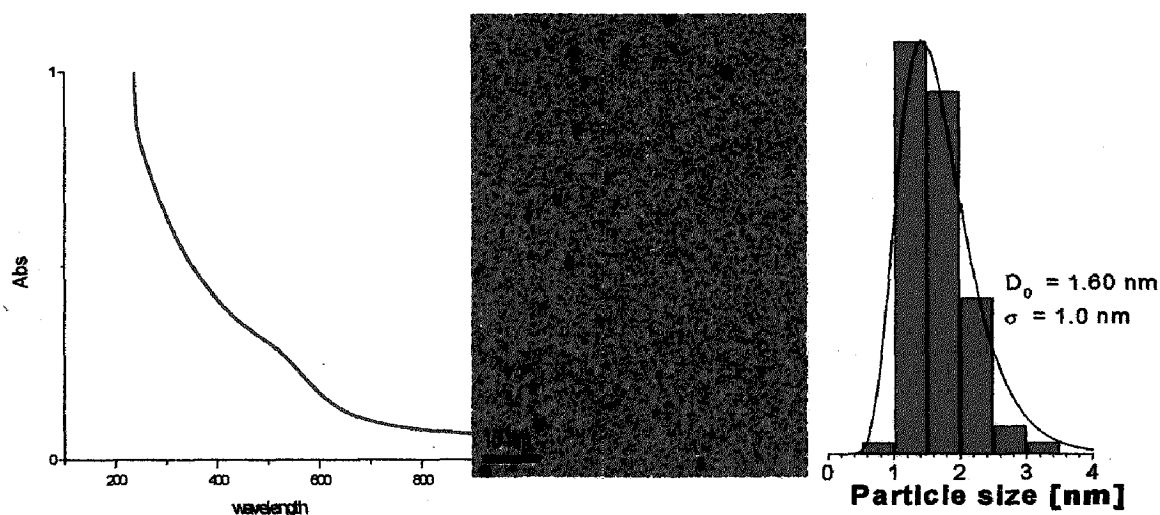


Figure 3.2.2: TEM image, UV-vis spectrum and size distribution of gold nanoclusters stabilized by PVP(K-90) at conditions II using Sigma-Aldrich microreactor

In conditions I and II, the mols of HAuCl_4 , NaBH_4 , PVP and flow rate of HAuCl_4 were kept constant. Only the flow rate of NaBH_4 was changed. The average particle size for condition I and II were 1.5 ± 0.8 and 1.6 ± 1.0 nm, respectively (Figure 3.2.1 and 3.2.2).

So it can be concluded that increase in flow rate of NaBH_4 solution around 300 ml/h is not a favourable condition for getting the Au nanoclusters with smaller size.

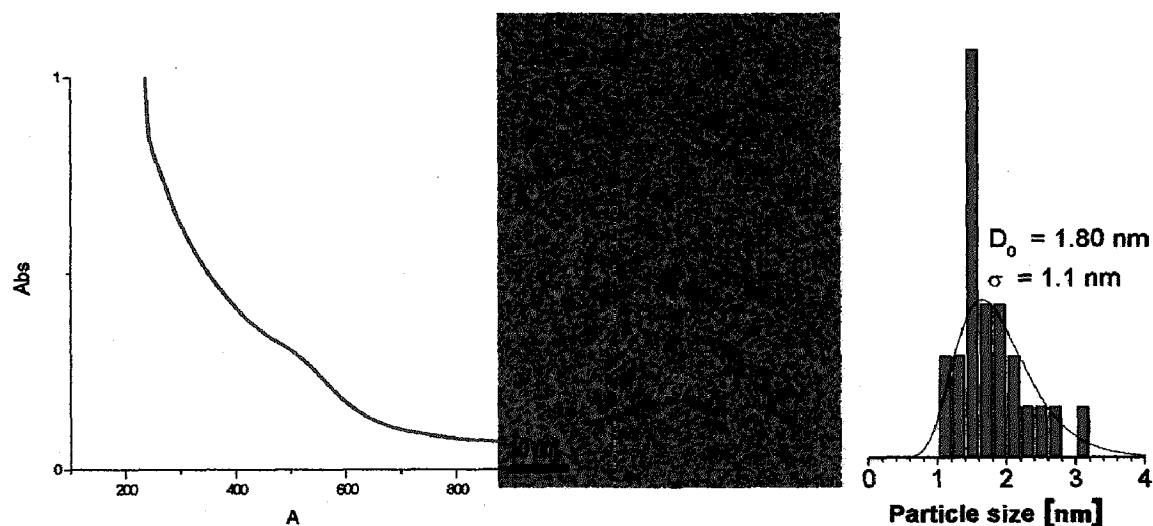


Figure 3.2.3: TEM image, UV-vis spectrum and size distribution of gold nanoclusters stabilized by PVP(K-90) at conditions III using Sigma-Aldrich microreactor

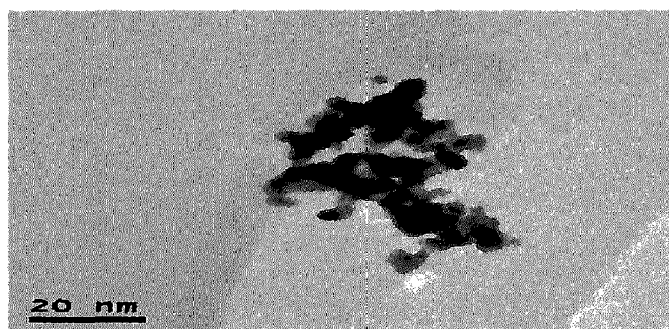


Figure 3.2.4: TEM image of gold nanoclusters stabilized by PVP(K-90) at conditions IV using Sigma-Aldrich microreactor

In conditions III and IV, mols of HAuCl_4 , NaBH_4 and flow rate of HAuCl_4 and NaBH_4 were kept constant. Only the mole of PVP was reduced. Precipitation occurred in condition IV. By this result it was concluded that decreasing the concentration of PVP is not favourable condition to synthesize smaller Au particles.

This may be due to the fact that decreasing the amount of PVP leads to less protection and the Au nanoclusters get aggregated.

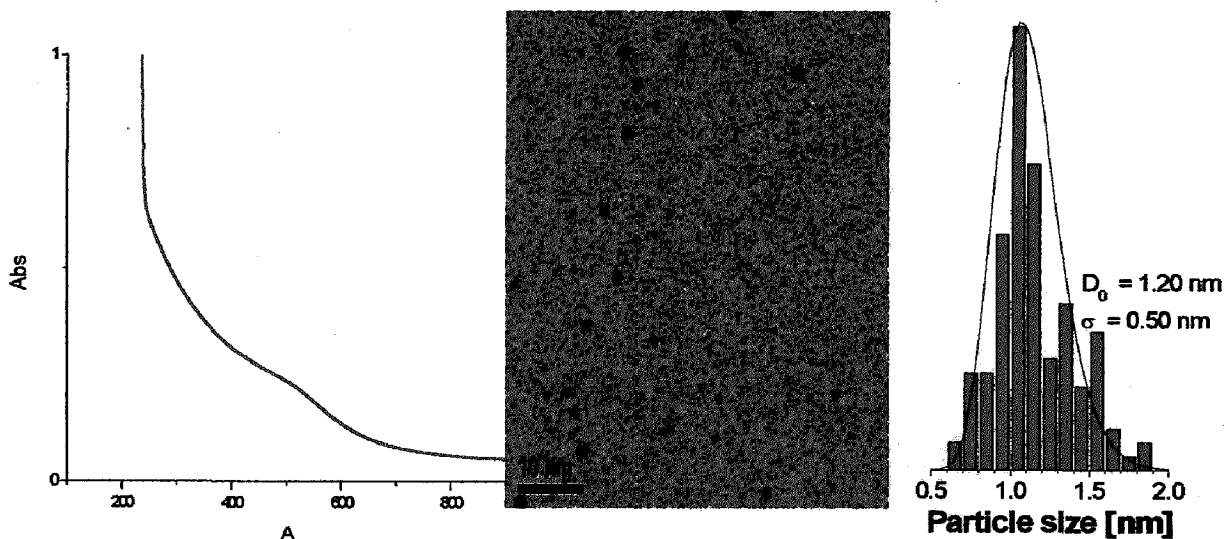


Fig 3.2.5: TEM image, UV-vis spectrum and size distribution of gold nanoclusters stabilized by PVP(K-90) at conditions V using Sigma-Aldrich microreactor

In the Vth condition, mols of HAuCl_4 and PVP were halved as compared to that in condition III. The average diameter of Au nanoclusters was $1.2 \pm 0.5 \text{ nm}$. So, dilution is a favorable condition to get smaller Au particles.

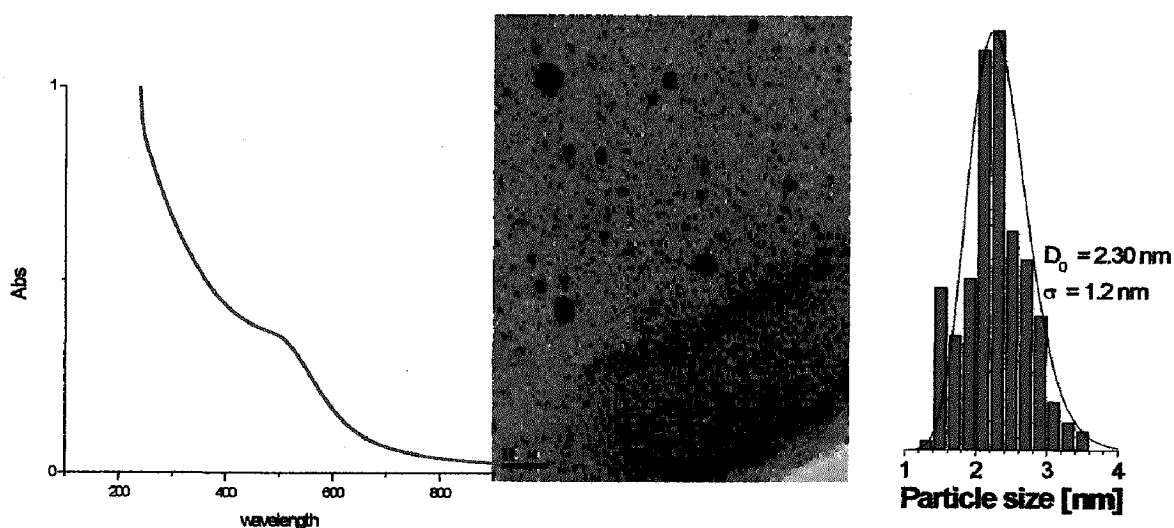


Figure 3.2.6: TEM image, UV-vis spectrum and size distribution of gold nanoclusters stabilized by PVP(K-90) at conditions VI using Sigma-Aldrich micro reactor

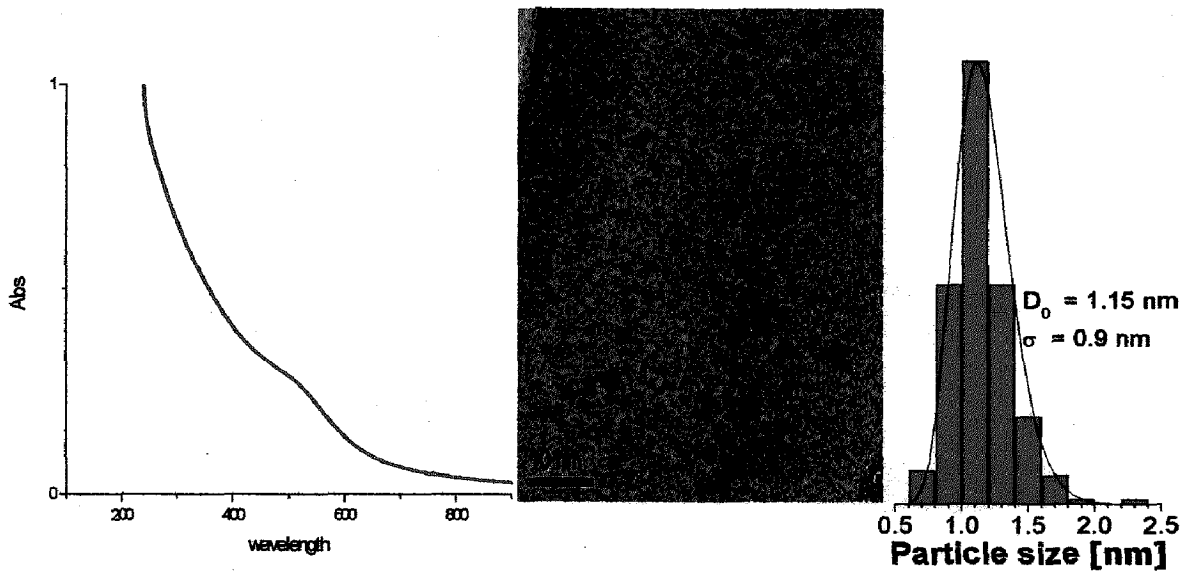


Figure 3.2.7: TEM image, UV-vis spectrum and size distribution of gold nanoclusters stabilized by PVP(K-90) at conditions VII using Sigma-Aldrich micro reactor

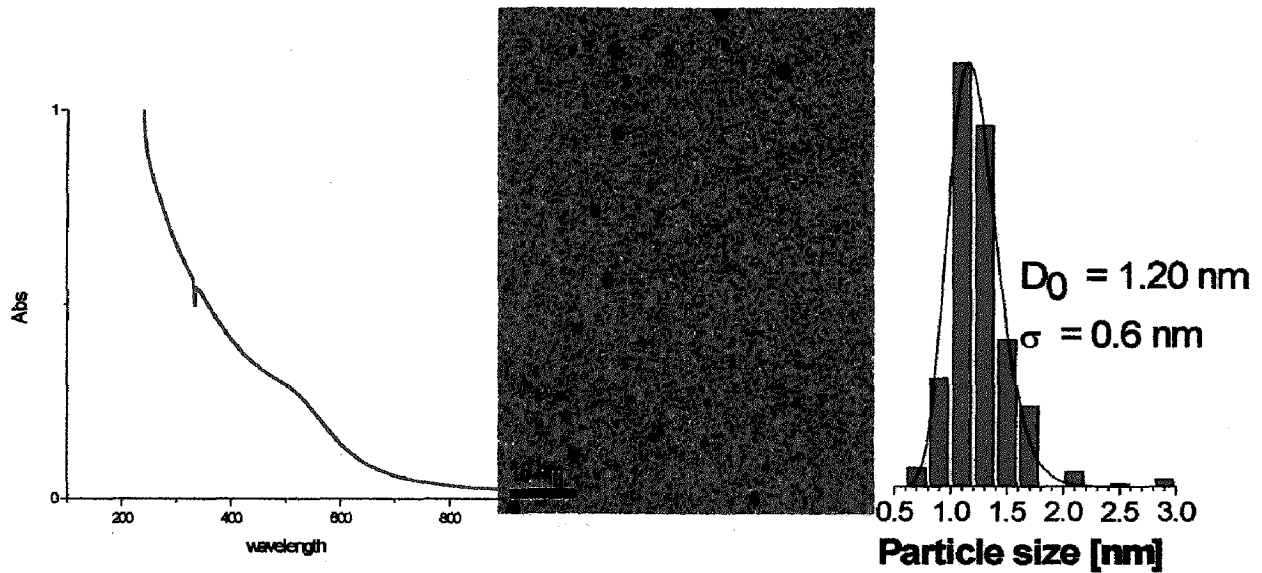


Figure 3.2.8: TEM image, UV-vis spectrum and size distribution of gold nanoclusters stabilized by PVP(K-90) at conditions VIII using Sigma-Aldrich microreactor

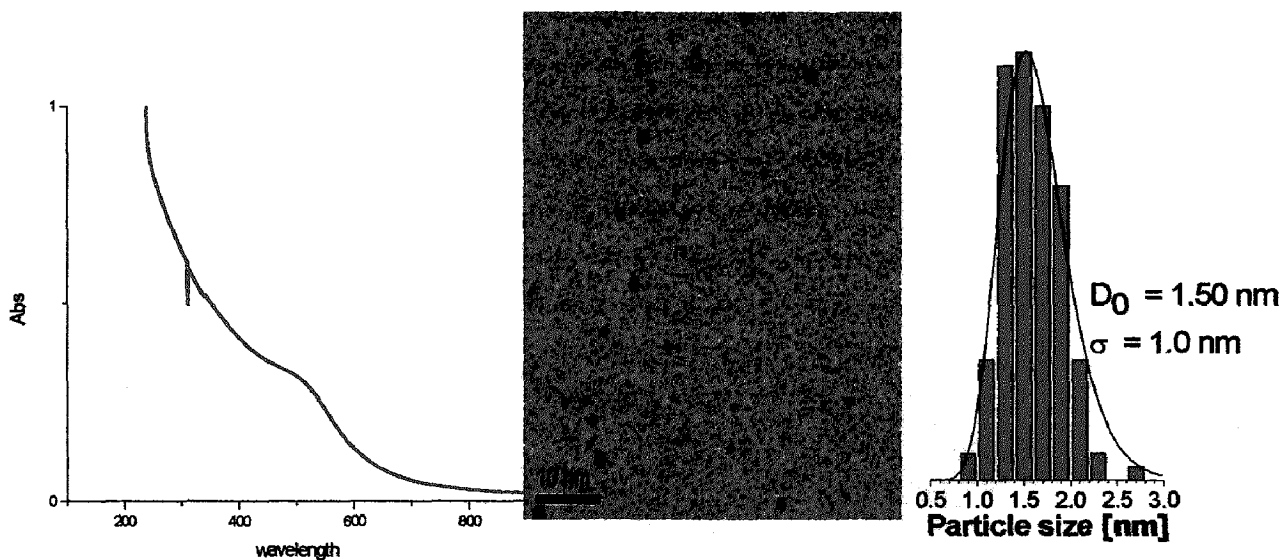


Figure 3.2.9: TEM image, UV-vis spectrum and size distribution of gold nanoclusters stabilized by PVP(K-90) at conditions IX using Sigma-Aldrich microreactor

Entries VI, VII, VIII, and IX in Table 3.1.1 show the conditions in which mols of NaBH_4 , HAuCl_4 , and PVP were kept constant and only the flow rates of NaBH_4 and HAuCl_4 solution were changed. The best optimized condition was obtained for entry VII where the flow rate of HAuCl_4 was 200ml/h and that of NaBH_4 was 55.8 ml/h.

3.3 Characterization of Au:Star poly(MOVE)

In this study, star poly(MOVE) was used for the stabilization of gold nanoclusters. The effect of flow rate of HAuCl_4 and NaBH_4 solution were investigated. The TEM images particle size histograms and the UV-Vis spectra are shown in Figure 3.3.1 and Figure 3.3.2. The different conditions that were applied for the synthesis of Au:star poly(MOVE) are listed in Table 3.3.1.

Table 3.3.1 Different optimization conditions for the preparation of Au:star poly(MOVE)

Entry	HAuCl_4 (mmol)	NaBH_4 (mmol)	StarMOVE (mmol)	Flowrate(ml/h) HAuCl_4	Flowrate(ml/h) NaBH_4	Particle daimeter(nm)
I	0.025	0.25	1.25	300	55.8	1.9±0.8
II	0.025	0.25	1.25	400	74.4	4.0±1.5

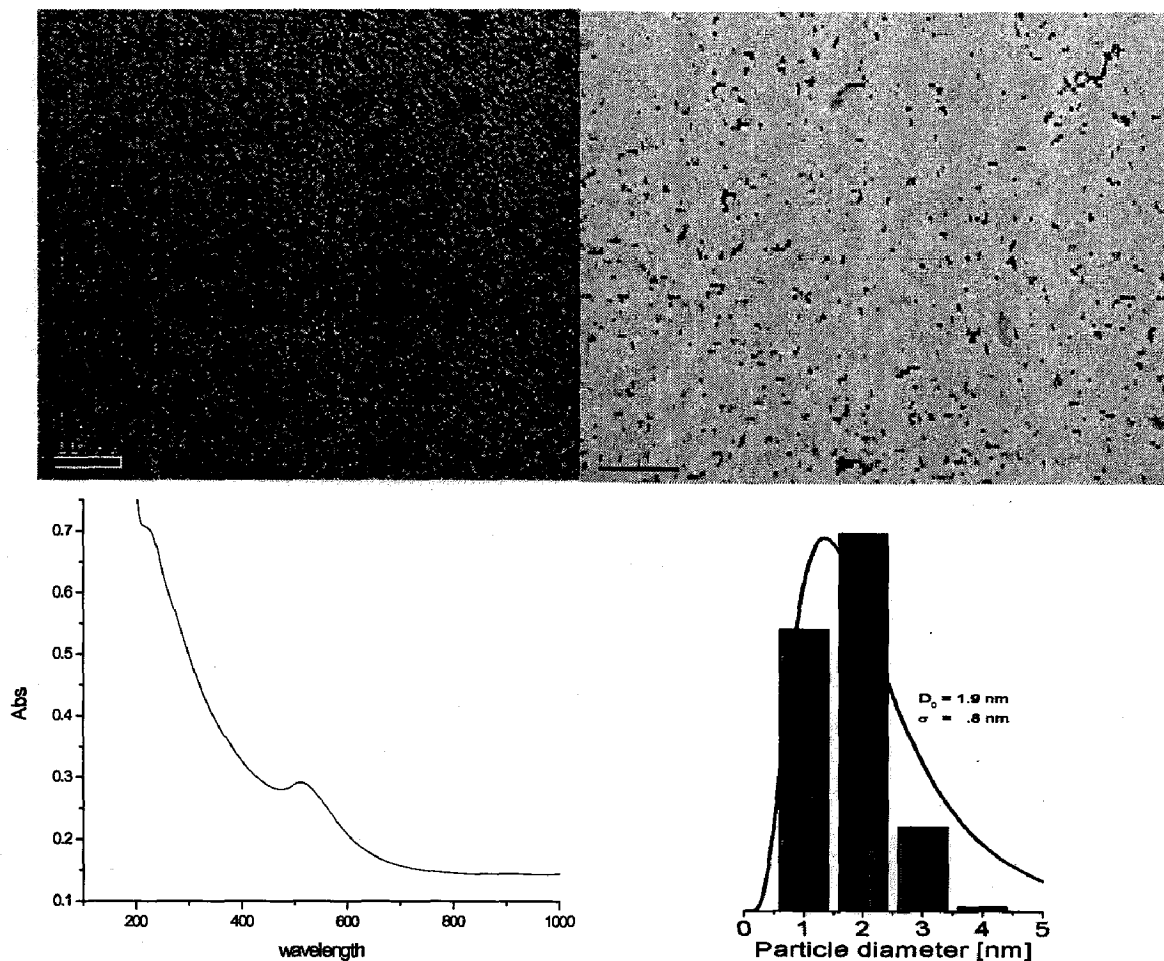


Figure 3.3.1: TEM images, UV-vis spectrum and size distribution of gold nanoclusters stabilized by star MOVE at condition I using Techno-application COMET X-01 microreactor

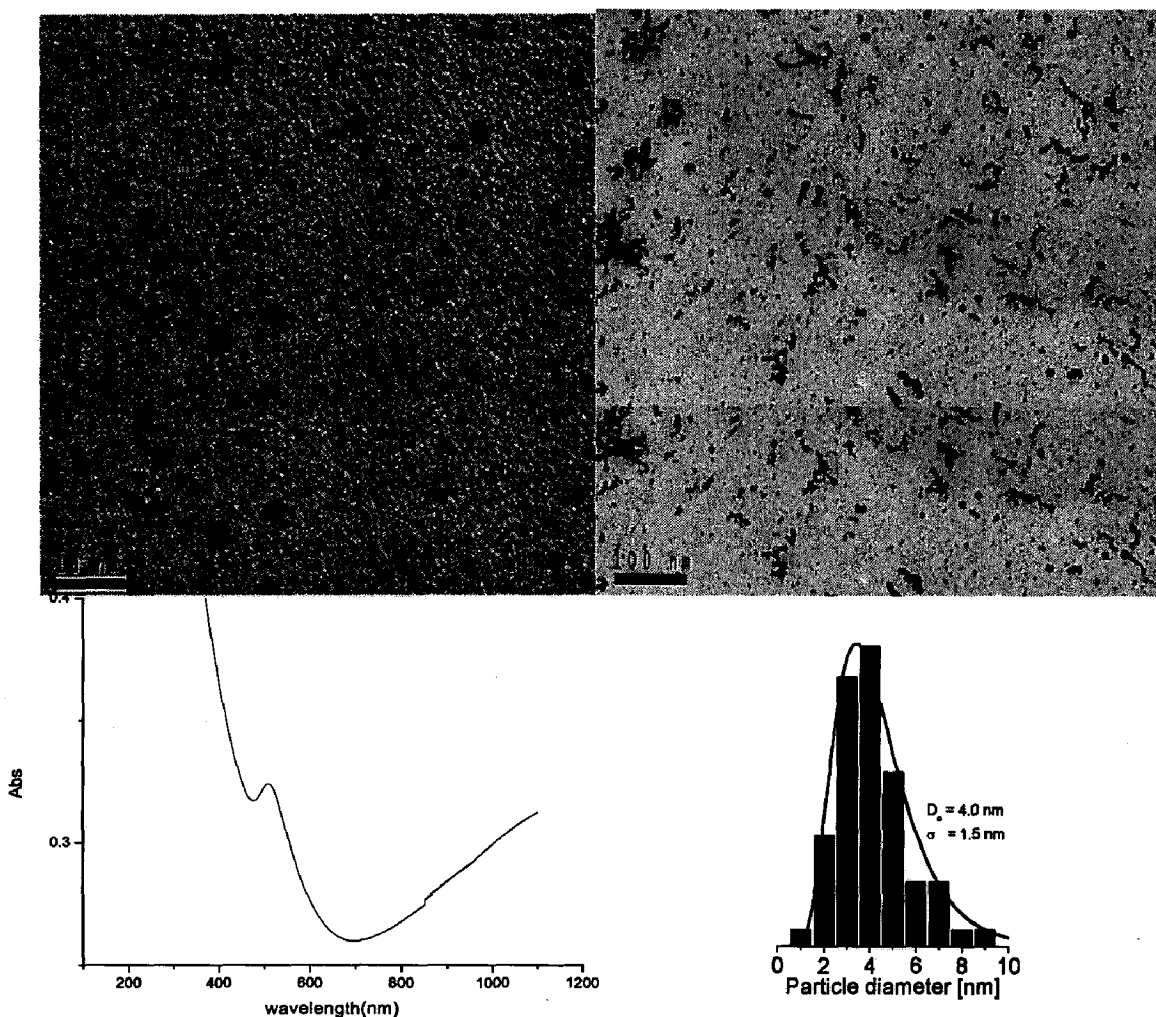


Figure 3.3.2: TEM images, UV-vis spectrum and size distribution of gold nanoclusters stabilized by star MOVE at condition II using Techno-application COMET X-01 microreactor

For the synthesis of Au:star poly(MOVE) nanoclusters, not too many conditions were tried because larger size of gold nanoparticles were obtained. The average gold nanoparticle size ranges from 1.9 nm to 4 nm and precipitation also occurred. From the UV- visible spectra one can see that the baseline is moved upward at longer wavelength regime that is due to the larger size of the particles and surface plasmon resonance at 520 is also observed that indicates the Au particle size is larger than 2 nm. This may be due to the fact that mixing is not good when COMET X-01 microreactor is used.

AEROBIC OXIDATION REACTIONS



It has been reported that gold nanoclusters stabilized by water soluble polymer poly(N-vinyl-2-pyrrolidone) (Au:PVP(K-30)) perform as excellent catalyst in the aerobic oxidation of benzylic alcohols in water under ambient conditions [62]. Notable features of alcohol oxidation catalyzed by Au:PVP clusters are listed as follows: i) Au:PVP is easily prepared from commercially available precursors. Au:PVP is non-hazardous and can be stored for months either as a solid powder or as an aqueous dispersion [63a], ii) Au:PVP behaves as a quasi-homogeneous catalyst in aqueous solution and can be recovered by centrifugal ultrafiltration [60-64], and iii) the catalytic activity per unit cluster surface area increases rapidly with decreasing size from ca. 10 to 1.3 nm. The smallest Au:PVP clusters exhibit the highest activity probably due to their non-metallic electronic structures [62].

This chapter contains a comparison of catalytic activity of Au:PVP(K-30) nanoclusters synthesized by the batch process and Au:PVP(K-90) nanoclusters synthesized by the Sigma-Aldrich microreactor S02 towards aerobic oxidation of different alcohols.

4.1.1 Oxidation of Benzyl Alcohol

Aerobic oxidation of benzyl alcohol was carried out to observe the catalytic activity of the prepared catalysts (Figure 4.1.1). A test tube ($\phi = 30$ mm) was placed with benzyl alcohol (27 mg, 0.25 mmol), K_2CO_3 (103.7 mg, 0.75 mmol), and H_2O (5 ml). An aqueous solution of Au:PVP(K-90) (0.5 mmol, 10 ml) was added and the reaction mixture was stirred vigorously (1300 rpm) at 300 K. The reaction mixture was sampled at every 30 min interval, quenched with 2 M HCl solution and extracted 3 times with ethyl acetate (0.5 ml). Then, the extracted organic layer was analyzed by gas chromatography. The yield was obtained from the calibration curve.

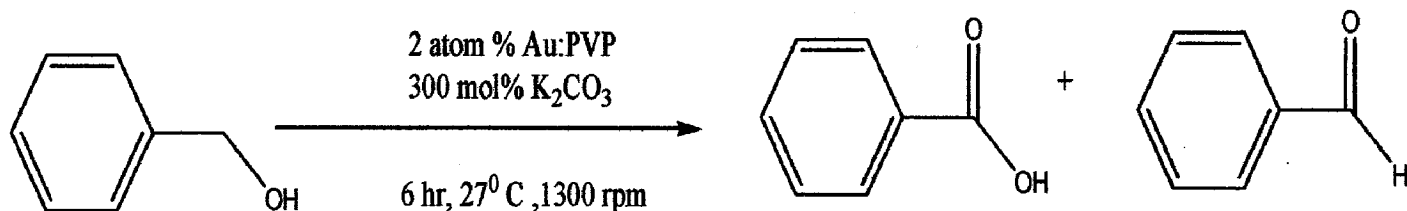


Figure 4.1.1: Oxidation of benzyl alcohol

The progress of oxidation reaction of benzyl alcohol using the catalysts is shown in Figure 4.1.2. In the starting few hours, benzaldehyde was observed but its yield decrease as the time proceeded. The final observed product was benzoic acid with both Au:PVP(K-30) and Au:PVP(K-90) nanoclusters.

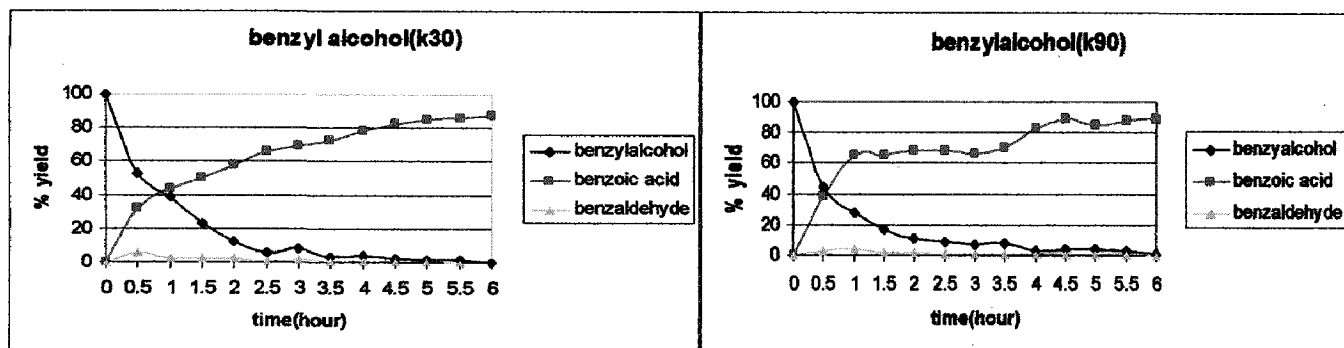


Figure 4.1.2: Progress of oxidation of benzyl alcohol with Au:PVP(K-30) and Au:PVP(K-90)

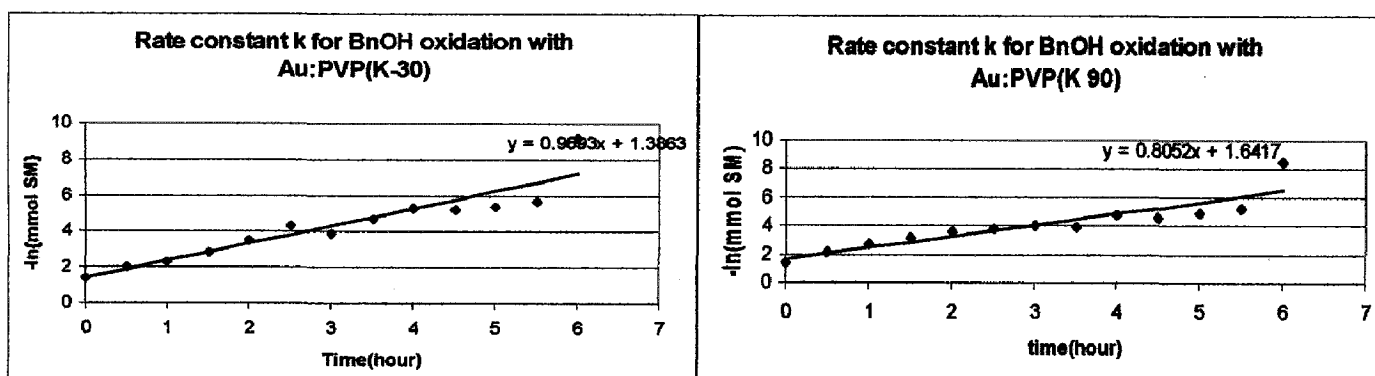


Figure 4.1.3: Kinetics of oxidation reaction of benzyl alcohol with Au:PVP(K-30) and Au:PVP(K-90)

The conversion C into the product was estimated from the measured yield of starting material remained as a function of reaction time for Au:PVP(K-90). A linear relationship between $-\ln(1-C)$ or $-\ln(\text{SM})$ and the reaction time is observed that indicating the reaction is first order with respect to the substrate (Figure 4.1.3). The slope of the straight line gives the rate constant. The same procedure was adapted for the catalytic oxidation of p-methoxy benzylalcohol, p-nitro benzylalcohol and the results were compared with Au:PVP(K-30) and Au:PVP(K-90) to see the effect of viscosity of polymer on the aerobic oxidation reactions.

4.1.2 Oxidation of p-methoxy benzy lalcohol

The procedure for p-methoxy benzyl alcohol (34.5 mg, 0.25 mmol) oxidation was same as that for benzyl alcohol. The progress of oxidation reaction of p-methoxy benzylalcohol is shown in Figure 4.1.4.

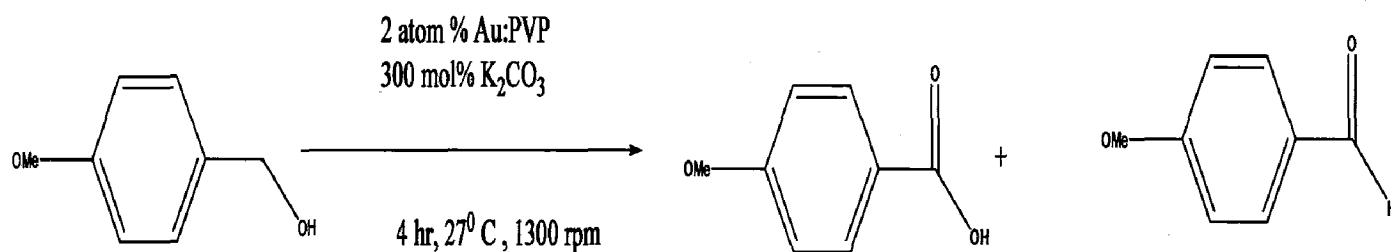


Figure 4.1.4: Oxidation of benzyl alcohol

In the starting few hours, p-methoxy benzaldehyde was observed (Figure 4.1.5), that was in higher yield as compared to the corresponding aldehyde observed with benzyl alcohol, but its yield decreased as the time proceeded. The final observed product was p-methoxy benzoic acid with both Au:PVP(K-30) and Au:PVP(K-90) nanoclusters. The rate constants have been compared for Au:PVP(K-30) and Au:PVP(K-90) in Figure 4.1.6.

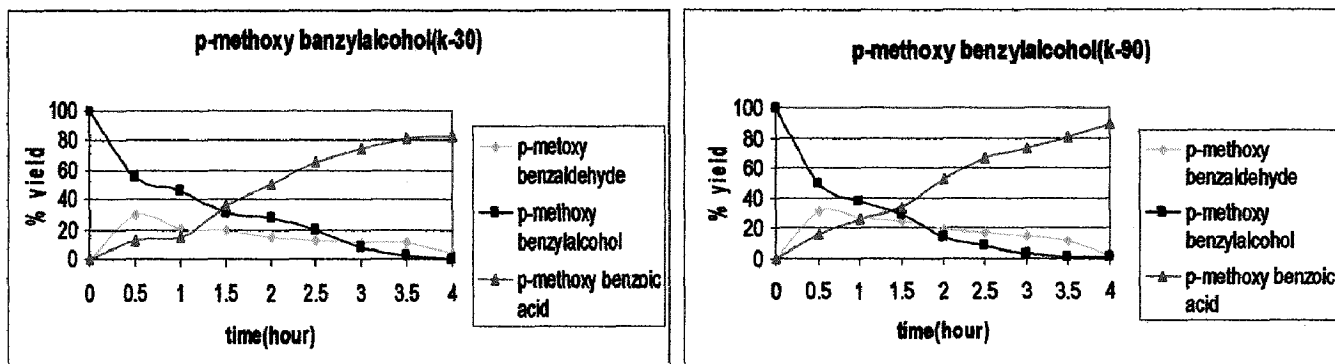


Figure 4.1.5: Progress of oxidation reaction of p-methoxy benzyl alcohol with Au:PVP(K-30) and Au:PVP(K-90)

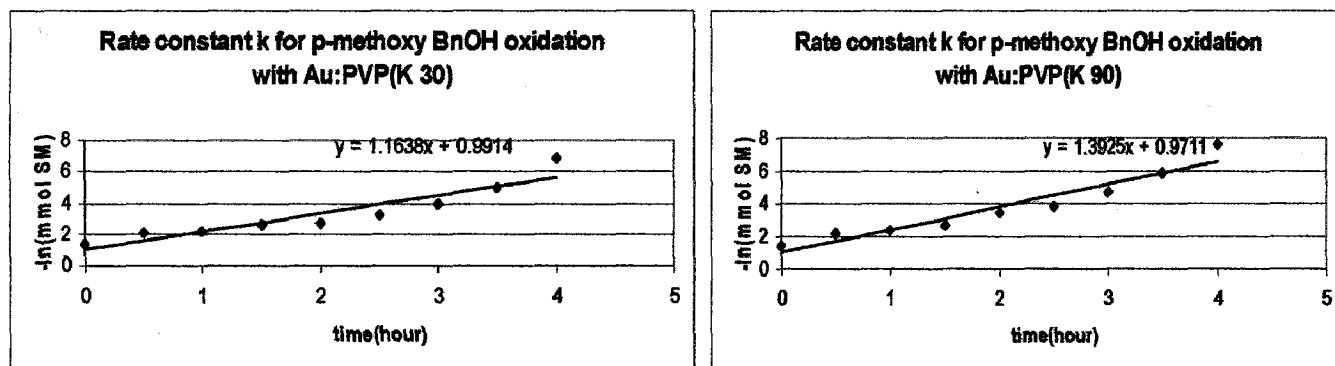


Figure 4.1.6: Kinetics of oxidation reaction of p-methoxy benzyl alcohol with Au:PVP(K-30) and Au:PVP(K-90)

4.1.3 Oxidation of p-nitro benzyl alcohol

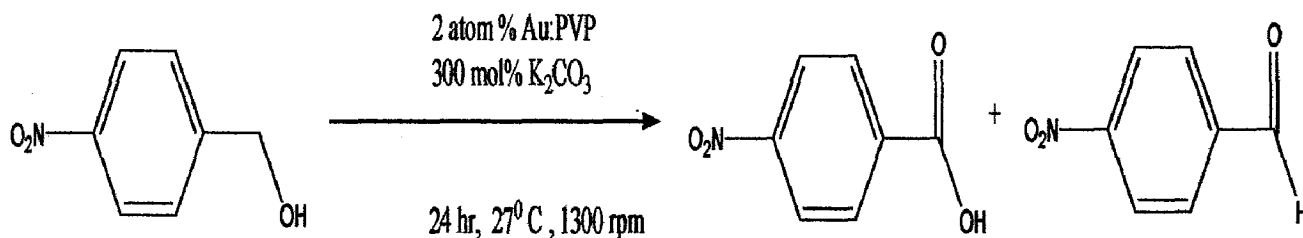


Figure 4.1.8: Oxidation of p-nitro benzyl alcohol

The procedure for the aerobic oxidation reaction of p-nitro benzyl alcohol (38.2 mg, 0.25 mmol) was same as that for benzyl alcohol and p-methoxy benzyl alcohol. All the results of the aerobic oxidation reactions that were performed are summarized in Table 4.1.1

Table 4.1.1 Summary of yield and rate constants for different aerobic oxidation reactions

Entry	Substrate	Catalyst	Final product	% Yield	Rate constant(h ⁻¹)	Time(hours) for completion of the reaction
I	Benzylalcohol	Au:PVP(K-30)	Benzonic acid	87	0.969	6
		Au:PVP(K-90)	Benzonic acid	89	0.805	
II	p-methoxy benzyl alcohol	Au:PVP(K-30)	p-methoxy benzonic acid	82	1.16	4
		Au:PVP(K-90)	p-methoxy benzonic acid	89	1.39	
III	p-nitro benzyl alcohol	Au:PVP(K-30)	p-nitro benzonic acid	81		
		Au:PVP(K-90)	p-nitro benzonic acid	86		24

From the results in the Table 4.1.1 it can be concluded that Au:PVP(K-90) nanoclusters prepared by Sigma Aldrich X-01 microreactor show almost comparable catalytic activity towards aerobic oxidation reaction as Au:PVP(K-30) synthesized by the batch method. This may be due to smaller the size of NPs of Au:PVP(K-90) (1.1 ± 0.4 nm).

4.2 Some Preliminary Studies on the Catalytic Growth of Carbon Nanotubes

4.2.1 Carbon Nanotubes

Since their discovery, carbon nanotubes have been found to possess extraordinary properties compared to conventional materials. Because of their great potential for a diverse range of applications, carbon nanotubes have been the most intensively researched nanomaterial. They can be used in electronics, composite materials, batteries, solar cells, sensors, semiconductors, and tips for scanning instruments [65-67].

4.2.2 Fabrication methods

The primary methods for the fabrication of carbon nanotubes are arc discharge, laser vaporization, and chemical vapor deposition. High pressure carbon monoxide (HiPco), electrospinning, and template methods that use anodic aluminum oxide have been used to make the carbon nanotubes [68].

4.2.2a Chemical vapor deposition (CVD)

Chemical vapor deposition is a well known technique in the semiconductor and microelectronic industry. To grow carbon nanotubes using this process, carbon containing gases pass through a furnace in which catalyst materials are present at a temperature of about 600 to 1200°C. The major parameters for the growth of carbon nanotubes in CVD are hydrocarbon gas as a carbon source, catalyst, and the growth temperature. As carbon sources, carbon monoxide (CO), methane (CH₄), acetylene (C₂H₂), ethylene (C₂H₄), and alcohol have been used. Transition metals such as Fe, Co, and Ni are used as the catalysts for the growth of carbon nanotubes. Figure 4.2.1 is a schematic diagram of a chemical vapor deposition system for the growth of carbon nanotubes.

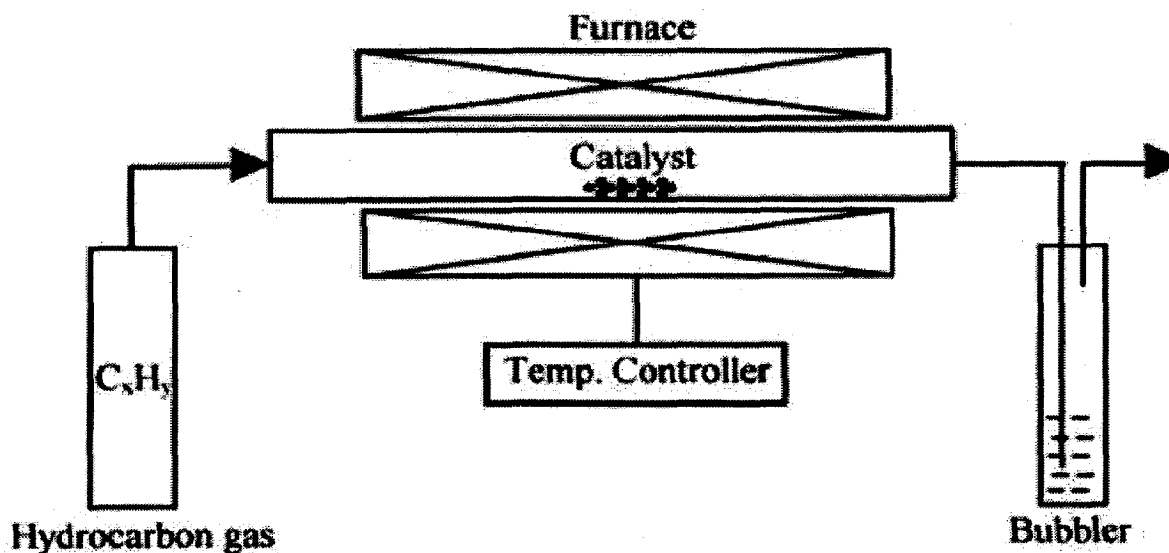


Figure 4.2.1: Schematic diagram of a chemical vapor deposition system.

Generally, a high reaction temperature (900 - 1200°C) is needed for single-walled carbon nanotubes growth, while a low reaction temperature is needed (600 - 900°C) for multi-walled carbon nanotubes growth. Whereas multi-walled carbon nanotubes can grow from a mixture of most carbon-containing gases and an inert gas, single-walled carbon nanotubes can only be grown from carbon-containing gases such as CO, CH₄, etc. These gases have reasonable stability in the temperature range of 900 - 1200°C, in a mixture of H₂ and an inert gas such as Ar [69].

The CVD method for producing carbon nanotubes includes two steps. The first step is coating the catalyst material such as Fe, Ni, and Co on the substrate by sputtering or other methods. The catalyst layer is then annealed or etched. Annealing of the metal layer makes clusters, which are sites for the nucleation of carbon nanotubes. Ammonia gas (NH₃) is generally used to etch out the catalyst metal layer and provide nucleation sites.

The second step is the actual growth of carbon nanotubes on the substrate. When the substrate-catalyst interaction is strong, carbon nanotubes grow up with the catalyst particle rooted at its base (base growth model) [69]. On the other hand, when the substrate-catalyst interaction is weak, the catalyst metal particle is lifted up by the growing carbon nanotube (tip growth model) [69]. Figure 4.2.2 shows the base growth model of carbon nanotubes.

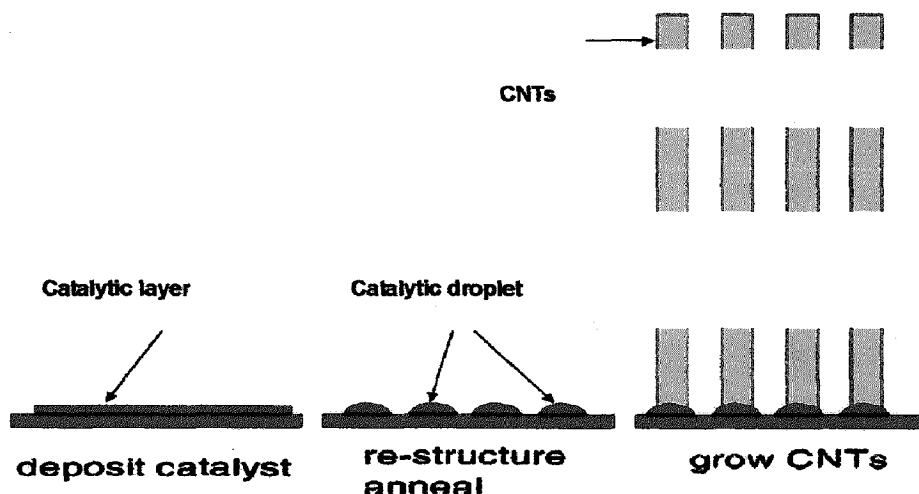


Figure 4.2.2: Schematic diagram of base growth model of carbon nanotubes

In the CVD process, the formation of single-walled carbon nanotubes or multi-walled carbon nanotubes can be controlled by the size of the catalyst particle. In general, when the particle size is a few nanometers, single-walled carbon nanotubes form, whereas particles of a few tens of nanometers favor multi-walled carbon nanotubes formation [70]. CVD is the best process to grow aligned carbon nanotubes on desired substrates for specific applications. This is not feasible with arc discharge or laser evaporation methods. CVD is the most suitable process for generating doped carbon nanotubes, e.g., with boron (B), nitrogen (N), or both. Also, carbon nanotube production with CVD is easy to scale up and economical. However, CVD grown multi-walled carbon nanotubes are usually less crystalline and exhibit many more defects than arc-discharge produced multi-walled carbon nanotubes.

4.2.3 Experimental Procedure

4.2.3a Preparation of Au supported catalyst

Au:PVP (K-90) was used as the catalyst for the growth of carbon nanotubes. The Au:PVP synthesized by chemical reduction method using microreactor and the supporting oxide (aluminium oxide) were suspended in methanol to get 0.6 wt% Au/Al₂O₃ catalyst, followed by evaporation. Other metal oxides such as MgO was also studied as the support material.

4.2.3b Growth of Carbon Nanotubes

For the growth of CNTs, 20 mg of the catalyst was placed in a quartz tube. A furnace was heated to the CVD temperature in a flow of Ar (99.999% purity, 350 sccm) with two different heating rates: (i) heating at a constant rate of 13°C/ min to CVD temperature (normal-heat CVD), and (ii) the sample was quickly inserted into the furnace maintained at the CVD temperature (rapid-heat CVD). The temperature program for furnace is shown in Figure 4.2.3. After reaching the CVD temperature, 700 – 900°C, the gas was switched to a mixture of C₂H₂ (1 vol %)–H₂ (5 vol %) and Ar under a total flow rate of 350 sccm. The reaction lasted for 10 min, and after the reaction, the furnace was cooled down to room temperature under Ar flow. Table 4.2.1 below shows typical chemical vapor deposition conditions for the growth of carbon nanotubes.

Table 4.2.1 Process conditions for the carbon nanotubes growth in CVD

ENTRY	GAS	SUPPORT	TEMP °C
1	CH ₄ +H ₂	Magnesium Oxide,wako	700
2	C ₂ H ₂ +H ₂	Aluminum Oxide (neutral), Wako	700
3	C ₂ H ₂ +H ₂	Aluminum oxide (basic),Aldrich	700
4	C ₂ H ₂ +H ₂	Aluminum oxide (basic),Aldrich	900
5	C ₂ H ₂ +H ₂	Aluminum oxide(acidic), Aldrich	900
6	C ₂ H ₂ +H ₂	Aluminum oxide(neutral), Aldrich	900

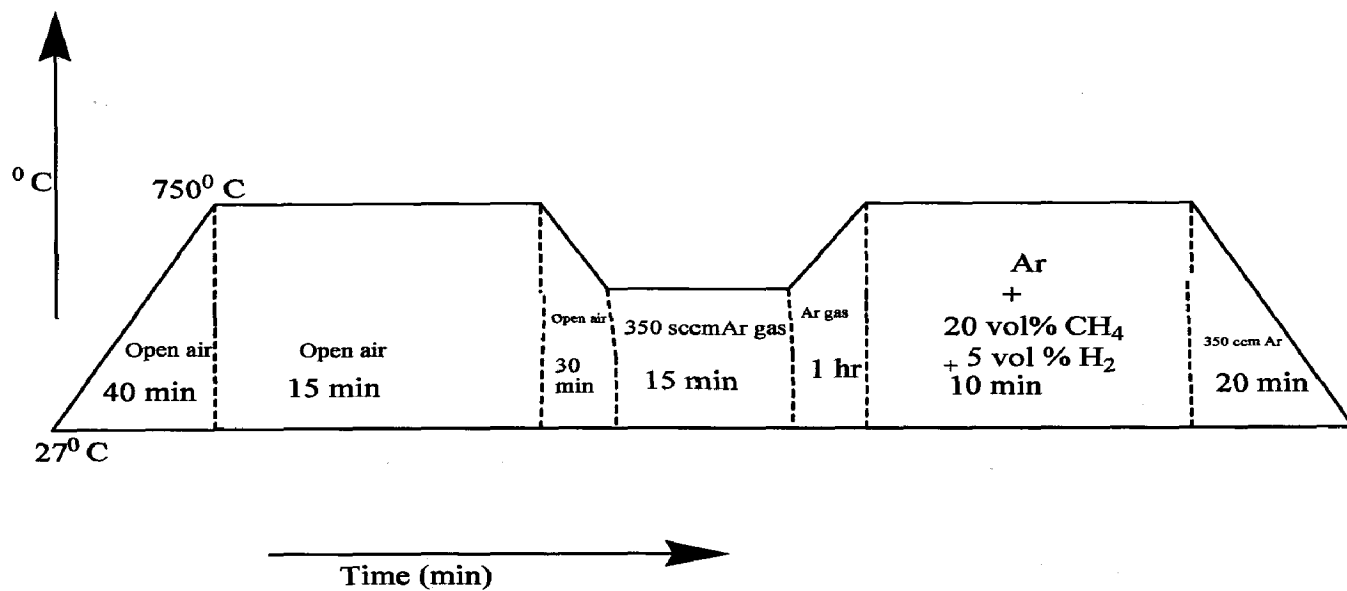


Figure 4.2.3: Temperature program of electric furnace for the growth of carbon nanotubes

The obtained products were characterized by scanning electron microscopy (SEM :JEOL FE-SEM:JSM-6700F) and the images are shown below (Figure 4.2.4, 4.2.5, 4.2.6, 4.2.7, 4.2.8, and 4.2.9).

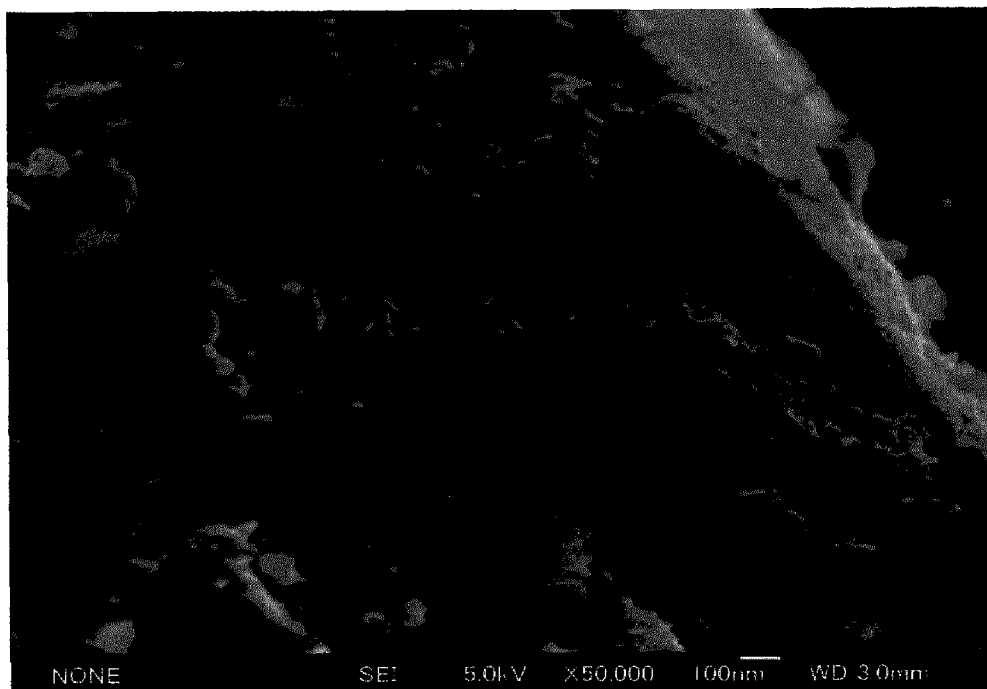


Figure 4.2.4: SEM image of product obtained under the condition listed in Entry 1

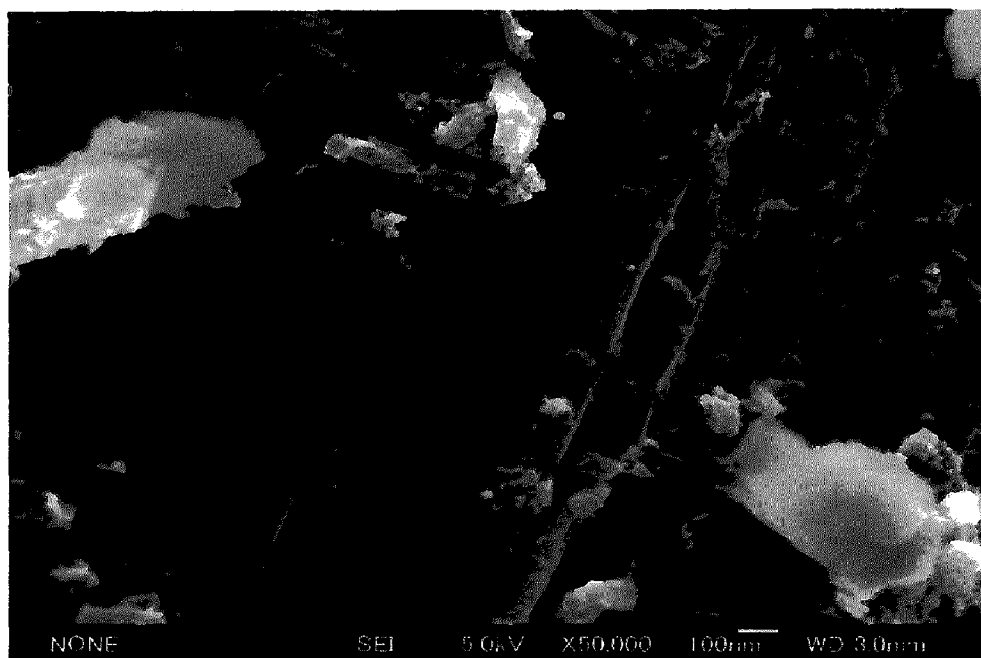


Figure 4.2.5: SEM image of product obtained under the condition listed in Entry 2

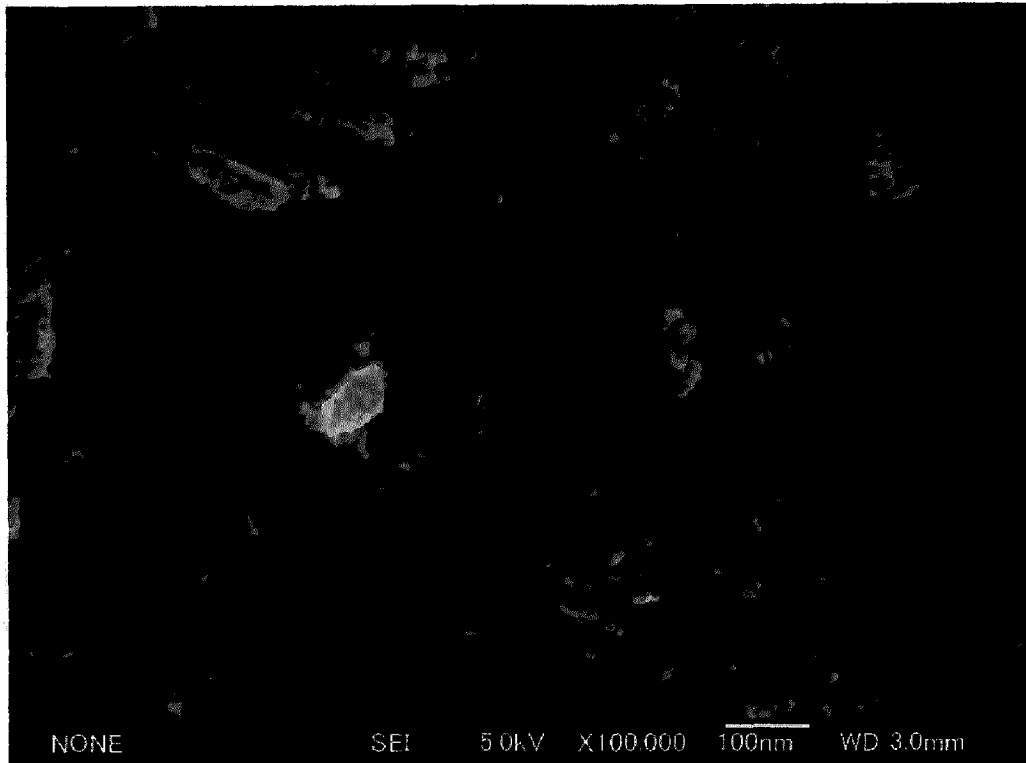


Figure 4.2.6: SEM image of product obtained under the condition listed in Entry 3

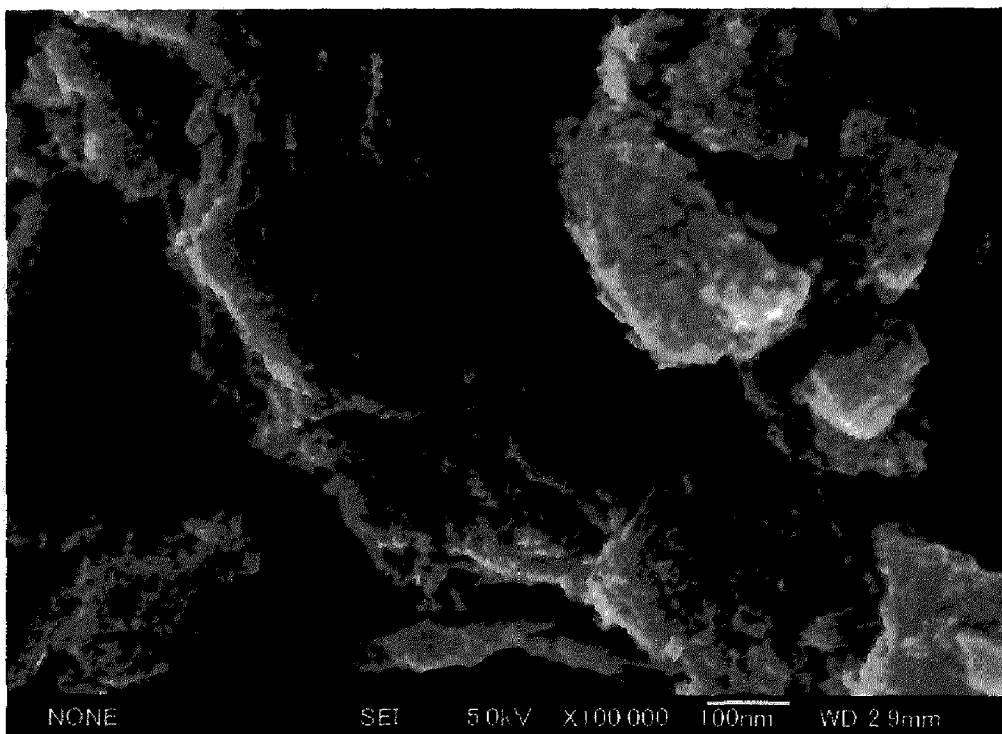


Figure 4.2.7: SEM image of product obtained under the condition listed in Entry 4

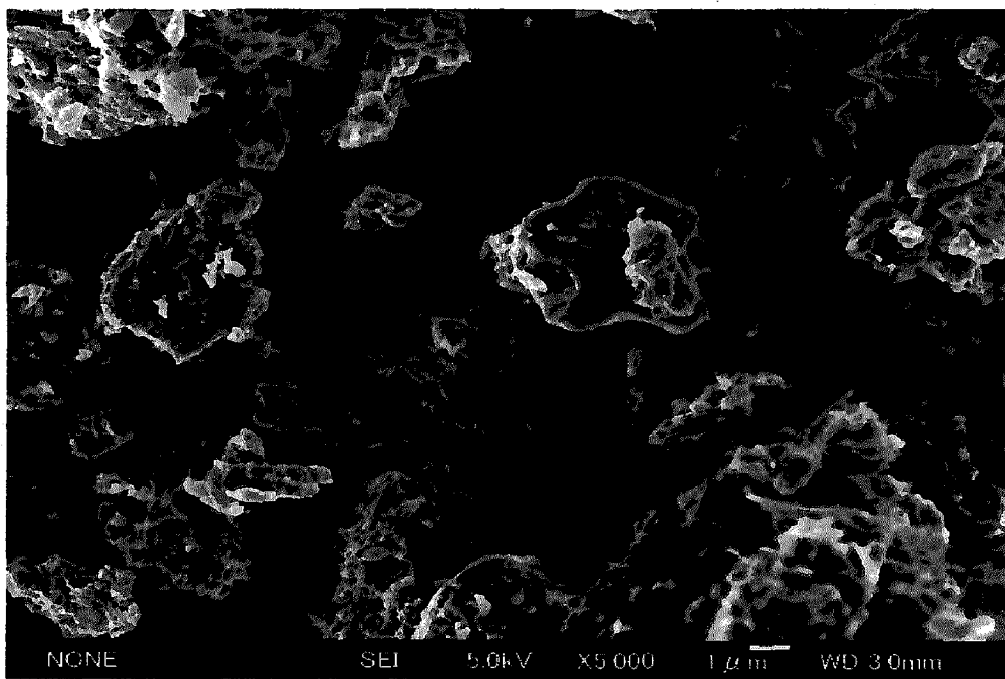
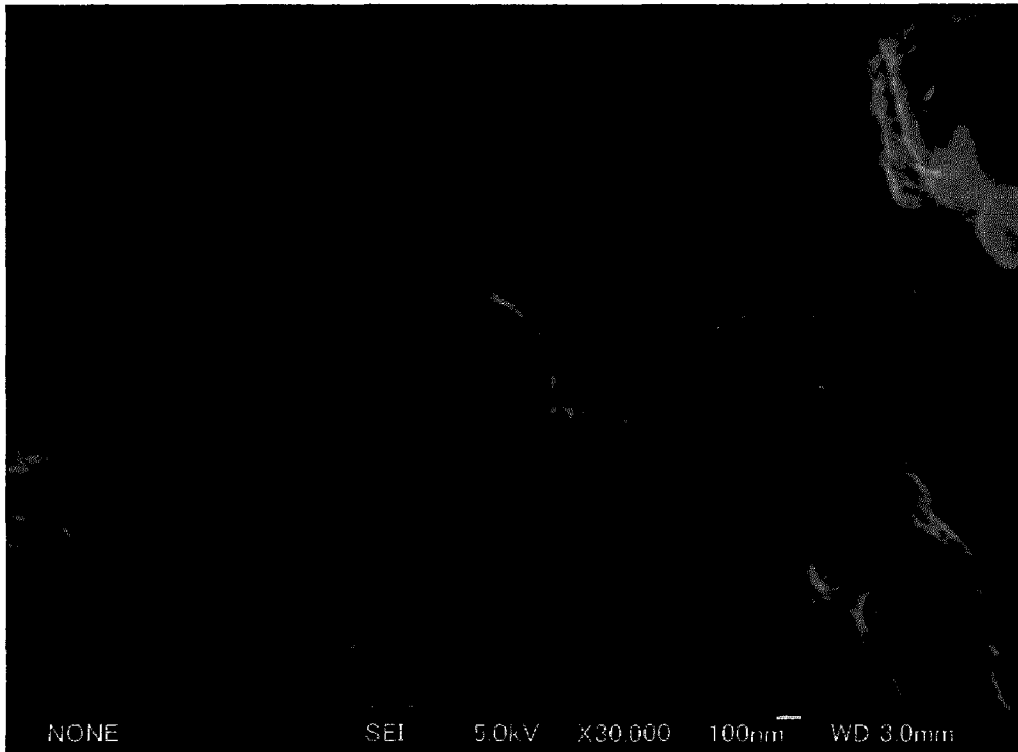


Figure 4.2.8: SEM image of product obtained under the condition listed in Entry 5

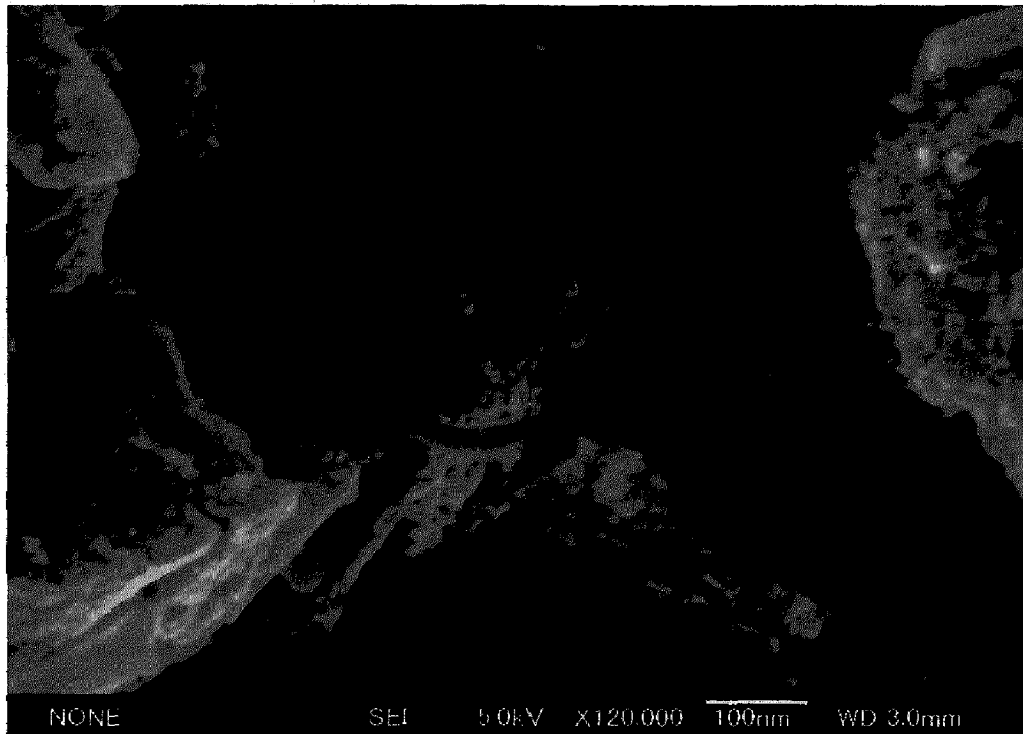
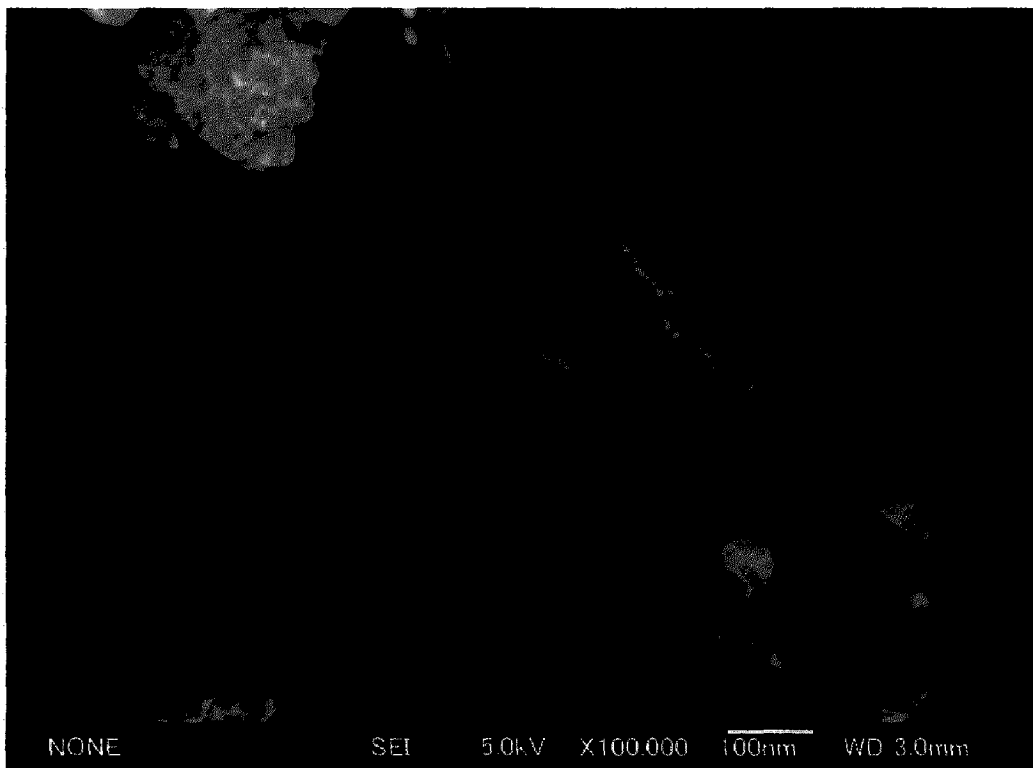


Figure 4.2.9: SEM image of product obtained under the condition listed in Entry 6

Carbon nanotubes were formed only with aluminium oxide (neutral) and aluminium oxide (acidic) (standard grade - 150 mesh) (Figure 4.2.8 and Figure 4.2.9) and the formation rapidly increases in the temperature range (700- 900°C). Further analysis of the materials by TEM and Raman spectroscopy are currently under progress.

CHAPTER 5

CONCLUSIONS



Gold nanoclusters with very small size have been prepared by microreactor based method. Au:PVP (K-90) mono-dispersed clusters have been successfully prepared with 1.15 ± 0.4 nm mean size under the optimized conditions of Sigma-Aldrich type S02 microreactor. This method can be used for the preparation of smaller Au nanoclusters stabilized by high molecular and relatively more viscous polymers, effectively. Au:Star poly(MOVE) nanoclusters were prepared under the optimized conditions of Techno- applications Comet X-01 microreactor. The particle size distribution of prepared Au: Star polymer was in the range 1.9 to 4 nm. It was found that Techno- applications Comet X-01 microreactor is not suitable for the formation of monodispersed small Au:star poly(MOVE) nanoclusters. It can be concluded that monodispersed, small size Au nanoclusters protected by hydrophilic polymers having high viscosity NCs can be prepared effectively by Sigma-Aldrich Microreactor. The Au:PVP(K-90) catalyst, prepared by the microreactor(Sigma-Aldrich S02) shows almost comparable activity towards aerobic oxidation reactions as Au:PVP(K-30) catalyst that was prepared by the batch process. The viscosity of hydrophilic polymer does not play a major role in the aerobic oxidation reaction and only the size of the catalyst is important. Finally, Au:PVP nanoclusters have been demonstrated as a good catalyst for the growth of carbon nanotubes.

CHAPTER 5

REFERENCES

1. P. Atkins, J. D Paula, Physical Chemistry, *Oxford University Press*, 2002 , 908
2. A. Roucoux, J. Schulz, H. Patin, *Chem Rev.* 2002, 102, 3757-3778
3. D. Astruc, F. Lu, J. R. Aranzaes, *Angew. Chem. Int. Ed.* 2005, 44, 7852-7872
4. N. Pernicone, *Cattech*, 2003, 7, 196-204
5. G. A. Somorjai, Y.G. Borodko, *Catal. Lett.* 2001, 76, 1-5
6. M. Haruta, N. Yamada, T. Kobayashi, S. Iijima, *J. Catal.* 1987, 115, 301-309
7. R. Nishio, M. Sugiura, S. Kobayashi, *Org. Lett.* 2005, 7, 4831-4834
8. B. Yoon, H. Kim, C. M. Wai, *Chem. Comm.* 2003, 1040-1041
9. M.-C. Daniel, D. Astruc, *Chem. Rev.* 2004, 104, 293-346.
10. C. W. Corti, R. J. Holliday, D. T. Thompson, *Gold Bull.*, 2003, 35, 111
11. M. M. Maye, J. Luo, L. Han, N. N. Kariuki, C. J. Zhong, 2003, 36, 75
12. M. Haruta, M. Date, *Appl. Catal. A: General*, 2001, 222, 427
13. D. T. Thompson, *Gold Bull.*, 1998, 31, 111; 1999, 32, 12
14. D. Compton, L. Cornish, E. vander Lingen, *Gold Bulletin*, 2003, 36, 10-16; 36, 51
15. D. I. Gittins, D. Bethell, D. J. Schiffrin, R. J. Nichols, *Nature*, 2000, 408, 67
16. M. Shirai, K. Haraguchi, K. Hiruma, T. Katsuyama, *Gold Bulletin* 1999, 32, 80
17. M. Himmelhaus, H. Takei, Sensors, Actuators B, *Chemical*, 2000, 63, 24
18. D. J. Maxwell, J. R. Taylor, S. Nie, *J. Am. Chem. Soc.* 2002, 124, 9606
19. T. A. Taton, C. A. Mirkin, R. L. Letsinger, *Science*, 2000, 289, 17
20. S. J. Park, T. A. Taton, C. A. Mirkin. *Science*, 2002, 295, 1503.
21. M.-C Daniel, D. Astruc, *Chem. Rev.* 2004, 104, 293-346.
22. a) Z. Li, C. Brouwer, C. He, *Chem. Rev.* 2008, 108, 3239. b) E. J.-Nunez, A.M. Echavarren, *Chem. Rev.* 2008, 108, 3326. c) A. Arcadi, *Chem. Rev.* 2008, 108, 3266. d) D.J. Gorin, B.D. Sherry, F. D. Toste, *Chem. Rev.* 2008, 108, 3351 e), J. Muzart, *Tetrahedron* 2008, 64, 5815. f) S. D. Gonzalez, N. Marion, S. P. Nolan, *Chem. Rev.* 2009, 109, 3612. g) A. Furstner, *Chem. Soc. Rev.* 2009, 38, 3208. h) N.T. Patil, Y. Yamamoto, *Chem. Rev.* 2008, 108, 3395.
23. a) M. Haruta, T. Kobayashi, H. Sano, N. Yamada, *Chem. Lett.* 1987, 16, 405. b) M. Haruta, *Chem. Record* 2003, 3, 75.

c) A.S, K Hashmi, G Hachings, Angrew. *Chem . Int. Ed.* **2006**, *45*, 7896. d) T. Matsumoto, L. Prati, M. Rossi, *Chem. Soc. Rev* **2008**, *37*, 2077. f) A. Corma, H. Garcia, *Chem. Soc. Rev.* **2008**, *37*, 2096. g) F. Moreau, G.C .Bond, A.O . Taylor, *J. Catal.* **2005**, *231*, 105. h) R.M. T. Sanchez, A. Ueda, K. Tanaka, M.Haruta, *J. Catal.* **1997**, *168*, 125. i) D.A., H Cunningham, W. Vogel, H. Kageyama. S. Tsubota, M. Haruta, *J. Catal.* **1998**, *177*, 1 j) F.Shi , Q.Zhang, Y. Ma, Y. He, Y. Deng, *J. Am.Chem Soc.* **2005**, *127*, 4182. k) D.T. Thompson, *Topics Catal. Today* **1997** , *36*, 153. m) B.E.Salisbury, W.T. Wallace, R. L.Whetten, *Chem. Ohys.* **2000**, *262*, 131. n) T. Hayashi, K. Tanaka, M. Harta, *J. Catal.* **1998**, *178*, 566. o) M. d, Hughes , Y- J. Xu,P Jenkins, P. McMorn, P. Landon, D.I.Enache, A. F. Carley, G.A. Attard, G.J. Htchings, F. King, E. H.Stitt, P. Johnston, K. Griffin, C. J. Kiely, *Natre* **2005**, *437*, 11332 p) S. C arretin , P. McMorn , P. Johnston, K. Griffin, C.J.Kiely, Hatchings, *Chem. Comm.* **2002**, 696. q) R. Zhao, D, Ji, G.Lv, g.Qian, L.Yan, X. Wang, J. Suo ,*Chem . comm.* **2004**, 904. r) Y.A Kalvachev, T.Hayashi, S. Tsubota, M. Haruta, *J. Catal.* **1999**, *186*, 228 s) R. D Wtaers, J. J Weimer, J. E. Smith, *Catal. Lett.* **1995** , *30*, 181. t) C. Qi, T. Akita, M. Okumura, M. Haruta, *Appl. Catal. A***2001**, *218*, 81 u) G. Mul, A. Zwijnenburg, B. v.d Linden, M . Makkee, J.A. Moulijn. *J. Catal.* **2001**, *201*, 28 v) E. E. Stangland, K. B. Stavens, R. P.Andres, W. N. Delgass, *J. Catal.* **2000**, *191*, 332 w) C. Bianchi, F. Prata, L. Prati, M. Rossi, *Topics Catal.* **2000**, *13*, 231. x) F. Porta, L. Prati, M. Rossi, *Topics Catal Today* **2000**, *61*, 165 y) F. Porta, L. Prati, M. Rossi, S.Couccia, G.Martra, *Catal.* **2004**, *224*, 397. z)M.Haruta, *Chemical Record* **2003**, *3*, 75. aa) L. Fu, N.Q . Wu, J. H . Ymg, F. Qu, D. L. Johnson, M. C. Kung, H. H. Kung, V. P. Dravid , *J. Chem. Phys. B* **2005**, *109*, 3704.

24. a) A. Bongiorno, U.Landman, *Phy. Rev.Lett.* **2005**, *95*, 1. b) U. Landman, B.Yoon, C. Zhang, U. Heiz, M. Arenz, *Topics Catal.* **2007**, *44*, 145. c) U. Heiz, A.Sanchez, S. Abbet, W.D. Schneider, *Eur. Phys. J.D* **1999**, *9*,35. d) A. Sanchez, A .Abbet, U. Heiz, W. D. Schneider, H. Hakkinen, R, N.Barnett, U. Landman, *J. Phys.Chem A* **1999**, *103*, 9573. e) B. Yoon, P. Koskinen, B. Huber, Koskined, B. Huber, O. Kostko, B. Issendorff,H Hakkinen, M. Moseler, U., Lamdman, *Chem. Phys.Chem.* **2007**, *8*, 157. f) C. Harding, V. Habibpour, S.Kunz, A . N. S Farnbacher, U Heiz, B. Yoon, ,U.Landman, *J. Am .Chem. Soc.***2009**, *131*, 538. g) M. S. Chen, D.W. Goodman, *Science* **2004**, *306*, 252 h) M. S. Chen, D.W. Goodman, *Catal. Today* **2006**, *111*, 22 i) N. Saliba, D. H. Parker, B. E. Koel, *Surf. Sci.* **1998**, *410*, 270. j) B. Hammer, J. K. Norskov, *Nature* **1995**, *376*, 238.

- k) J. A. Bokhoven, J.T. Miller, *J.Phys.Chem. C* **2007**, *111*, 9245 l) G.C. Bond , *Catal. Today* **2002**, *72*, 5 m) G.C . Bond, *J. Mol. Catal. A* **2000**, *156*, 1.
25. a) J. Jia, KHaraki, J. N. Kondo, K. Domen, K. Tamaru, *J. Phys. Chem. B* **2000**, *104*, 1115,.b) J. E. B ailie, H.A. Abdullah, J. A. Aanderson, C.H. Rochester , N. V.Richardson, N.Hodge ,J. G . Zhang, A. Burrows, C. J.Kiely, G. J. Hutchings, *Phys. Chem. Chem. Phys .* **2001**, *3*, 4113. c) Okumura, T. Akita, M. Harta, *Catal. Today* **2002**,*74*, 265. d) H. Sakurai, T. Akita, S. Tsukuda, M. Kiuchi, M. Haruta, *Appl. Catal A* **2005** , *291*, 179. e) M. L. Tafin, A. A. Chaou, F. Moffin, V. Caps. J). Rousset, *Chem. Comm.* **2005**, 388.
26. Y. D. Kim, *Int. J. Mass. Spectrum.* **2003**, *299*, 864.
27. D. Stolcic, M. Fischer, G. Gantefor, Y. D. Kim, Q. Sun, P. Jena, *J. Am. Chem. Soc.* **2003**, *125*, 2848.
28. A. Gniewek, J. J. Ziolkowski, A.M. Trzeciak, L. Kepinski, *J. Catal.* **2006**, *239*, 272-281.
29. M. Brust, M. Walker, D. Bethell, D. J. Schiffrin, R. Whyman, *J. Chem. Soc., Chem. Commun.*,**1994** , 801-802
30. H. Hirai, *J. Macromol. Sci., Chem.* **1979**, *A13*, 633-649.
31. H. Tsunoyama, H. Sakurai, Y. Negishi, T. Tsukuda, *J. Am. Chem. Soc.* **2005**, *127*, 9374-9375
32. H. Tsunoyama, H. Sakurai, N. Ichikuni, Y. Negishi, T. Tsukuda, *Langmuir*, **2004** , *20*, 11293-11296
33. R. Narayanan, M. A. El-Sayed, *J. Am. Chem. Soc.* **2003** , *125*, 8340-8347.
34. Y. Li, X. M. Hong, D. M. Collard, M. A. El-Sayed, *Org. Lett.* **2000**, *2*, 2385-2388.
35. H. Tsunoyama, T. Tsukuda, H. Sakurai, *Chem. Lett.*, **2007**, *36*, 212-213
36. Y. B. Liu, C. Khemtong, J. Hu, *Chem. Comm.*, **2004**, 398-399
37. S. Kanaoka, N. Yagi, Y. Fukuyama, S. Aoshima, H. Tsunoyama, T. Tsukuda and H. Sakurai, *J. Am. Chem. Soc.* **2007**, *129*, 12060
38. P. G N. Mertens, I.F.J. Vankelecom, P. A. Jacobs, and D. E. De Vos, *Gold Bull.* **2005**, *38* 157-162
39. B.P.S. Chauhan, J.S. Rathore, T. Bando, *J. Am. Chem. Soc.*, **2004**, *126*, 8493-8500
40. A. Biffis, and L. Minati, *J. Catal.* **2005**, *236*, 405-409
41. A. B. R. Mayer, J. E. Mark, *J. Polym. Sci. Part a-Polym. Chem.* **1997**, *35*, 3151-3160.
42. R.M. Crooks, M .Q. Zhao, L. Sun, V. Chechik, L.K. Yeung, *Acc. Chem. Res.*, **2001**, *34* 181-190.

43. M.J. Hostetler, J.E. Wingate, C.J. Zhong, J.E. Harris, R.W. Vachet, M.R. Clark, J.D. Londono, S.J. Green, J.J. Stokes, G.D. Wignall, G.L. Glish, M.D. Porter, N.D. Evans, and R.W. Murray, *Langmuir*, **1998**, *14*, 17-30.
44. M. Tamura, H. Fujihara, *J. Am. Chem. Soc.*, **2003**, *125*, 15742-15743.
45. W. W. Weare, S. M. Reed, M. G. Warner, J. E. Hutchison, *J. Am. Chem. Soc.*, **2000**, *122*, 12890-12891.
46. L. Wu, B. L. Li, Y. Y. Huang, H. F. Zhou, Y. M. He, Q. H. Fan, *Org. Lett.* **2006**, *8*, 3605-3608.
47. S. R. Isaacs, E.C. Cutler, J.S. Park, T.R. Lee, Y.S. Shon, *Langmuir* **2005**, *21*, 5689-5692
49. L.S. Ott, R.G. Finke, *Coordination Chem. Rev.* **2007**, *251* 1075-1100
50. R. Sheldon, *Chem. Comm.* **2001**, 2399-2407.
51. a) H. Tsunoyama, H. Sakurai, T. Tsukuda, *Chem. Phys. Lett.* **2006**, *429*, 528. b) H. Tsunoyama, H. Sakurai, N. Ichikuni, Y. Negishi, T. Tsukuda, *Langmuir* **2004**, *20*, 1193. c) H. Tsunoyama, T. Tsukuda, H. Sakurai, *Chem. Lett.* **2007**, *36*, 213.
53. S. Kanaoka, N. Yagi, Y. Fukuyama, S. Aoshima, H. Tsunoyama, T. Tsukuda, H. Sakurai, *J. Am. Chem. Soc.* **2007**, *129*, 12060.
54. a) H. Sakurai, H. Tsunoyama, T. Tsukuda, *J. Organomet. Chem.* **2007**, *692*, 368. b) H. Sakurai, H. Tsunoyama, T. Tsukuda, *Trans. Mater. Res. Soc. Jpn.* **2006**, *31*, 521.
55. I. Kamiya, H. Tsunoyama, T. Tsukuda, H. Sakurai, *Chem. Lett.* **2007**, *36*, 646.
56. H. Tsunoyama, N. Ichikuni, H. Sakurai, T. Tsukuda, *J. Am. Chem. Soc.* **2009**, *131*, 7086-7093.
57. H. Hirai, H. Chawanya, N. Toshima, *React. Polym.* **1985**, *3*, 127
58. V. Hessel, S. Hardt, H. Loewe, *Chemical Micro Process Engineering: Fundamentals, Modelling and Reactions*; Wiley-VCH: Weinheim, Germany, 2004. b) V. Hessel, H. Loewe, A. Müller, Kolb, G. *Chemical Micro Process Engineering: Processing and Plants*; Wiley-VCH: Weinheim, Germany, 2005.
59. H. Tsunoyama, H. Sakurai, N. Ichikuni, Y. Negishi, T. Tsukuda, *Langmuir* **2004**, *20*, 11293-11296.
60. Shalom, D.; Wootton, R. C. R.; Winkle, R. F.; Cottam, B. F.; Vilar, R. *Mater. Lett.* **2007**, *61*, 1146-1150.
61. Toshima, N.; Harada, M.; Yamazaki, Y.; Asakura, K. *J. Phys. Chem.* **1992**, *96*, 9927.

62. a) H. Tsunoyama, H. Sakurai, Y. Negishi, T. Tsukuda, *J. Am. Chem. Soc.* **2005**, 127, 9374.
b) H. Tsunoyama, H. Sakurai Tsukuda, *Chem. Phys. Lett.* **2006**, 429, 528.
63. a) H. Tsunoyama, H. Sakurai, N. Ichikuni, Y. Negishi, Tsukuda, *Langmuir* , **2004**, 20, 11293.
64. H. Sakurai, H. Tsunoyama, T. Tsukuda, *Trans. Mater. Res. Soc. Jpn.* **2006**, 31, 521.
65. A.G. Rinzler, J. H. Hafner, P. Nikolaev, L. Lou, S.G. Kim, D. Toma'nek, *et al. Science* **1995**, 269, 1550–3.
66. S. J. Tans, A. R. M. Verschueren, C. Dekker. *Nature* **1998**, 393, 49–52.
67. X. K. Wang, X. W. Lin, S. N. Song, V. P. Dravid, J. B. Ketterson, R. P. H. Chang, *Carbon*, **1995**, 33, 949–58.
68. J. Robertson, *Materials Today*, **2007**, 10, 36-43.
70. Y. Ando, *Materials Today*, **2004**, 22-29.